

DATABASE DEVELOPMENT FOR TSUNAMI INFORMATION SYSTEM

A THESIS SUBMITTED TO
THE GRADUATE SCHOOL OF NATURAL AND APPLIED SCIENCES
OF
MIDDLE EAST TECHNICAL UNIVERSITY

BY

KORAY KAAAN ÖZDEMİR

IN PARTIAL FULFILLMENT OF THE REQUIREMENTS
FOR
THE DEGREE OF MASTER OF SCIENCE
IN
CIVIL ENGINEERING

SEPTEMBER 2014

Approval of the thesis:

**DATABASE DEVELOPMENT FOR TSUNAMI INFORMATION
SYSTEM IN TURKEY**

Submitted by **KORAY KAAN ÖZDEMİR** in partial fulfillment of the
requirements for the degree of **Master of Science in Civil Engineering**
Department, Middle East Technical University by,

Prof. Dr. Canan Özgen
Dean, Graduate School of **Natural and Applied Sciences** _____

Prof. Dr. Ahmet Cevdet Yalçiner
Head of Department, **Civil Engineering** _____

Prof. Dr. Ahmet Cevdet Yalçiner
Supervisor, **Civil Engineering Department, METU** _____

Examining Committee Members:

Prof. Dr. Ayşen Ergin
Civil Eng. Dept., METU _____

Prof. Dr. Ahmet Cevdet Yalçiner
Civil Eng. Dept., METU _____

Assist. Prof. Dr. Gülizar Özyurt Tarakcıoğlu
Civil Eng. Dept., METU _____

Dr. Işıkhan Güler
Civil Eng. Dept., METU _____

Dr. Hülya Karakuş Cihan
Yüksel Project Int. Co _____

Date: 04.09.2014

I hereby declare that all information in this document has been obtained and presented in accordance with academic rules and ethical conduct. I also declare that, as required by these rules and conduct, I have fully cited and referenced all material and results that are not original to this work.

Name, Last Name: Koray Kaan ÖZDEMİR

Signature:

ABSTRACT

DATABASE DEVELOPMENT FOR TSUNAMI INFORMATION SYSTEM

ÖZDEMİR, Koray Kaan

M.Sc., Civil Engineering Department

Supervisor: Prof. Dr. Ahmet Cevdet YALÇINER

September 2014, 116 pages

Tsunamis are believed to be one of the natural enemies of human kind and evolution as the damage it gives at the shores can be described as lethal in means of loss of lives, tangible damage to the economy and concrete living on the shore, threat to health in variety of sicknesses after drawdown of water.

Since this phenomena has been lethal lately even in a country like Japan which was prepared for any fatal earthquakes and tsunamis, it is in great importance to use the technology and history in accordance to create a public warning in time. For this purpose, in this study, the development of a database for a simple tsunami warning system is discussed.

The methodology consists of defining the lethal historical tsunamis in the area, simulating possible most dangerous tsunami scenarios, evaluating the post effects of the simulated tsunamis, creating basis for developing an informative system in correlation with formerly simulated tsunami scenarios

Keywords: Tsunami modeling, warning system, database, NAMI DANCE

ÖZ

TSUNAMİ UYARI SİSTEMİ İÇİN VERİTABANI GELİŞTİRİLMESİ

ÖZDEMİR, Koray Kaan

Yüksek Lisans, İnşaat Mühendisliği Bölümü

Tez Yöneticisi: Prof. Dr. Ahmet Cevdet YALÇINER

February 2014, 116 sayfa

Tsunamiler kıyılarda yarattığı canlı hayatına karşı tehlikesi, ekonomiye ve kıyıdaki yaşama maddi olarak etkisi ve sular çekildikten sonra yarattığı çeşitli sağlık sorunlarıyla, insan oğlu ve evriminin doğal düşmanlarından biri olarak düşünülür.

Tsunami olgusu son zamanlarda Japonya gibi her türlü ölümcül deprem ve tsunamiye hazırlıklı olan bir ülkede bile etkili olabildiyse, her geçen gün gelişen teknolojik ve tarihi bilgileri kullanıp genel bir uyarı oluşturmak önemli bir yer kazanmaktadır. Bu çalışmada yukarıdaki nedenlerden dolayı bir tsunami uyarı sistemi için veri tabanı oluşturulması planlanmış ve tartışılmıştır.

Çalışmada öncelikle tarihi tsunamilerin incelenmesi; belirlenen tehlikeli tsunamilerin günümüz coğrafyasında benzetimlerinin yapılması; tarihi tsunamiler ve benzetimlerin sonuçlarının değerlendirilmesi; değerlendirmeler sonucunda uyarı sistemi için bu bilgileri kullanan bir veri tabanının ve basit bir yazılımın oluşturulması yolları izlenmiştir.

Anahtar Kelimeler: Tsunami benzetimi, uyarı sistemi, veri tabanı, NAMI DANCE

To my uncle Gürsel Eylan (1960-2013),

ACKNOWLEDGEMENTS

I would like to express my gratitude to Prof. Dr. Ayşen Ergin who opened my path for being a civil engineer on my 4th year of my undergraduate education when I have lost all the motivation to be one.

I would like to thank to my supervisor Prof. Dr. Ahmet Cevdet Yalçınar to accept me as not just one of his students but one of his colleagues for over four years and for being patient during my long time of writing this thesis. He has influenced me not just in being an engineer but also to become a leader and think wise in every tough situation I had over years.

I would like to thank also to Dr. Işıksan Güler for being an idol for me in being an engineer with the social attributes and his efforts to teach me all he knew.

I am grateful to Mr. Okan Taktak for being a great boss and a leader for me in my period as a civil engineer in Derinsu Underwater Engineering.

Besides being a good friend and colleague, I want to express my deepest gratitude to Gökhan Güler who has helped me with the coding in this thesis and sharing his valuable time with me.

A big thanks to ‘Alt Kat’ Crew for great times, take home exams and memories. It would not be that fun without them.

All members of the Ocean Engineering and Research Center gave me a lot of courage, knowledge, shared their friendships and passion for engineering with me. I can only say that I am really glad to meet and spend my years with them.

I want to thank to METU Jazz Society and Board of Engineering Students of Technology (BEST), LBG Ankara for giving me the opportunity to lead them and develop my personality.

I would like to thank to all members of my band, Rocky Swing Project to accompany me for the last 12 years and raising me.

My best friend Can Kuşhan has all the rights to deliver my sincere wishes for being with me since we were just children.

I also want to thank to my aunt Melahat Dum for making me wiser and my uncle Metin Dum for his helps over years.

My sincere thanks goes to my uncles Ömer Eylen for showing me the way of being a good engineer and Şakir Eylen for just not being an uncle but a good friend.

My special thanks goes to my brother, Kamil Özdemir for being a bright light on my route to be a civil engineer and supporting me in every way he could.

I have no words but just gratitude and happiness for my parents, Ayşe and Hamdi Özdemir for believing in me, giving everything they could, always supporting me in my life.

I am in a big debt to my future wife Kıvılcım Sıla Gümüş for being patient, making everything more beautiful, always motivating me and showing her love all the time.

Finally, I would like to dedicate this thesis to my uncle Gürsel Eylen for showing me to be a good person in this relentless life, being a good person for all his life.

TABLE OF CONTENTS

ABSTRACT	v
ÖZ.....	vi
ACKNOWLEDGEMENTS	viii
TABLE OF CONTENTS	x
LIST OF FIGURES.....	xii
1. INTRODUCTION	1
2. LITERATURE SURVEY	3
2.1 Tectonic Characteristics of the Marmara Region.....	3
2.2 Historical Tsunamis in the Sea of Marmara.....	5
2.3 Past Attempts of Tsunami Modeling for the Sea of Marmara	10
3. ESTIMATION OF TSUNAMI SOURCES AND SIMULATIONS	13
3.1 Estimation of Source Parameters	13
3.1.1 Geological Characteristics of the Sea of Marmara.....	14
3.1.2 Estimation of Probable Tsunami Source Mechanisms for the Marmara Sea	16
3.2 Tsunami Simulations for the Marmara Sea Region	21
3.2.1 NAMI DANCE – Tsunami Numerical Modeling Code.....	21
3.2.2 Scenarios Used in Simulations in the Sea of Marmara	23
3.2.2.1 Simulation of Source PI.....	25
3.2.2.2 Simulation of Source PIN.....	31
3.2.2.3 Simulation of Source PI + GA.....	37
3.2.2.4 Simulation of Source GA	43
3.2.2.5 Simulation of Source YAN.....	49
3.2.2.6 Simulation of Source CMN	55
4. DATABASE FOR THE WARNING SYSTEM IN THE SEA OF MARMARA 63	
4.1 Idea and Method.....	63
4.2 Formation of the Database	64

4.3	Working Stages of Tsunami Warning System	74
4.3.1	Input Stage	74
4.3.2	Processing Stage	75
4.3.2.1	First Checks	75
4.3.2.2	Reading the Database	77
4.3.2.3	Calculating the Geographical Distance between Coordinates and the Haversine Formula	77
4.3.2.4	Sorting Results and Choosing the Right Source	79
4.3.3	Output Stage.....	79
5.	CONCLUSIONS and FURTHER RECOMMENDATIONS	82
5.1	Conclusions on Tsunami Simulations.....	82
5.2	Conclusions on Software for Database	83
5.3	Recommended Future Studies.....	84
	REFERENCES.....	86
	APPENDIX A	88
A.	TSUNAMI CATALOGUE FOR TURKISH COASTS.....	88
	APPENDIX B	100
B.	RESULTS OF SIMULATIONS FOR 5KM FOCAL DEPTH.....	100

LIST OF FIGURES

FIGURES

Figure 2.1 Description of the Sea of Marmara with bathymetric data, ‘o’ points for seismicity.....	4
Figure 2.2 Locations of Tsunamigenic Events in Marmara Sea Region (Altinok, 2011, Redrawn)	9
Figure 3.1 Study Domain (Google Earth)	14
Figure 3.2 The NAF in the Marmara Sea (Armijo et al, 2005 and OYO – IMM, 2007)	15
Figure 3.3 Parameters of Selected Sources (OYO – IMM Report, 2007)	17
Figure 3.4 Studied and Selected Gauges in the Domain	24
Figure 3.5 Tsunami Source for PI	25
Figure 3.6 Sea states at t=10, 30, 60, and 90 min respectively according to the tsunami source PI	26
Figure 3.7 Distribution of Maximum (+) Wave Amplitude (top) and Minimum (-) Wave Amplitudes.....	27
Figure 3.8 Run-up Distribution According to the Tsunami Source PI.....	28
Figure 3.9 Time Histories of Water Surface Fluctuations at the Selected Gauge Locations for PI.....	30
Figure 3.10 Tsunami Source for PIN	31
Figure 3.11 Sea states at t=10, 30, 60, and 90 min respectively according to the tsunami source PIN	32
Figure 3.12 Distribution of Maximum (+) Wave Amplitude (top) and Minimum (-) Wave Amplitudes.....	33
Figure 3.13 Run-up Distribution According to the Tsunami Source PIN.....	34
Figure 3.14 Time Histories of Water Surface Fluctuations at the Selected Gauge Locations for PIN.....	36
Figure 3.15 Tsunami Source for PI+GA	37
Figure 3.16 Sea states at t=10, 30, 60, and 90 min respectively according to the tsunami source PI+GA	38
Figure 3.17 Distribution of Maximum (+) Wave Amplitude (top) and Minimum (-) Wave Amplitudes.....	39
Figure 3.18 Run-up Distribution According to the Tsunami Source PI+GA.....	40
Figure 3.19 Time Histories of Water Surface Fluctuations at the Selected Gauge Locations for PI+GA.....	42
Figure 3.20 Tsunami Source for GA.....	43

Figure 3.21 Sea states at t=10, 30, 60, and 90 min respectively according to the tsunami source GA	44
Figure 3.22 Distribution of Maximum (+) Wave Amplitude (top) and Minimum (-) Wave Amplitudes.....	45
Figure 3.23 Run-up Distribution According to the Tsunami Source GA	46
Figure 3.24 Time Histories of Water Surface Fluctuations at the Selected Gauge Locations for GA.....	48
Figure 3.25 Tsunami Source for YAN.....	49
Figure 3.26 Sea states at t=10, 30, 60, and 90 min respectively according to the tsunami source YAN	50
Figure 3.27 Distribution of Maximum (+) Wave Amplitude (top) and Minimum (-) Wave Amplitudes.....	51
Figure 3.28 Run-up Distribution According to the Tsunami Source YAN	52
Figure 3.29 Time Histories of Water Surface Fluctuations at the Selected Gauge Locations for YAN.....	54
Figure 3.30 Tsunami Source for CMN	55
Figure 3.31 Sea states at t=10, 30, 60, and 90 min respectively according to the tsunami source CMN	56
Figure 3.32 Distribution of Maximum (+) Wave Amplitude (top) and Minimum (-) Wave Amplitudes.....	57
Figure 3.33 Run-up Distribution According to the Tsunami Source CMN.....	58
Figure 3.34 Time Histories of Water Surface Fluctuations at the Selected Gauge Locations for CMN	60
Figure 4.1 Screenshot of the Input Screen	74
Figure 4.2 Coordinate Warning Message.....	75
Figure 4.3 Magnitude Warning Message	77
Figure 4.4 Spherical Triangle Solved by the Law of Haversines	78
Figure 4.5 Selection of the Source as Output.....	80
Figure 4.6 Visual Outputs of the Code	81
Figure 4.7 Visual Outputs of the Code	81
Figure 4.8 Sample Output of Elapsed Time Message.....	81
Figure B.1 Distribution of Maximum (+) Wave Amplitude (top) and Minimum (-) Wave Amplitudes.....	100
Figure B.2 Sea states at t=10, 30, 60, and 90 min respectively according to the tsunami source PI.....	101
Figure B.3 Time Histories of Water Surface Fluctuations at the Selected Gauge Locations for PI.....	102
Figure B.4 Distribution of Maximum (+) Wave Amplitude (top) and Minimum (-) Wave Amplitudes.....	103
Figure B.5 Sea states at t=10, 30, 60, and 90 min respectively according to the tsunami source PIN	104

Figure B.6 Time Histories of Water Surface Fluctuations at the Selected Gauge Locations for PIN.....	105
Figure B.7 Distribution of Maximum (+) Wave Amplitude (top) and Minimum (-) Wave Amplitudes.....	106
Figure B.8 Sea states at t=10, 30, 60, and 90 min respectively according to the tsunami source PI+GA	107
Figure B.9 Time Histories of Water Surface Fluctuations at the Selected Gauge Locations for PI+GA.....	108
Figure B.10 Distribution of Maximum (+) Wave Amplitude (top) and Minimum (-) Wave Amplitudes.....	109
Figure B.11 Sea states at t=10, 30, 60, and 90 min respectively according to the tsunami source GA	110
Figure B.12 Time Histories of Water Surface Fluctuations at the Selected Gauge Locations for GA.....	111
Figure B.13 Distribution of Maximum (+) Wave Amplitude (top) and Minimum (-) Wave Amplitudes.....	112
Figure B.14 Sea states at t=10, 30, 60, and 90 min respectively according to the tsunami source YAN	113
Figure B.15 Time Histories of Water Surface Fluctuations at the Selected Gauge Locations for YAN.....	114
Figure B.16 Distribution of Maximum (+) Wave Amplitude (top) and Minimum (-) Wave Amplitudes.....	115
Figure B.17 Sea states at t=10, 30, 60, and 90 min respectively according to the tsunami source CMN.....	116
Figure B.18 Time Histories of Water Surface Fluctuations at the Selected Gauge Locations for CMN	117

LIST OF TABLES

TABLES

Table 2.1 Earthquakes Occurred between 0-1900 in the Marmara Sea Region, Ambraseys, 2002	6
Table 3.1 Coordinates of Domain	14
Table 3.2 Fault Parameters for PI	18
Table 3.3 Fault Parameters for YAN and GA.....	19
Table 3.4 Fault Parameters for PIN and CMN.....	20
Table 3.5 Names and Coordinates of the Selected Gauges.....	24
Table 3.6 Results of PI Simulation at the Selected Gauge Points.....	29
Table 3.7 Results of PIN Simulation at the Selected Gauge Points.....	35
Table 3.8 Results of PI+GA Simulation at the Selected Gauge Points.....	41
Table 3.9 Results of GA Simulation at the Selected Gauge Points	47
Table 3.10 Results of YAN Simulation at the Selected Gauge Points.....	53
Table 3.11 Results of CMN Simulation at the Selected Gauge Points	59
Table 4.1 Database.....	66
Table 4.2 Corner Coordinates of the Domain	75
Table 4.3 Decision Matrix for the Atlantic (Tinti, et al., 2012).....	76
Table 4.4 Decision Matrix for the Mediterranean (Tinti, et al., 2012).....	76
Table A.1 Tsunamis Occurred on and Near Turkish Coasts (Altinok, 2011).....	88
Table A.1 (Continued)	89
Table A.1 (Continued)	90
Table A.1 (Continued)	91
Table A.1 (Continued)	92
Table A.1 (Continued)	93
Table A.1 (Continued)	94
Table A.1 (Continued)	95
Table A.1 (Continued)	96
Table A.1 (Continued)	97
Table A.1 (Continued)	98
Table A.1 (Continued)	99
Table B.1 Results of PI Simulation at the Selected Gauge Points	100
Table B.2 Results of PIN Simulation at the Selected Gauge Points	103
Table B.3 Results of PI+GA Simulation at the Selected Gauge Points	106
Table B.4 Results of GA Simulation at the Selected Gauge Points.....	109
Table B.5 Results of GA Simulation at the Selected Gauge Points.....	111
Table B.6 Results of YAN Simulation at the Selected Gauge Points	112
Table B.7 Results of CMN Simulation at the Selected Gauge Points.....	115

CHAPTER 1

INTRODUCTION

Origin of “tsunami” word is in Japanese meaning “harbor wave”, which does not reflect its real wild and fatal characteristics. Generated mostly by a seismic event on the earth or space, tsunamis are a result of a high amount of water displacement. The energy that tsunamis possess is the main key to the damage at the shoreline. Traveling from 600-800 km/h, tsunamis are not a danger to escape easily. However, when earthquakes are considered, the period to increase public awareness and create escape zones is considerably high and usable.

On March 11, 2011 a deadly earthquake of magnitude 9.0 in Richter scale hit Tōhoku Region for 6 minutes. Since the epicenter was approximately 70 km away from the shore and 32 km deep, a tsunami was inevitable. The period that the tsunami waves would hit the shore was estimated as 10 to 30 minutes initially. Even if the waves hit the shore after one hour, the results were devastating. Waves overflowing vertical breakwaters and sea walls of 10 meters high, reaching to 15 meters in some regions created a damage of 300 billion US Dollars and around 20000 casualties. (Wikipedia, 2014). Moreover, as a post event damage, nuclear power plant in Fukushima created a life threat for Japan and it is still questionable.

Even if Japanese authorities created a tsunami warning, it is clear that the warning was not sufficient. The necessary information and caution tips shall be given to the community. To obtain this goal a simple and effective tsunami warning system for a region can be built that is under tsunami threat in case of a seismic event. Even though

property will be lost for sure, it is still possible to retain the lives under danger in case of a tsunami.

In this study, Sea of Marmara is taken as the study area. Since Marmara Region of Turkey is an active earthquake region, has multiple sea basins and contains an important number of population, it comes up as a good candidate for developing a database for earthquake warning system. Although tsunamis are not frequent in this region, historical data reveals that seismic events in the history caused numerous tsunamis happening in the region.

In a possible tsunami in Marmara Sea, from the former studies it can be concluded that the necessary period to evacuate a coastal area is around 15 minutes. A well prepared tsunami simulation can take up to 1 hour. In a metropolitan city like İstanbul, giving a warning without information can create chaos.

Study is focusing on to create a simple software that takes simple inputs from the initial data obtained from reliable sources, compare it with the already simulated possible tsunamis with the numerical modeling software NAMI DANCE and warn authorities about the severity of the ongoing event. Simulating the possible events are the most time consuming phase in this chain. Thus, a database is necessary containing the results this pre-processed simulations which are constructed with respect to the historical events.

Following chapters are put in order to give a literature survey about the problem in Chapter 2, presenting the theory of tsunamis and creating the scenarios to be simulated in Chapter 3. In Chapter 4, results of the simulations are discussed and in Chapter 5 a broad discussion is given.

CHAPTER 2

LITERATURE SURVEY

The Sea of Marmara is located in the Marmara Region of Turkey, connecting the Black Sea and the Aegean Sea by the Strait of Çanakkale and the Bosphorus of İstanbul. Including İstanbul, this region is a home for over 20 million citizens. Along the coastline, seven cities take place of eleven cities in the region. The industry and trade capitals of Turkey are the main important zones in the region which are İstanbul and Kocaeli. İzmit Bay contains numerous commercial ports, power plants and sea structures. Being the historical capital of Ottoman Empire, Byzantine Empire and East Rome for a period, İstanbul has a great importance of cultural heritage. With 17 million people living in the city and a considerable number at the coastline, any earthquake based tsunami will create a threat.

In order to discuss the possible danger in this region due to tsunami phenomenon, the bathymetry and the tectonic characteristics of the region shall be understood. Following sections contain information about these characteristics, historical data and information about modelling.

2.1 Tectonic Characteristics of the Marmara Region

Turkey is under the influence of more than one seismic faults, the most important being the North Anatolian Fault (NAF) which is a major continental strike slip fault and creates the dextral motion between the Anatolian and Black Sea blocks as a result of the collision between the Arabian and Eurasian plates. (Barka and Kadinsky-Cade, 1988; McClusky et al., 2000). The connection between the Gulf of Corinth in the west

and east of Turkey is linked by this fault. In the 20th century. This fault created 11 large earthquakes having magnitudes more than 6.7 in Richter scale. In August 1999, an earthquake of 7.4 in magnitude in İzmit exhibited a right lateral strike slip faulting on fault length about 120 km (Burka et al., 2002; Delouis et al., 2002; Michel and Avouac, 2002). Focal mechanisms that are observed shows a dextral strike slip faulting when the surface ruptures are analyzed (Barka and Kadinsky-Cade, 1988)

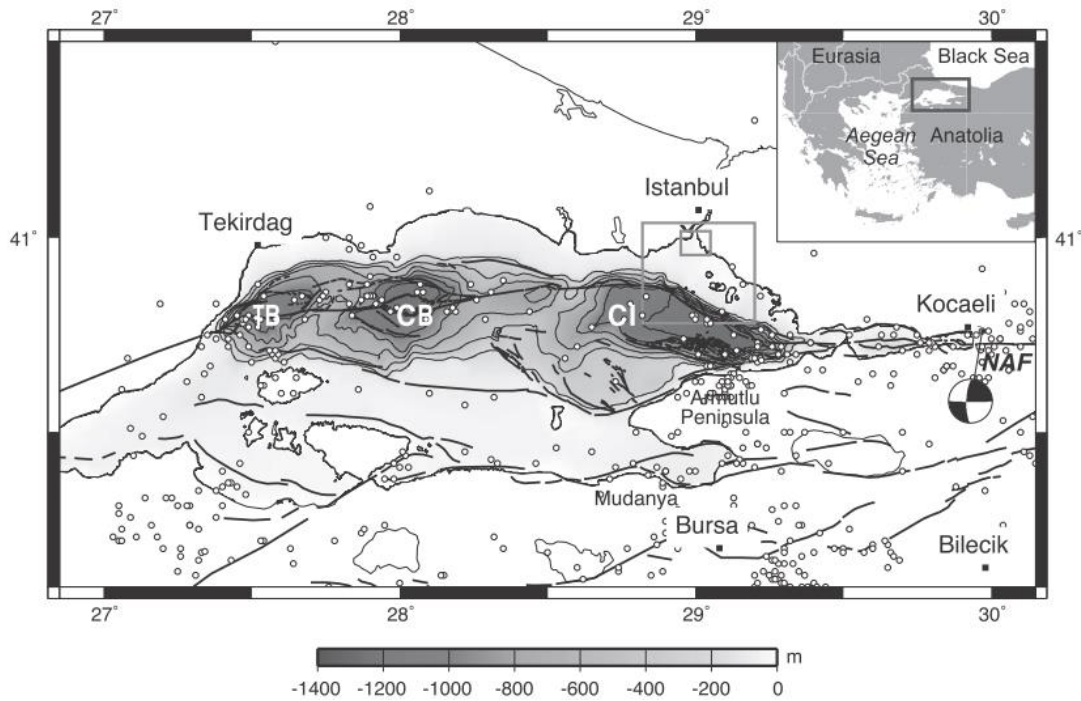


Figure 2.1 Description of the Sea of Marmara with bathymetric data, ‘o’ points for seismicity.

As seen in Figure 2.1, the Sea of Marmara is consisting of past seismic activity and branches of faults. The NAF divides into branches in the Marmara Sea as can be seen in the figure and then enters the northern Aegean region. In the history, the seismicity in this area is found to be high considering especially the northern branch of the NAF. In 1509, 1766, 1776, 1819, 1894 and 1912 earthquakes having magnitudes more than 7.0 were experienced before 1999.

The 1999 earthquakes enabled scientists to retrieve new and useful data about the region. However, they all showed high probability of an earthquake happening offshore and close to İstanbul. As future earthquakes are expected to break segments

of the emerged NAF, tsunami generation generated by seafloor displacement and landslides shall be considered.

2.2 Historical Tsunamis in the Sea of Marmara

When historical data are observed, it can clearly be concluded that the Marmara Sea have been hit by tsunamis frequently. According to Altinok et al., 2001a, over 40 tsunamis could have occurred in the Marmara Sea between 120 and 1999AD.

NAF is observed as one of the most active faults in the area because of its high stress accumulation during the previous century.

Table 2.1 Earthquakes Occurred between 0-1900 in the Marmara Sea Region, Ambraseys, 2002

	Year	Latitude	Longitude	Ms	General Effects										Region
					1	2	3	4	5	6	7	8	9	10	
1	32	40.5	30.5	7	1	4	2	2	2	0	2	2	0	0	Nicaea
2	68	40.7	30	7.2	1	4	2	2	2	0	2	2	0	0	Nicaea
3	121	40.5	30.1	7.4	1	3	4	3	3	2	2	0	0	0	Nicomedia
4	123	40.3	27.7	7	1	3	1	2	2	0	0	0	0	0	Cyzicus
5	160	40	27.5	7.1	1	3	6	3	2	0	2	2	2	0	Hellespont
6	180	40.6	30.6	7.3	1	4	2	2	3	0	2	0	0	0	Nicomedia
7	268	40.7	29.9	7.3	1	3	3	3	3	0	2	0	0	0	Nicomedia
8	358	40.7	30.2	7.4	1	3	6	3	3	3	2	2	2	2	Izmit
9	362	40.7	30.2	6.8	1	4	3	2	2	0	1	1	0	0	Izmit
10	368	40.5	30.5	6.8	1	4	2	2	2	0	2	1	0	0	Persis
11	368	40.1	27.8	6.8	1	4	1	2	2	0	0	0	0	0	Germe
12	407	40.9	28.7	6.8	2	4	2	2	1	0	1	1	0	0	Hebdomon
13	437	40.8	28.5	6.8	3	4	1	2	1	1	1	1	0	0	Istanbul
14	447	40.7	30.3	7.2	1	3	5	3	3	3	2	2	2	2	Nicomedia
15	460	40.1	27.6	6.9	1	4	3	4	2	2	2	2	2	0	Cyzicus
16	478	40.7	29.8	7.3	2	3	5	3	3	3	2	2	0	1	Helenopolis
17	484	40.5	26.6	7.2	1	3	8	3	3	2	2	2	2	0	Callipolis
18	554	40.7	29.8	6.9	2	4	4	2	2	2	2	1	2	0	Nicomedia
19	557	40.9	28.3	6.9	2	4	3	2	2	2	1	1	0	0	Silivri
20	740	40.7	28.7	7.1	3	4	5	2	3	2	2	2	0	2	Marmara
0	823	0	0	0	0	0	0	0	0	0	0	0	0	0	Panium
21	860	40.8	28.5	6.8	3	4	2	2	1	1	2	1	0	0	Marmara
22	869	40.8	29	7	2	4	1	2	2	1	2	2	0	0	CP

Table 2.1 (Continued)

	Year	Latitude	Longitude	Ms	General Effects										Region
					1	2	3	4	5	6	7	8	9	10	
23	967	40.7	31.5	7.2	1	3	4	3	3	3	2	2	0	0	Bolu
24	989	40.8	28.7	7.2	3	4	3	2	2	2	2	0	0	1	Marmara
25	1063	40.8	27.4	7.4	1	3	5	3	3	3	2	2	0	0	Panio
26	1065	40.4	30	6.8	1	4	2	2	1	0	1	1	0	0	Nicaea
27	1296	40.5	30.5	7	1	4	2	2	2	1	2	2	0	0	Bithynia
28	1343	40.7	27.1	6.9	1	3	6	3	2	2	1	1	0	0	Ganos
29	1343	40.9	28	7	2	4	3	2	2	1	2	0	0	1	Heraclea
30	1354	40.7	27	7.4	1	2	7	3	3	3	2	2	1	0	Hexamili
31	1419	40.4	29.3	7.2	1	4	3	2	3	2	2	0	2	0	Bursa
0	1489	0	0	0	0	0	0	0	0	0	0	0	0	0	Saros?
32	1509	40.9	28.7	7.2	2	2	15	2	2	3	1	2	2	2	CP
33	1556	40.6	28	7.1	1	3	3	3	3	2	0	2	0	0	Gonen
34	1625	40.3	26	7.1	3	4	5	3	0	0	0	2	0	0	Saros
35	1659	40.5	26.4	7.2	2	4	5	2	0	0	0	2	0	0	Saros
36	1672	39.5	26	7	2	4	3	2	2	0	0	2	0	0	Biga
37	1719	40.7	29.8	7.4	1	2	17	3	3	3	2	2	2	0	Izmit
38	1737	40	27	7	1	3	19	3	3	0	1	2	2	0	Biga
39	1752	41.5	26.7	6.8	1	3	17	3	2	2	2	2	2	0	Edirne
40	1754	40.8	29.2	6.8	2	3	9	3	2	2	2	2	0	2	Izmit
41	1766	40.8	29	7.1	2	3	16	2	3	2	2	2	0	1	Marmara
42	1766	40.6	27	7.4	1	2	20	3	3	3	2	2	2	0	Gonas
43	1855	40.1	28.6	7.1	1	2	24	3	3	1	1	2	2	0	Bursa
44	1859	40.3	26.1	6.8	2	3	25	3	1	2	1	2	2	2	Saros
45	1893	40.5	26.2	6.9	2	3	31	3	2	1	1	2	0	1	Saros
46	1894	40.7	29.6	7.3	2	2	81	1	3	3	2	2	2	2	Izmit
47	1912	40.7	27.2	7.3	1	2	99	1	2	2	2	2	1	2	Ganos
48	1912	40.7	27	6.8	1	3	32	1	2	1	1	2	2	0	Ganos
49	1944	39.5	26.5	6.8	2	2	67	1	1	1	1	1	2	0	Edremit
50	1953	40.1	27.4	7.1	1	2	45	1	2	2	2	2	1	0	Gonen

Table 2.1 (Continued)

	Year	Latitude	Longitude	Ms	General Effects										Region
					1	2	3	4	5	6	7	8	9	10	
51	1957	40.7	31	7.1	1	2	81	1	2	2	2	2	1	0	Abant
52	1964	40.1	28.2	6.8	1	2	70	1	1	1	1	1	1	0	Manyas
53	1967	40.7	30.7	7.2	1	2	99	1	3	2	2	2	1	0	Mudurnu
54	1999	40.7	30	7.4	1	1	0	1	3	3	2	2	1	1	Izmit
55	1999	40.8	31.2	7.1	1	1	0	1	2	2	2	1	1	0	Duzce

1, Location: 1, on land; 2, offshore; 3, at sea. 2, Epicentral region: 1, instrumental; 2, well-defined macroseismic; 3, less well defined; 4, adopted. 3, Number of sites used. 4, Magnitude: 1, instrumental; 2, macroseismic $M_s \geq 0.5$; macroseismic $M_s < 0.35$. 5, Maximum effects: 1, considerable damage; 2, heavy damage; 3, destructive, extensive reconstruction, with social and economic repercussions. 6, Loss of life: 1, small; 2, significant; 3, great. 7, Extent of damage: 1, local; 2, widespread. 8, Felt area: 1, small; 2, large. 9, Ground effects: 1, surface faulting; 2, ground failures and landslides. 10, Seismic sea waves: 1, damaging; 2, observed.

As observed in Table 2.1, 55 earthquakes over magnitude of 6.5 happened in the region between 0 – 1900 (Ambraseys, 2002) after 1999 Kocaeli shock and increase of stress on underwater faults directed Parsons et al. (2000) to calculate the probability of an underwater earthquake as $62 \pm 15\%$. This calculation also directs us to the result of encountering a tsunami in the following nearby years are more possible than ever.

The most recent tsunami catalogue for Turkish Coasts has been prepared by Altinok et al. (2011). In this study, all the available past catalogues and documents were traced and re-evaluated based on the guidelines defined in GITEC (Genesis and Impact of Tsunamis on the European Coasts) and TRANSFER (Tsunami Risk and Strategies for the European Region) projects.

According to this catalogue, from 17th century BC to 1999, 35 tsunamis have been occurred in the Marmara Sea. Locations of some of the remarkable tsunamis in Marmara Sea are given below in Figure 2.2.

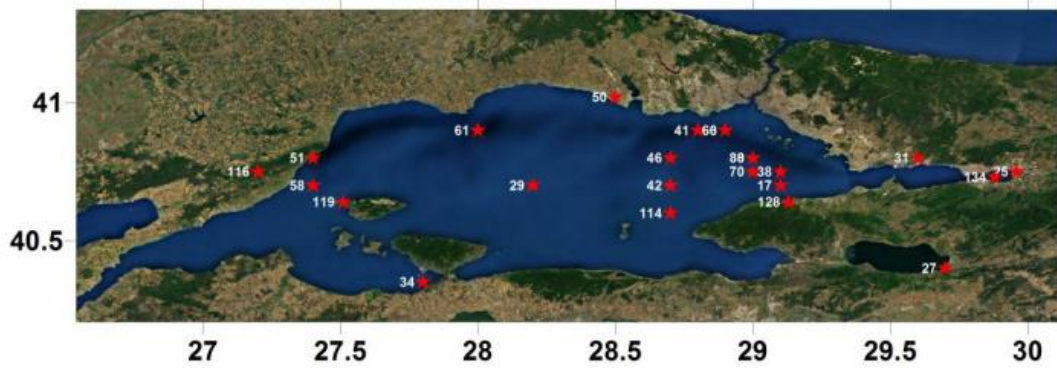


Figure 2.2 Locations of Tsunamigenic Events in Marmara Sea Region (Altinok, 2011, Redrawn)

In 1509 earthquake a big portion of Yenikapı area in İstanbul had been inundated. 500 – 600 meters of mainland was penetrated by the sea. (Altinok et al., 2011) The famous port of the time, Theodosius Port was destroyed by the waves overtopping the breakwater. Overtopping the city walls, waves also inundated the important locations in İstanbul. Moreover, waves assumed to be as 6 meters destroyed the shipyard, castle walls and the city in İzmit. (Oztin and Bayulke, 1991)

Marmaray constructions ended in 2013 revealed a massive amount of archaeological remains from 8000 years ago. Footprints were found dated 6000BC. 37 ships of different dimensions were found of different centuries. Amphora, ceramics and etc. were also other findings of a 45000 item list.

Another tsunami in 1894, July 10th made witnesses to observe 200 meters of penetration from Büyükçekmece to Kartal in İstanbul having run-ups of 2.5 meters. (Yalciner et al., 2002)

According to Altinok et al., 2003 an earthquake with $M_w = 7.3$ took place near Ganos Fault resulting in death of 2000 people. Sea disturbances also caused the sea level rise up to 3 meters and led to damage at the coasts of İstanbul.

Finally in 1999 earthquake of $M_w=7.4$ occurred in northern strand of the NAF (Altinok, 2001) Vertical displacements up to 3 meters have been observed during

detailed field surveys. The international tsunami survey team investigated the area and talked with witnesses. According to their studies, the wave run-up heights measured up to 2.5 meters along the north coast from Tütünçiftlik and Hereke and up to 2.9 meters at Degirmendere and lower values from Degirmendere to Karamursel (Yalciner et al., 2002). More than 300 meters of inundation happened in Kavakli (Altinok et al., 2011).

2.3 Past Attempts of Tsunami Modeling for the Sea of Marmara

The model TWO_LAYER was initiated by Alpar et al. (2001) and Yalciner et al. (2002) and created by Toho Tohoku University Disaster Control Research Centre in Japan. In this model the non-linear long wave equations are solved by using the finite difference method and the leap-frog solution procedure for two interfacing layers; the water body in the sea and the moving mass at the sea bottom.

A scenario of underwater landslides is assumed to occur at the southeast part of Cinarcik Basin, offshore the towns of Yalova and Cinarcik. (Alpar et. al., 2001) The results of the simulation; arrival time of tsunami waves are less than 5 min to southeastern coasts and around 10 min to northern coasts. Flow depth on land will exceed 3m along approximately 15 km of coastline of the northern and southern shores.

Yalciner et al., 2002 simulates two landslide and one earthquake induced tsunami scenarios. According to the results of these simulations, the waves reach the near coasts at approximately 5 min and depending on the source and coastal topography 3-6 m of wave heights occur near the shore. Herbert et. al. (2005) models different scenarios by solving Equation 2.1; conservation of mass and Equation 2.2; conservation of momentum in spherical coordinates using finite difference method with centering in time and using an upwind scheme in space (Heinrich et al., 1998; Hebert et al., 2001a, b).

$$\frac{\partial(\mu+h)}{\partial t} + \nabla[v(\mu + h)] = 0 \quad (\text{Eqn.2.1})$$

$$\frac{\partial(v)}{\partial t} + (v\nabla)v = -g\nabla\mu + \Sigma \quad (\text{Eqn.2.2})$$

They simulate an earthquake that may be occurred in the Eastern Marmara, Cinarcik Basin, for different rake angles. The maximum waves along the coastline ranges between 0.5 – 1 m for rake angles of 180° and 150°, whereas they reach up to 2 m for rake angles of 120° and 90°. Another scenario is an earthquake in the Western Marmara covering Tekirdag and Central Basins. In this case rake angles differ from 120° to 180°. The maximum waves along the coastline ranges between 0.8 – 1 m for rake angle of 120°. Finally they consider the rupture of whole seismic gap with rake angles 120° - 150° and 150° - 180°. The maximum wave heights vary between 0.5 – 2 m.

CHAPTER 3

ESTIMATION OF TSUNAMI SOURCES AND SIMULATIONS

Active faults and corresponding rupture parameters are studied and these studies are presented in this chapter. Geographical data which consists of bathymetry and topography data were gathered and processed in order to use numerical model for understanding tsunami characteristics in the region. Results of simulations conducted by numerical model are given in this chapter.

3.1 Estimation of Source Parameters

Most of the tsunamis happened in the Marmara Sea are originated from earthquakes or earthquake triggered submarine landslides. Thus, in this region the main causes for the tsunami sources can be considered as the displacement of the sea floor by fault rupture and submarine landslides. Since the data acquired shows earthquake induced tsunami sources mostly, submarine landslides are disregarded in this study. Study region was selected as Marmara Sea and the boundaries of the study are shown below in Figure 3.1 Study Domain (Google Earth).



Figure 3.1 Study Domain (Google Earth)

Bathymetric data used in this thesis is derived from the data used in OYO – IMM Report (2007). Original data has the spatial reference of ED_50 3 degrees. However to use in NAMI DANCE, a new projection is used which is WGS 84. Grid size of the bathymetry is 90 meters. This creates 3256 grids in x direction and 984 grids in y direction.

The corner coordinates of the domain are presented in Table 3.1.

Table 3.1 Coordinates of Domain

Spatial Reference	Coordinates (WGS84)	
Longitude	26.542	30.020
Latitude	40.210	41.260

3.1.1 Geological Characteristics of the Sea of Marmara

Northern Marmara is formed of basins extending from east to west in a trough. The basins are named as Çınarcık, Central and Tekirdağ basins respectively from east to west. The maximum depth of these basins are determined to be 1200 m (Yalciner et al., 2002). Moreover, between Tekirdağ and Central Basin, there is the Western High and between Central and Çınarcık Basin, there is the Central High.

Izmit and Ganos faults are located at the eastern and western ends of the trough. Macroscopically, it is considered that the Marmara Sea is a pull-apart basin formed by the extensional step-over between these right-lateral faults (Armijo et al., 2005, Figure 3.2). Moreover, the faulting topography showing the various type of faults (right-lateral fault, normal fault and reverse fault) is observed in the sea floor.

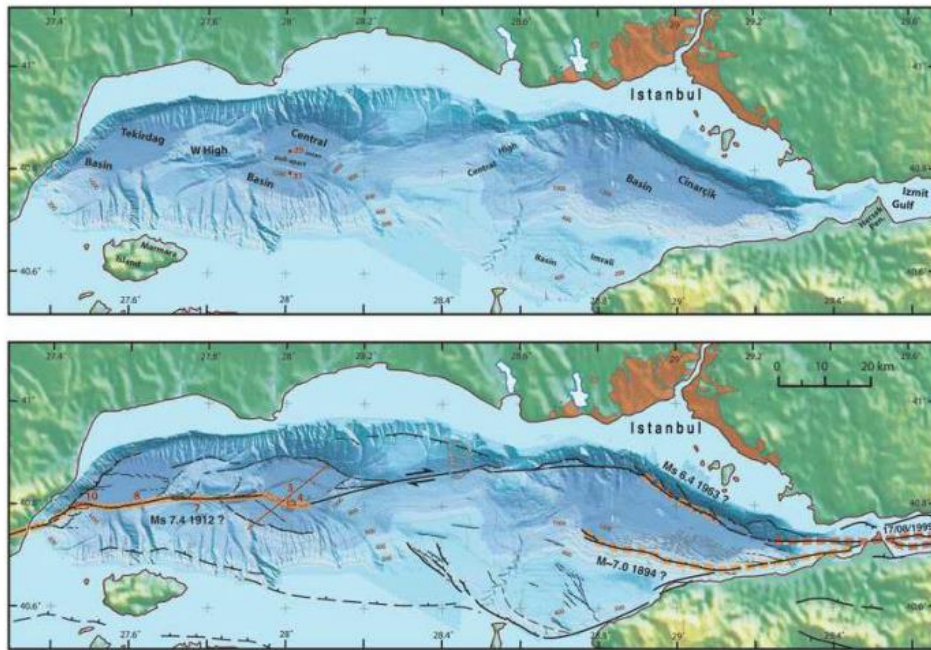


Figure 3.2 The NAF in the Marmara Sea (Armijo et al, 2005 and OYO – IMM, 2007)

Cinarcik Basin is formed by the step-over of Izmit and Prince's Island faults. Another normal fault that completes Izmit and Prince's Island faults is lying on northwest direction.

Along the edges of the Central Basin, normal faults are found. The young inner basin, which is formed due to the extensional step-over between Prince's Islands and the Ganos faults, is covered by the older one while the older outer basin is bounded by the continental shelf slopes.

Unlike Cinarcik and Central basins, Tekirdag basin does not have a step-over structure. However, the Ganos fault is thru the southern edge of the basin. It is estimated that Ganos fault has a right-lateral characteristic, but there is a normal fault portion at the north side and a reverse fault at the southwest.

Since the western part of the Central High and the Western High prolong straight through the narrow valleys, it can be estimated that the faults in these highs are pure right-lateral faults.

Therefore, as a whole, North Anatolian Fault (NAF) in the Marmara Sea shows a right-lateral fault having various features according to the tectonics. During the modeling studies, the features of faults in the Marmara Sea should be carefully considered.

3.1.2 Estimation of Probable Tsunami Source Mechanisms for the Marmara Sea

As mentioned in the previous chapters, earthquake induced tsunamis are investigated in the study. Thus the sources for tsunami are originated from a submarine earthquake.

For this kinds of earthquakes, following parameters are used to define the initial tsunami wave;

- Epicenter
- Focal Depth
- Dip, rake and strike angles
- Width and length of the fault plane
- Vertical displacement of fault

OYO-IMM Report (2007) gives a detailed descriptions of the parameters for sources. The parameters are shown in Figure 3.3.

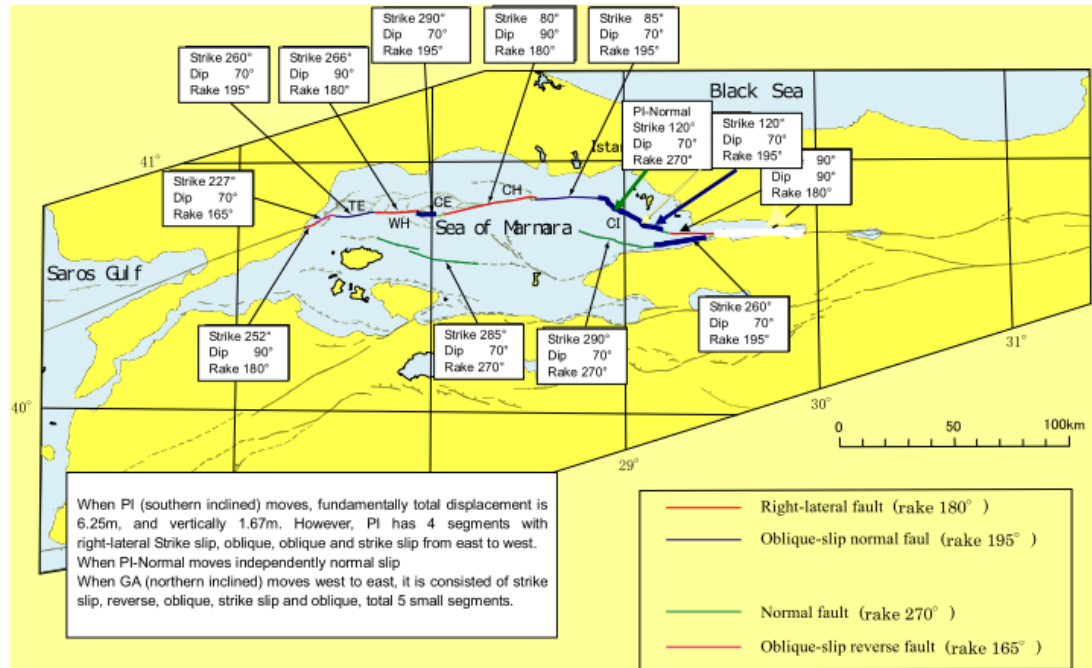


Figure 3.3 Parameters of Selected Sources (OYO – IMM Report, 2007)

Displacement parameter is of great importance and influential on the results. Displacements in OYO – IMM Report (2007) are taken between 1.6-3.0 meters in scenarios according to their segment types. However, in this study this parameter is taken as 5.0 meters assuming there is uncertainty in estimating these parameters.

In this study, parameters are taken according to the parameters that are given in OYO – IMM Report (2007). The faults selected are listed below.

- Prince's Island Fault(PI) – Strike Slip and Normal
- Ganos Fault (GA) – Oblique Normal and Oblique Reverse
- Yalova Fault (YAN) - Normal
- Central Marmara Fault (CMN) – Normal

Parameters and characteristics of the faults are presented in Table 3.2, Table 3.3 and Table 3.4.

In Chapter 3 results with respect to the parameters given in Table 3.4 are presented. However, further simulations are conducted with taking focal depth as 5km. Results of these simulations are presented in APPENDIX B.

Table 3.2 Fault Parameters for PI

Fault	Type	Latitude	Longitude	Depth	Strike	Dip	Rake	Length	Width	Vertical Disp	
		Degree(ED50)	Degree(ED50)	km	degree	degree	degree	km	km	Thesis	OYO - IMM
PI	Right-Lateral	40.72793	29.47313	2.00	84.44	90	180	4.717	16.000	0.00	0.00
		40.733309	29.23572	2.00	92.06	90	180	20.066	16.000	0.00	0.00
		40.733306	29.22818	2.00	90.2	90	180	0.636	16.000	0.00	0.00
	Oblique-Lateral	40.75691	29.12942	2.00	108.15	70	195	8.753	17.027	5.00	1.67
		40.7861	29.06928	2.00	123.15	70	195	6.024	17.027	5.00	1.67
		40.81653	28.99465	2.00	118.85	70	195	7.148	17.027	5.00	1.67
	Oblique-Normal	40.87251	28.90432	2.00	129.9	70	195	9.834	17.027	5.00	1.67
		40.87376	28.87843	2.00	94.37	70	195	2.187	17.027	5.00	1.67
		40.88033	28.75089	2.00	94.66	70	195	10.777	17.027	5.00	1.67
	Right-Lateral	40.87843	28.70595	2.00	87.64	70	195	3.795	18.027	5.00	1.67
		40.87328	28.64466	2.00	84.56	70	195	5.199	17.027	5.00	1.67
		40.86971	28.56006	2.00	87.73	70	195	7.144	17.027	5.00	1.67
	Oblique-Normal	40.87301	28.51766	2.00	96.8	90	180	3.593	16.000	0.00	0.00
		40.87298	28.4716	2.00	90.93	90	180	3.884	16.000	0.00	0.00
		40.8658	28.41844	2.00	80.93	90	180	4.553	16.000	0.00	0.00
	Right-Lateral	40.84761	28.26801	2.00	82.03	90	180	12.847	16.000	0.00	0.00
		40.8042	28.06159	2.00	75.73	90	180	18.074	16.000	0.00	0.00

Table 3.3 Fault Parameters for YAN and GA

Fault	Type	Latitude	Longitude	Depth	Strike	Dip	Rake	Length	Width	Vertical Disp	
		Degree(ED50)	Degree(ED50)	km	degree	degree	degree	km	km	Thesis	OYO - IMM
YAN	Oblique-Normal	40.72115	29.47103	2.00	257.96	70	195	7.058	17.027	5.00	1.67
		40.7075	29.38946	2.00	261.14	70	195	6.873	17.027	5.00	1.67
		40.69751	29.3092	2.00	260.98	70	195	10.952	17.027	5.00	1.67
	Normal	40.68121	29.18143	2.00	262.35	70	270	4.448	17.027	5.00	3.00
		40.6755	29.12936	2.00	273.96	70	270	4.562	17.027	5.00	3.00
		40.67791	29.07551	2.00	283.78	70	270	10.021	17.027	5.00	3.00
		40.69843	28.96007	2.00	294.84	70	270	3.154	17.027	5.00	3.00
		40.71005	28.92602	2.00	284.9	70	270	14.043	17.027	5.00	3.00
		40.8042	28.06159	2.00	263.3	70	195	2.143	17.027	5.00	1.67
		40.80152	28.03644	2.00	286.31	70	195	8.664	17.027	5.00	1.67
GA	Oblique-Normal	40.8217	27.93729	2.00	266.61	90	180	9.516	16.000	5.00	0.00
		40.71458	27.82494	2.00	271.96	90	180	10.494	16.000	5.00	0.00
	Oblique-Normal	40.8154	27.70062	2.00	260.87	70	195	12.441	17.027	0.00	1.67
	Oblique-Reverse	40.79464	27.55582	2.00	278.58	70	195	5.660	17.027	0.00	1.67
		40.80081	27.48929	2.00	258.14	70	165	3.046	17.027	0.00	1.67
	Right-Lateral	40.79441	27.45422	2.00	238.95	70	165	6.945	17.027	0.00	1.67
		40.76061	27.38506	2.00	257.18	90	180	4.519	16.000	0.00	0.00

Table 3.4 Fault Parameters for PIN and CMN

Fault	Type	Latitude	Longitude	Depth	Strike	Dip	Rake	Length	Width	Vertical Disp	
		Degree(ED50)	Degree(ED50)	km	degree	degree	degree	meters	meters	Thesis	OYO - IMM
PIN	Normal	40.75691	29.12942	2.00	108.15	70	270	8.753	17.027	5.00	3.00
		40.7861	29.06928	2.00	123.15	70	270	6.024	17.027	5.00	3.00
		40.81653	28.99465	2.00	118.85	70	270	7.148	17.027	5.00	3.00
		40.87251	28.90432	2.00	129.9	70	270	9.834	17.027	5.00	3.00
CMN	Normal	40.6755	29.12936	2.00	273.96	70	270	4.562	17.027	5.00	2.00
		40.67791	29.07551	2.00	283.78	70	270	10.021	17.027	5.00	2.00
		40.69843	28.96007	2.00	294.84	70	270	3.154	17.027	5.00	2.00
		40.71005	28.92602	2.00	284.9	70	270	14.043	17.027	5.00	2.00
		40.8042	28.06159	2.00	263.3	70	195	2.143	17.027	5.00	2.00

3.2 Tsunami Simulations for the Marmara Sea Region

Numerical simulations are conducted in this study to understand tsunami generation, propagation, coastal amplification and characteristics in the selected region.

Tsunami simulations are conducted using a numerical model named NAMIDANCE. In order to set the model up reliable tsunami genic data with accurate and reliable bathymetric data are needed. In determination of rupture parameters which are used as inputs for modelling studies, a conservative approach is necessary since the knowledge and information on rupture parameters are limited.

3.2.1 NAMI DANCE – Tsunami Numerical Modeling Code

Tsunami numerical models generally solve different forms of Navier-Stokes equations. The main equations used in NAMIDANCE, tsunami numerical modelling code used in this study, are non-linear shallow water equations with friction term which requires less computer memory decreasing computation duration. Moreover, it provides the results in acceptable error limit. Two dimensional non-linear shallow water equations are given below;

$$\frac{\partial \eta}{\partial t} + \frac{\partial M}{\partial x} + \frac{\partial N}{\partial y} = 0$$

$$\frac{\partial M}{\partial t} + \frac{\partial}{\partial x} \left(\frac{M^2}{D} \right) + \frac{\partial}{\partial y} \left(\frac{MN}{D} \right) + gD \frac{\partial \eta}{\partial x} + \frac{k}{2gD^2} M \sqrt{(M^2 + N^2)} = 0$$

$$\frac{\partial N}{\partial t} + \frac{\partial}{\partial x} \left(\frac{MN}{D} \right) + \frac{\partial}{\partial y} \left(\frac{N^2}{D} \right) + gD \frac{\partial \eta}{\partial y} + \frac{k}{2gD^2} N \sqrt{(M^2 + N^2)} = 0$$

Where;

η = water surface fluctuation

M & N = discharge fluxes in X & Y directions

D = total water depth

h = undisturbed basin

k = bottom friction coefficient

In this study, the computational tool NAMI DANCE is used in numerical modeling based on the solution of two dimensional nonlinear shallow water equations by finite difference method considering to related initial and boundary conditions. The numerical model was developed by Zaytsev, Yalciner, Pelinovsky, Chernov in C++ programming language by following leap frog scheme numerical solution procedures given by Shuto et al., 1990.

3.2.2 Scenarios Used in Simulations in the Sea of Marmara

In this thesis seismic sources are used in order to conduct simulations. By using the fault rupture parameters given in Table 3.2, Table 3.3 and Table 3.4, first tsunami wave form is calculated around the segments of rupture. After this step, tsunami sources are processed by NAMI DANCE for the selected scenarios.

In scope of this thesis six scenarios are simulated in single domain, based on the selection of main active faults, setting rupture parameters, and geographical data with sufficient resolution. The selected scenarios due to the main active faults are listed below;

- PI: Prince's Islands Fault (Oblique – Normal)
- PIN: Prince's Islands Fault (Normal)
- GA: Ganos Fault (Oblique-Normal and Oblique Reserve)
- YAN: Yalova Fault (Oblique-Normal and Normal)
- CMN: Central Marmara Fault (Normal)
- PI+GA

For every scenario, inputs and results of the simulations are given in next sections. In Marmara Sea, 82 gauges are studied and 12 of them are selected to demonstrate the arrival times of the waves and their amplitudes. Studied and the selected gauges are given in Figure 3.4. The names and coordinates of the selected gauges are shown in Table 3.5.

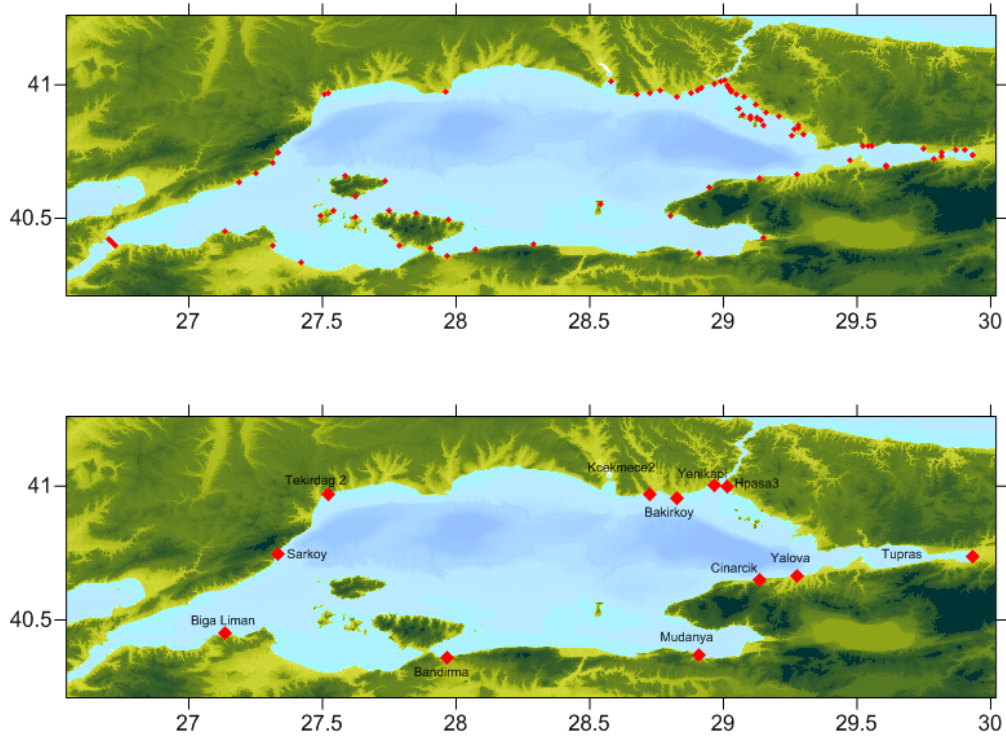


Figure 3.4 Studied and Selected Gauges in the Domain

Table 3.5 Names and Coordinates of the Selected Gauges

GAUGE	LONGITUDE	LATITUDE	DEPTH
BAKIRKOY	28.8262	40.9528	9.0
BANDIRMA	27.9683	40.3606	6.6
BIGALIMAN	27.1359	40.4516	3.9
CINARCIK	29.136	40.6515	4.8
HPASA3	29.0148	40.9957	9.1
KCEKMECE2	28.7238	40.9693	5.9
MUDANYA	28.9089	40.3675	8.4
SARKOY	27.3361	40.7449	5.3
TEKIRDAG2	27.5197	40.9711	9.5
TUPRAS	29.935	40.7372	8.3
YALOVA	29.2769	40.6634	8.1
YENIKAPI	28.9665	41.0018	9.7

3.2.2.1 Simulation of Source PI

PI fault which is on the North Marmara branch of the NAF (North Anatolian Fault) is assumed to be ruptured. Since PI fault is composed of 17 segments, all these segments are considered to be broken. These segments are composed of eight right lateral faults, four oblique-lateral and five oblique normal faults. Right lateral faults cause the generated waves to have small amplifications. Figure 3.5 demonstrates the tsunami source for PI.

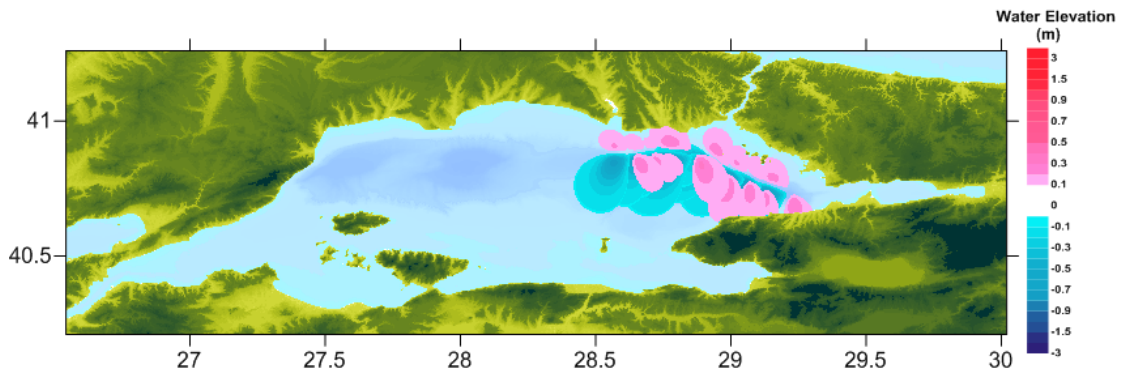


Figure 3.5 Tsunami Source for PI

Sea states for 10, 30, 60 and 90 minutes are given in Figure 3.6 for PI source. Figure 3.7 shows the maximum positive and maximum negative wave amplitudes in the domain. The values for maximum positive and maximum negative tsunami wave amplitudes are +3.0m and -4.5m respectively. Run-up distribution is also presented in Figure 3.8.

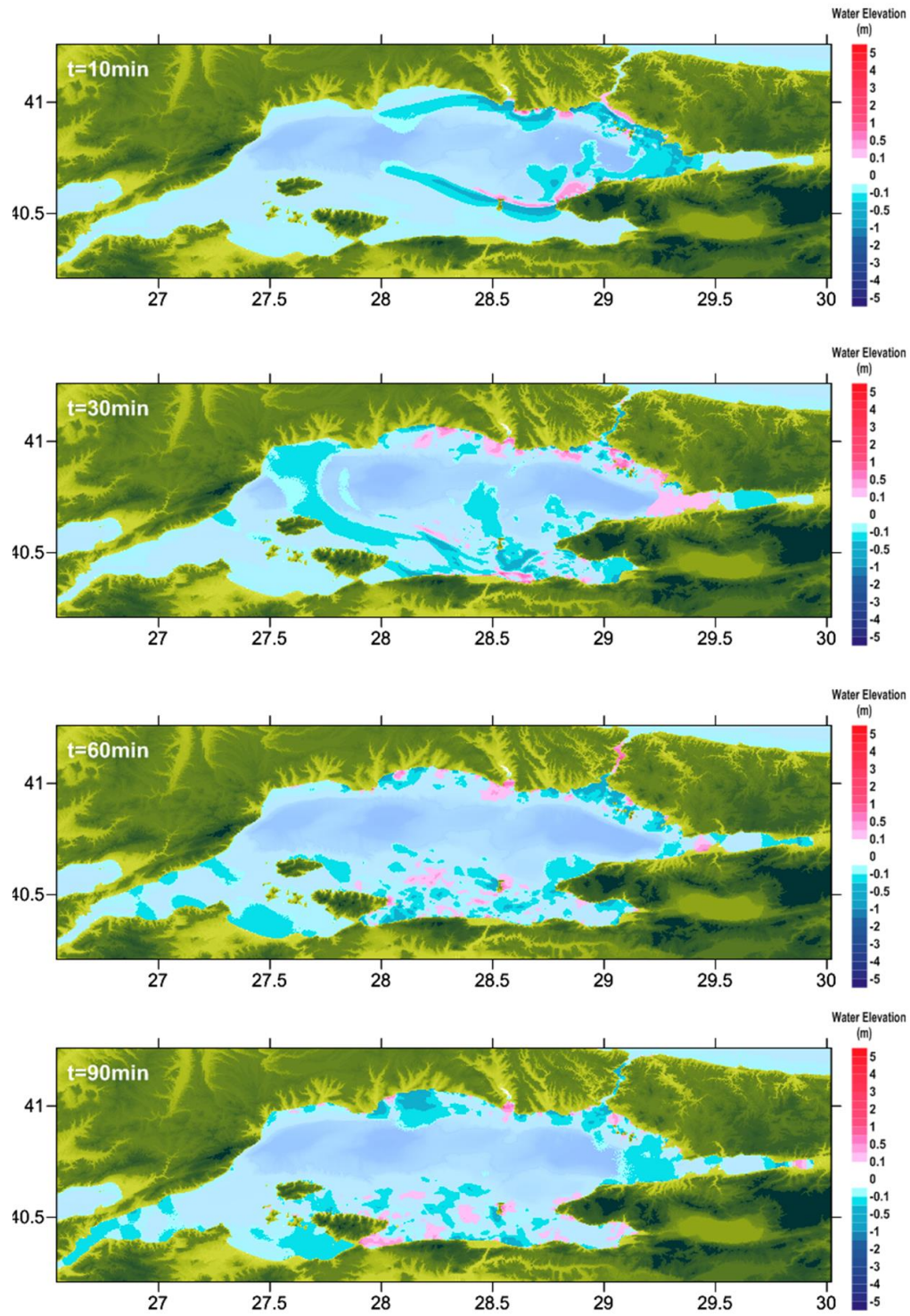


Figure 3.6 Sea states at $t=10, 30, 60$, and 90 min respectively according to the tsunami source PI

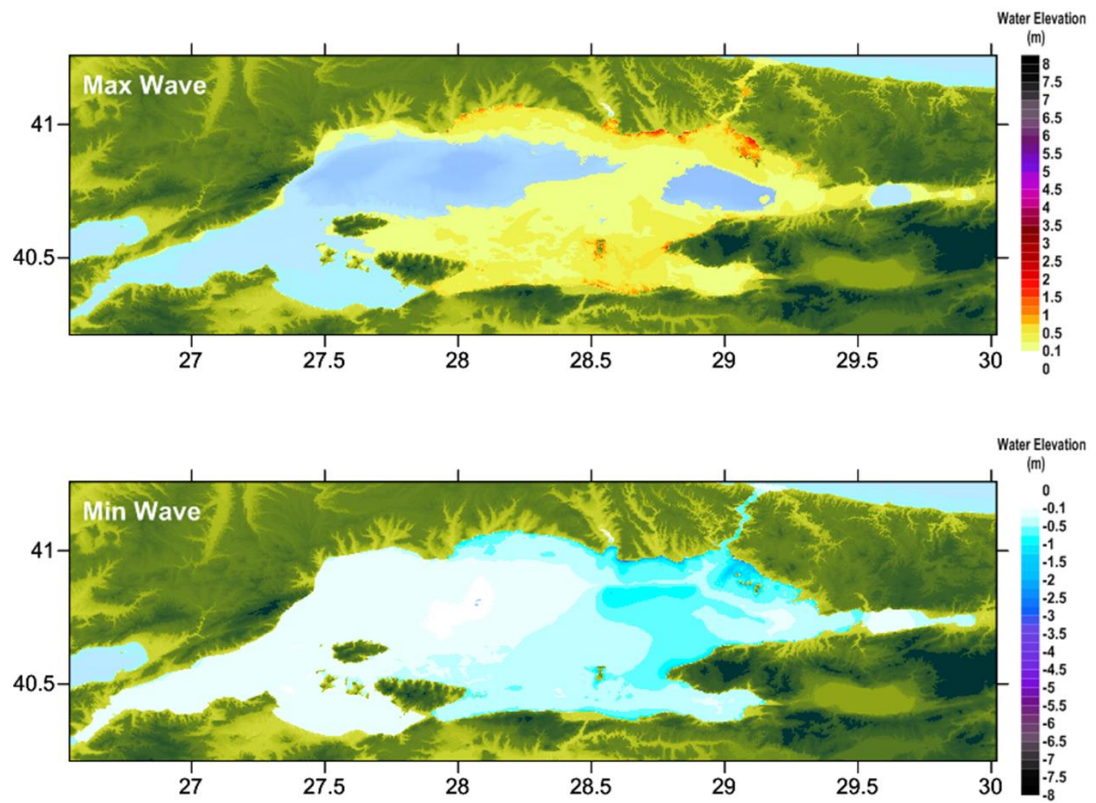


Figure 3.7 Distribution of Maximum (+) Wave Amplitude (top) and Minimum (-) Wave Amplitudes

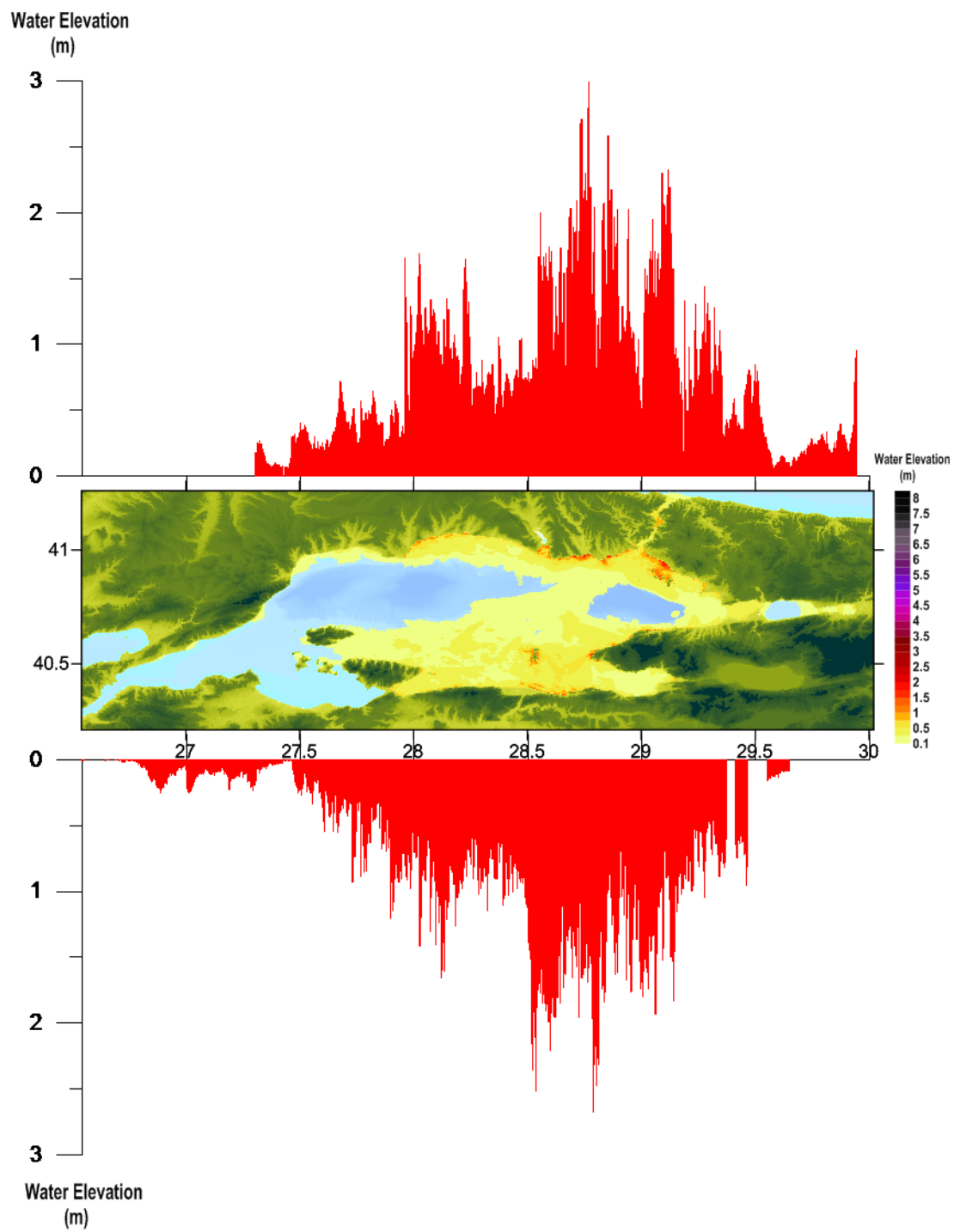


Figure 3.8 Run-up Distribution According to the Tsunami Source PI

Arrival times of the first and the maximum waves, water surface fluctuations measured at the selected gauges are given in Table 3.6. Time history diagrams of the water level fluctuations at the selected gauges are shown in Figure 3.9.

Table 3.6 Results of PI Simulation at the Selected Gauge Points

Name of gauge pt.	Depth at gauge pt.(m)	X	Y	Arrival time of initial wave (min)	Arrival time of max.wave (min)	Maximum (+) wave amp.(m)	Maximum (-) wave amp.(m)
Bakirkoy	9.0	28.826200	40.952800	0	21	1.1	-1.5
Bandirma	6.6	27.968300	40.360600	35	85	0.7	-0.6
BigaLiman	3.9	27.135900	40.451600	40	80	0.1	-0.3
Cinarcik	4.8	29.136000	40.651500	1	10	1.1	-1.3
Hpasa3	9.1	29.014800	40.995700	0	76	0.8	-1.0
Kcekmece2	5.9	28.723800	40.969300	0	15	1.4	-1.9
Mudanya	8.4	28.908900	40.367500	3	30	0.5	-0.5
Sarkoy	5.3	27.336100	40.744900	19	85	0.1	-0.3
Tekirdag2	9.5	27.519700	40.971100	20	82	0.3	-0.3
Tupras	8.3	29.935000	40.737200	43	85	0.3	-0.4
Yalova	8.1	29.276900	40.663400	0	29	0.5	-0.6
Yenikapi	9.7	28.966500	41.001800	0	27	0.8	-0.7

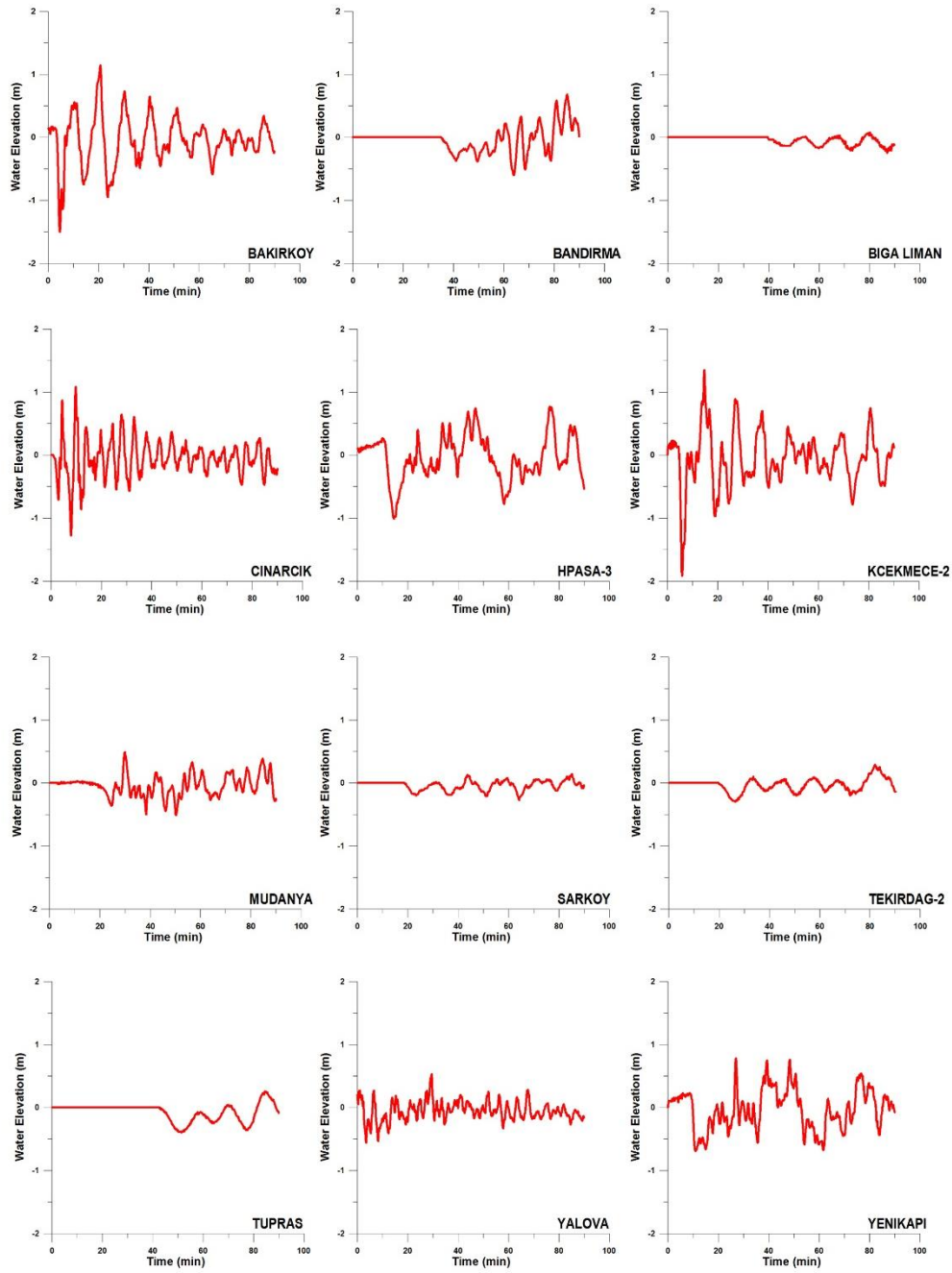


Figure 3.9 Time Histories of Water Surface Fluctuations at the Selected Gauge Locations for PI

From Table 3.6 and Figure 3.9 it is seen that the first wave arrives at İstanbul coasts immediately. A maximum amplitude of 1.4m and a maximum negative amplitude of -1.9m at Küçükçekmece gauge is observed (Kcekmece2)

PI source causes rather small amplitudes in eastern and western coasts of the Marmara Sea. Although in Cinarcik gauge a maximum positive amplitude of 1.1m and a maximum negative amplitude of -1.3m are observed, since the İzmit Bay is naturally protected the amplitudes are not high. However, further studies of wave oscillation should be conducted for this area.

3.2.2.2 Simulation of Source PIN

PIN source is the normal form of the first four oblique-normal segments of tsunami source PI. In the simulation of source PIN, it is assumed that the entire fault has been ruptured and they are all broken. PIN source can be seen in Figure 3.10.

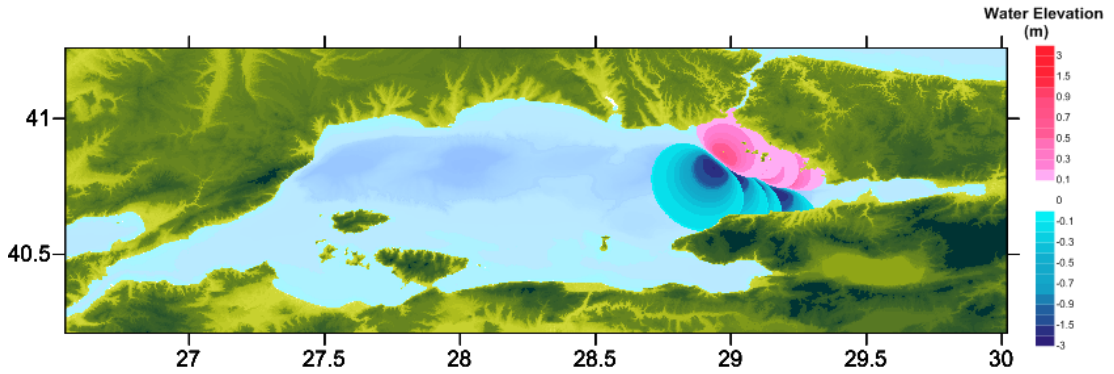


Figure 3.10 Tsunami Source for PIN

Sea states for 10, 30, 60 and 90 minutes are given in Figure 3.11 for PI source. Figure 3.12 shows the maximum positive and maximum negative wave amplitudes in the domain. The values for maximum positive and maximum negative tsunami wave amplitudes are +9.4m and -10.6m respectively. Run-up distribution is also presented in Figure 3.13.

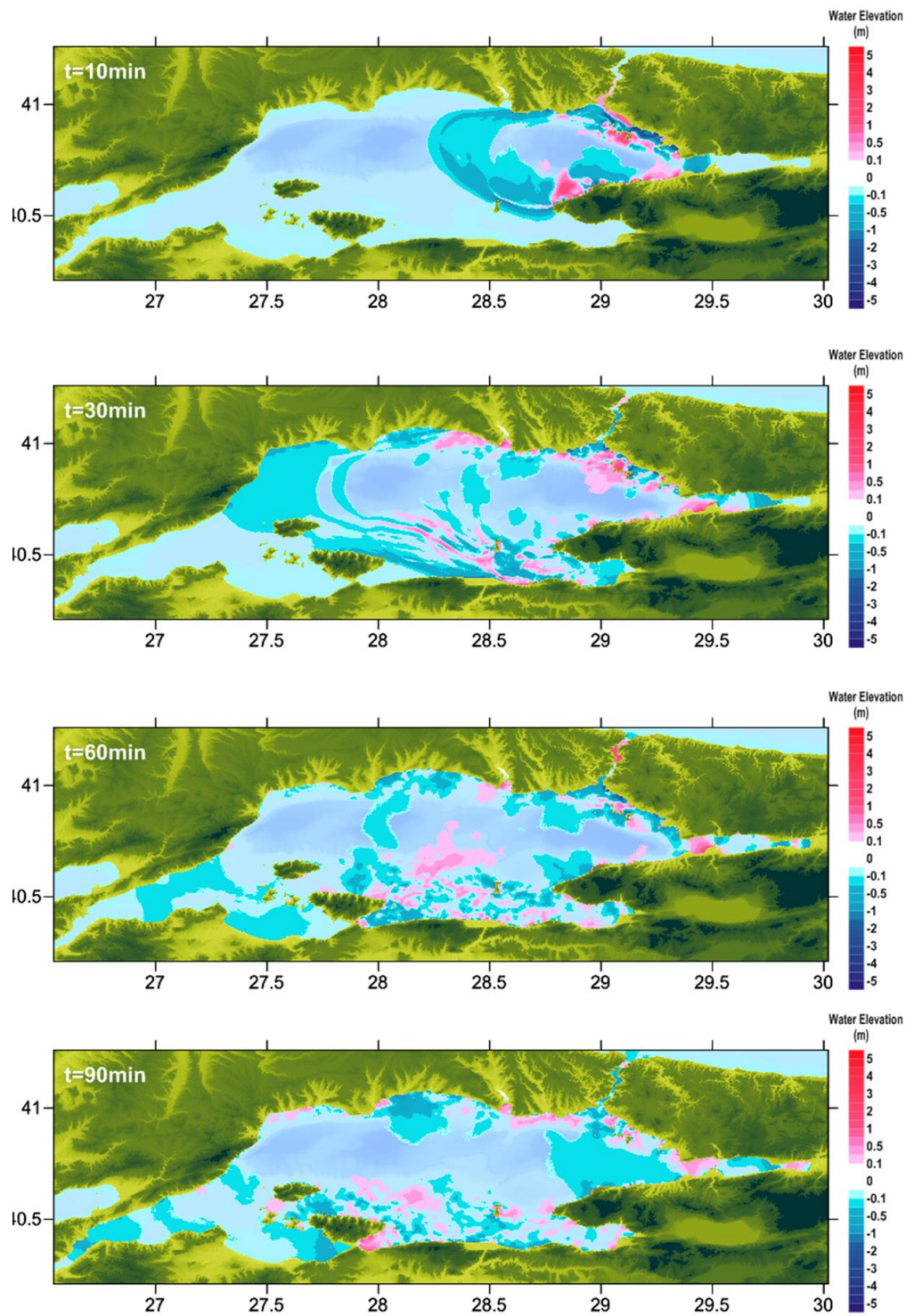


Figure 3.11 Sea states at $t=10, 30, 60$, and 90 min respectively according to the tsunami source PIN

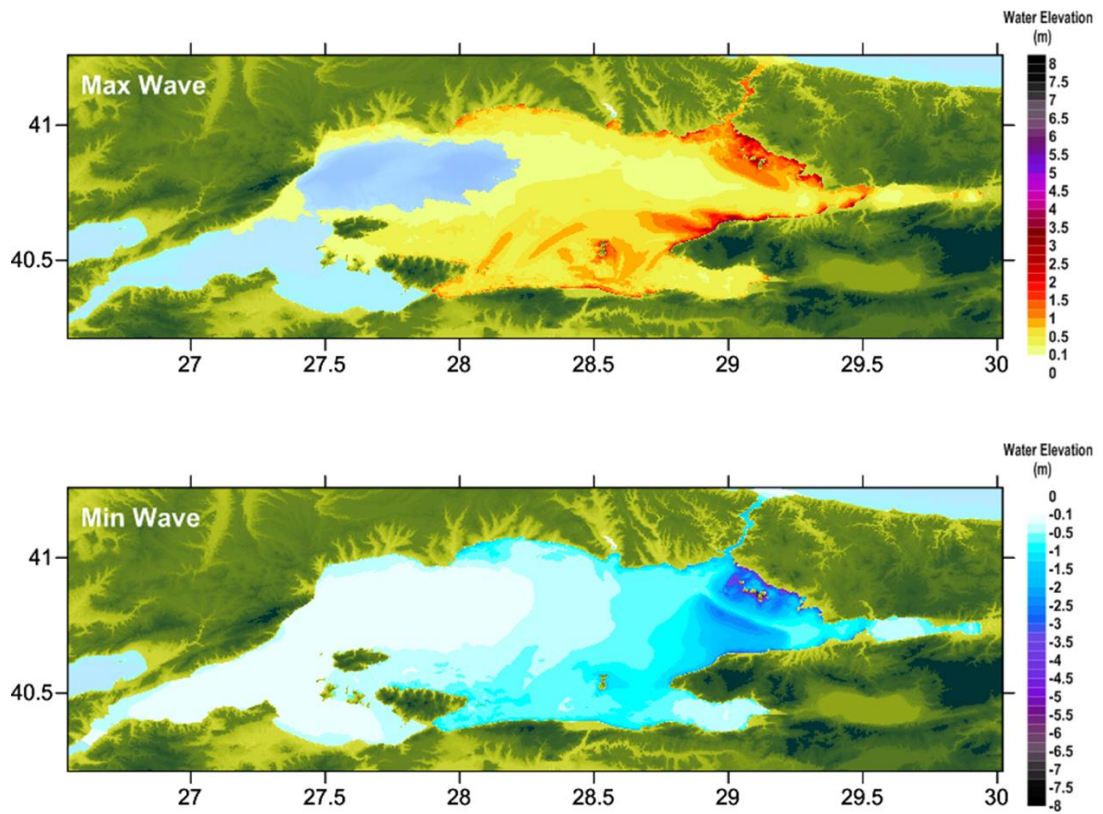


Figure 3.12 Distribution of Maximum (+) Wave Amplitude (top) and Minimum (-) Wave Amplitudes

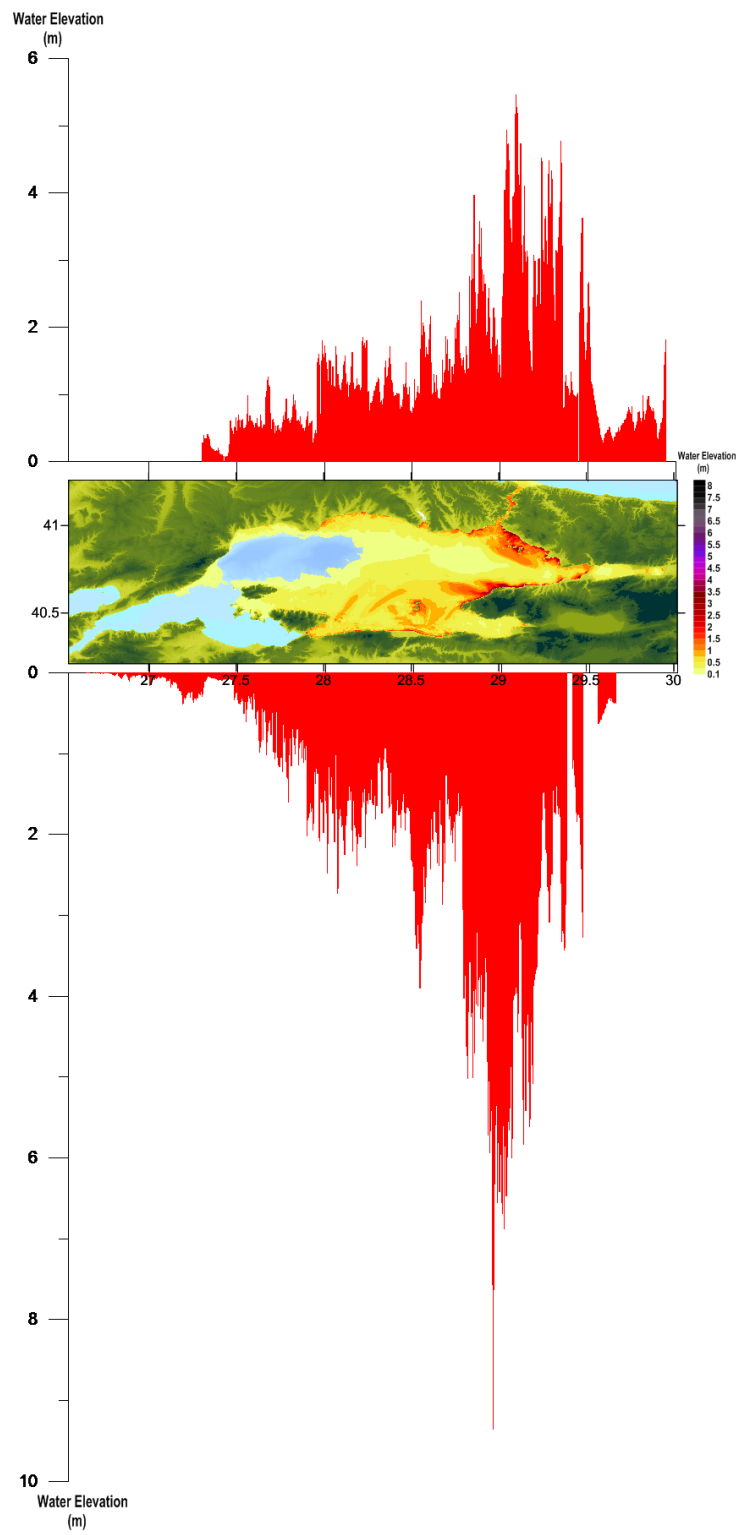


Figure 3.13 Run-up Distribution According to the Tsunami Source PIN

Arrival times of the first and the maximum waves, water surface fluctuations measured at the selected gauges are given in Table 3.7. Time history diagrams of the water level fluctuations at the selected gauges are shown in Figure 3.14.

Table 3.7 Results of PIN Simulation at the Selected Gauge Points

Name of gauge pt.	Depth at gauge pt.(m)	X	Y	Arrival time of initial wave (min)	Arrival time of max.wave (min)	Maximum (+) wave amp.(m)	Maximum (-) wave amp.(m)
Bakirkoy	9.0	28.826200	40.952800	0	22	1.3	-1.3
Bandirma	6.6	27.968300	40.360600	42	84	1.1	-1.1
BigaLiman	3.9	27.135900	40.451600	45	83	0.1	-0.3
Cinarcik	4.8	29.136000	40.651500	0	4	4.1	-3.4
Hpasa3	9.1	29.014800	40.995700	0	37	1.8	-2.0
Kcekmece2	5.9	28.723800	40.969300	2	17	1.0	-1.4
Mudanya	8.4	28.908900	40.367500	1	82	0.6	-0.7
Sarkoy	5.3	27.336100	40.744900	24	81	0.3	-0.3
Tekirdag2	9.5	27.519700	40.971100	25	46	0.3	-0.5
Tupras	8.3	29.935000	40.737200	28	78	0.5	-0.8
Yalova	8.1	29.276900	40.663400	0	9	1.8	-1.2
Yenikapi	9.7	28.966500	41.001800	0	27	1.3	-1.4

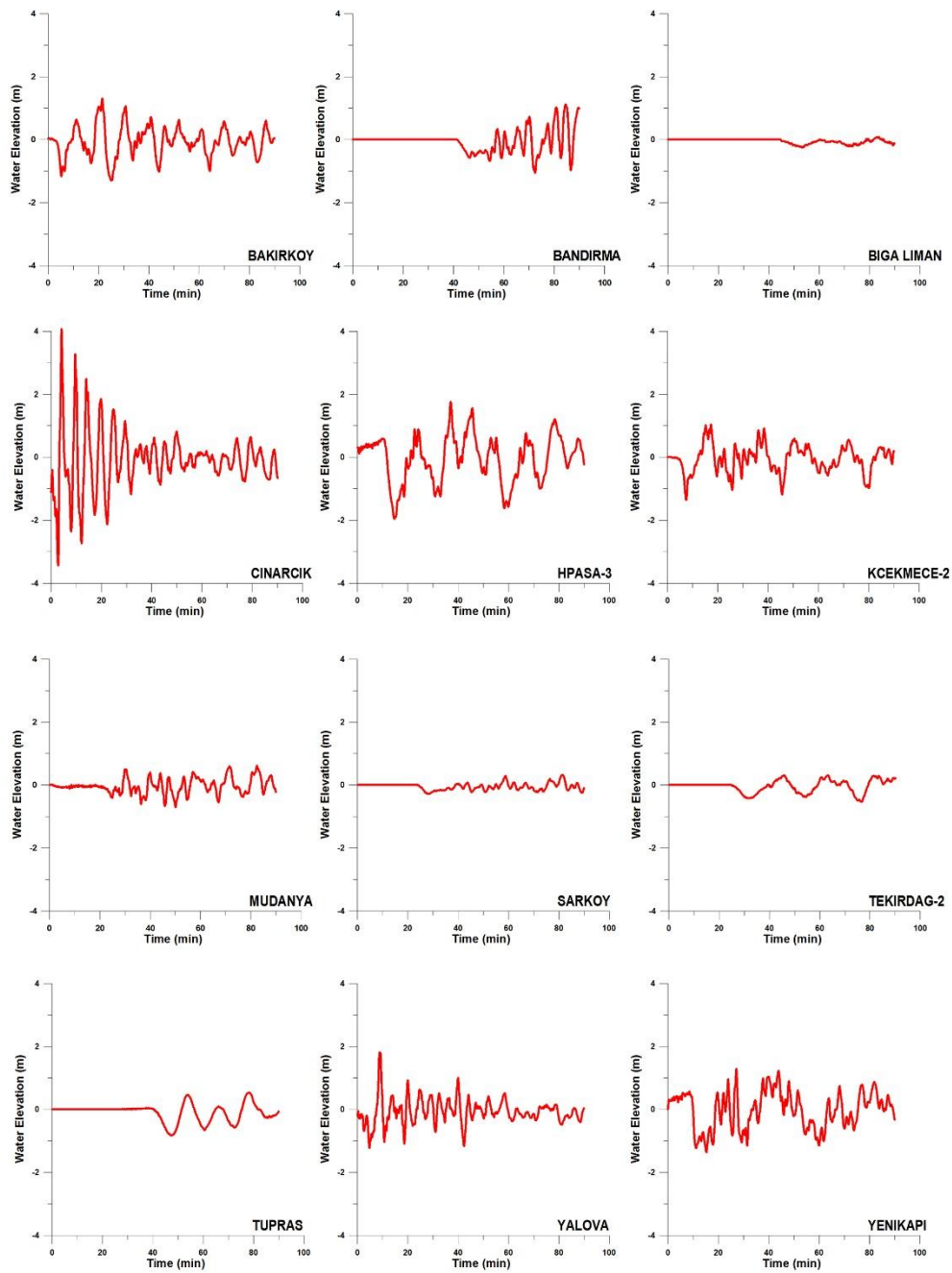


Figure 3.14 Time Histories of Water Surface Fluctuations at the Selected Gauge Locations for PIN

From Table 3.7 and Figure 3.14 it is seen that the first wave arrives at İstanbul coasts immediately with amplitude around 1m. A maximum amplitude of 1.8m and a maximum negative amplitude of -2.0m at Haydarpaşa gauge is observed (Hpasa3)

As PI source, PIN source also causes rather small amplitudes in western coasts of the Marmara Sea. Although again in Cinarcik gauge a maximum positive amplitude of 4.1m and a maximum negative amplitude of -3.4m are observed. Since the İzmit Bay is naturally protected the amplitudes are not high. However, further studies of wave oscillation should be conducted for this area.

3.2.2.3 Simulation of Source PI + GA

For PI+GA scenario, the entire north trough is assumed to be ruptured. That means all of the 26 segments are broken. Since eleven of these segments are right-lateral faults, the generated waves due to this segments have small amplitudes with respect to other faults. The source is shown in Figure 3.15.

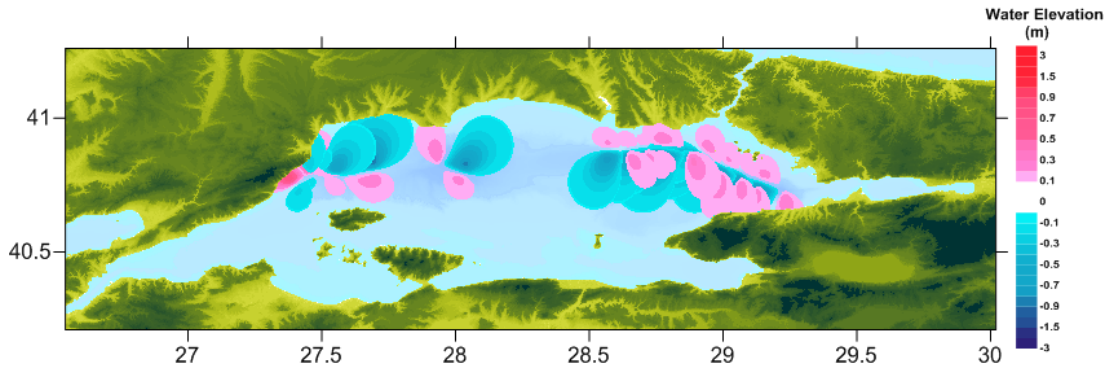


Figure 3.15 Tsunami Source for PI+GA

Sea states for 10, 30, 60 and 90 minutes are given in Figure 3.16 for PI source. Figure 3.17 shows the maximum positive and maximum negative wave amplitudes in the domain. The values for maximum positive and maximum negative tsunami wave amplitudes are +3.5m and -4.5m respectively. Run-up distribution is also presented in Figure 3.18.

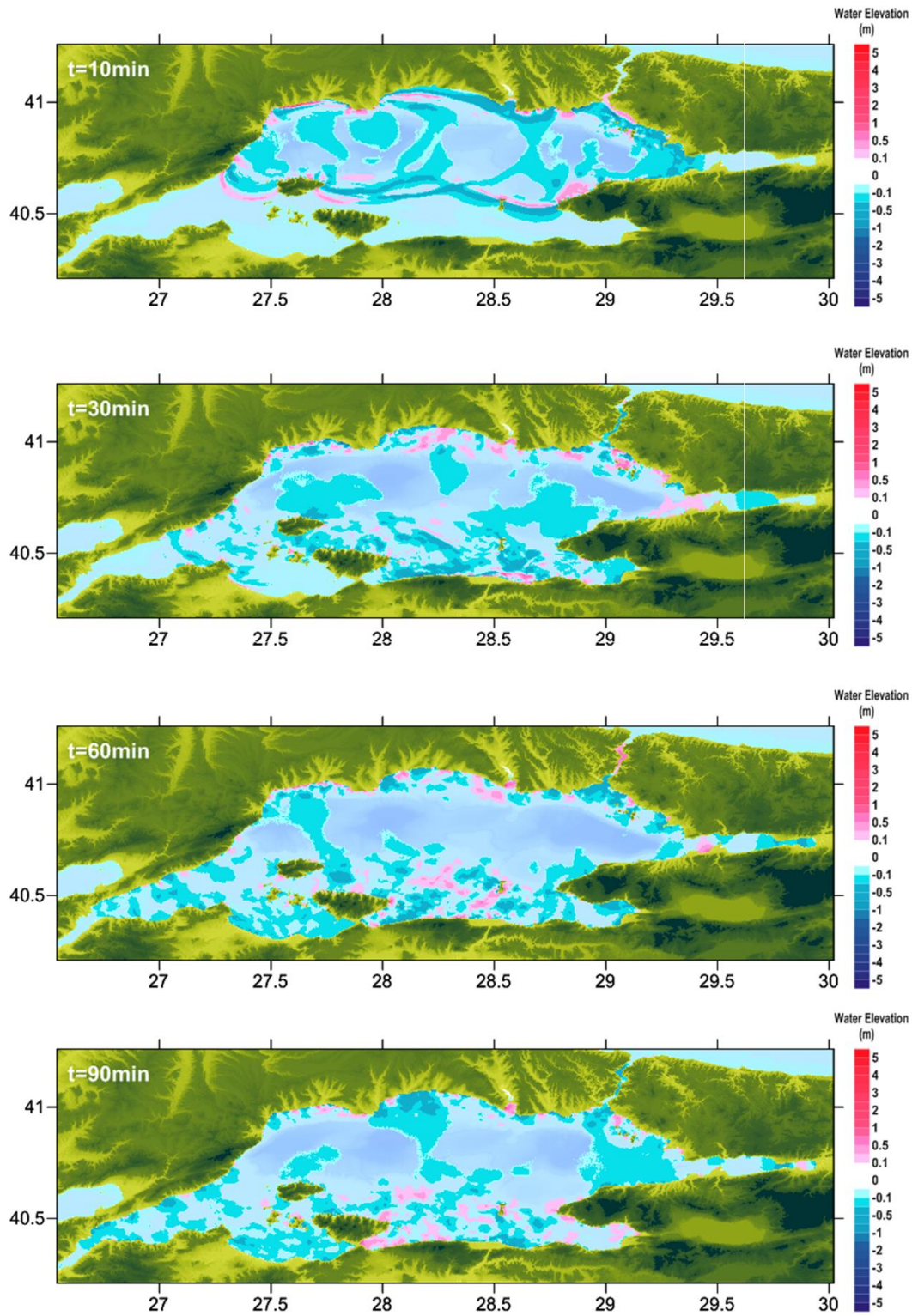


Figure 3.16 Sea states at $t=10, 30, 60$, and 90 min respectively according to the tsunami source PI+GA

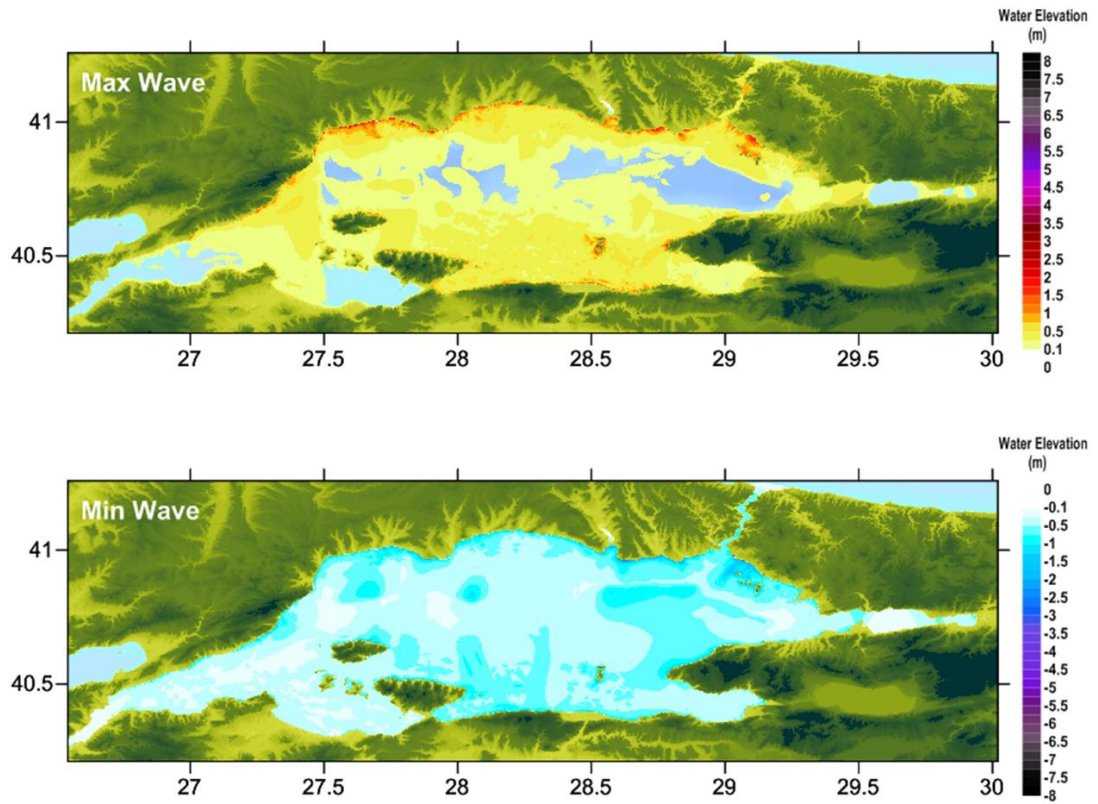


Figure 3.17 Distribution of Maximum (+) Wave Amplitude (top) and Minimum (-) Wave Amplitudes

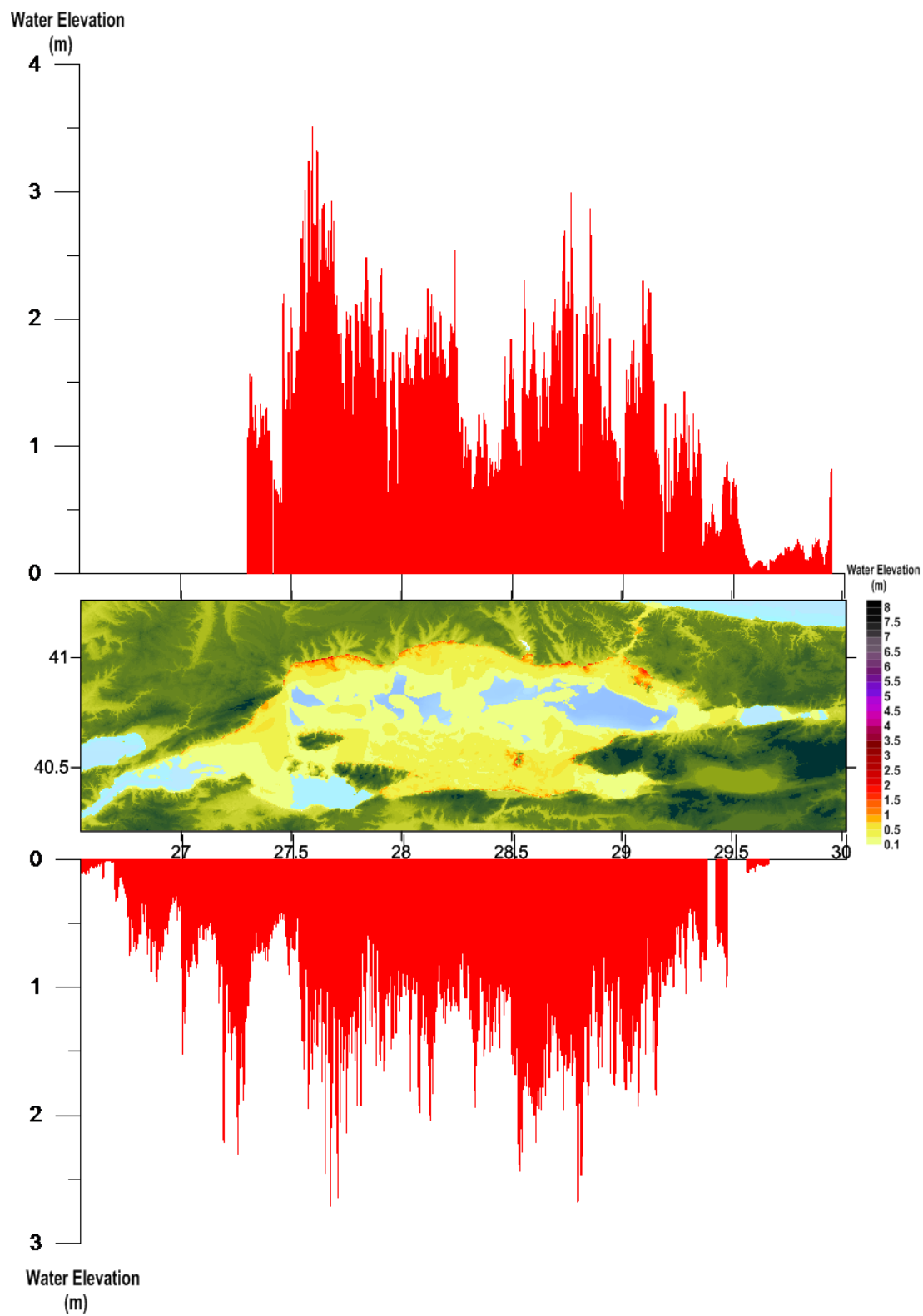


Figure 3.18 Run-up Distribution According to the Tsunami Source PI+GA

Arrival times of the first and the maximum waves, water surface fluctuations measured at the selected gauges are given in Table 3.8. Time history diagrams of the water level fluctuations at the selected gauges are shown in Figure 3.19.

Table 3.8 Results of PI+GA Simulation at the Selected Gauge Points

Name of gauge pt.	Depth at gauge pt.(m)	X	Y	Arrival time of initial wave (min)	Arrival time of max.wave (min)	Maximum (+) wave amp.(m)	Maximum (-) wave amp.(m)
Bakirkoy	9.0	28.826200	40.952800	0	21	1.2	-1.5
Bandirma	6.6	27.968300	40.360600	21	81	0.8	-0.8
BigaLiman	3.9	27.135900	40.451600	7	36	0.5	-0.6
Cinarcik	4.8	29.136000	40.651500	1	10	1.1	-1.3
Hpasa3	9.1	29.014800	40.995700	0	76	0.7	-1.0
Kcekmece2	5.9	28.723800	40.969300	0	12	1.3	-1.4
Mudanya	8.4	28.908900	40.367500	3	30	0.5	-0.6
Sarkoy	5.3	27.336100	40.744900	0	10	1.0	-1.0
Tekirdag2	9.5	27.519700	40.971100	0	12	0.6	-0.8
Tupras	8.3	29.935000	40.737200	43	85	0.1	-0.5
Yalova	8.1	29.276900	40.663400	0	29	0.5	-0.6
Yenikapi	9.7	28.966500	41.001800	0	27	0.8	-0.7

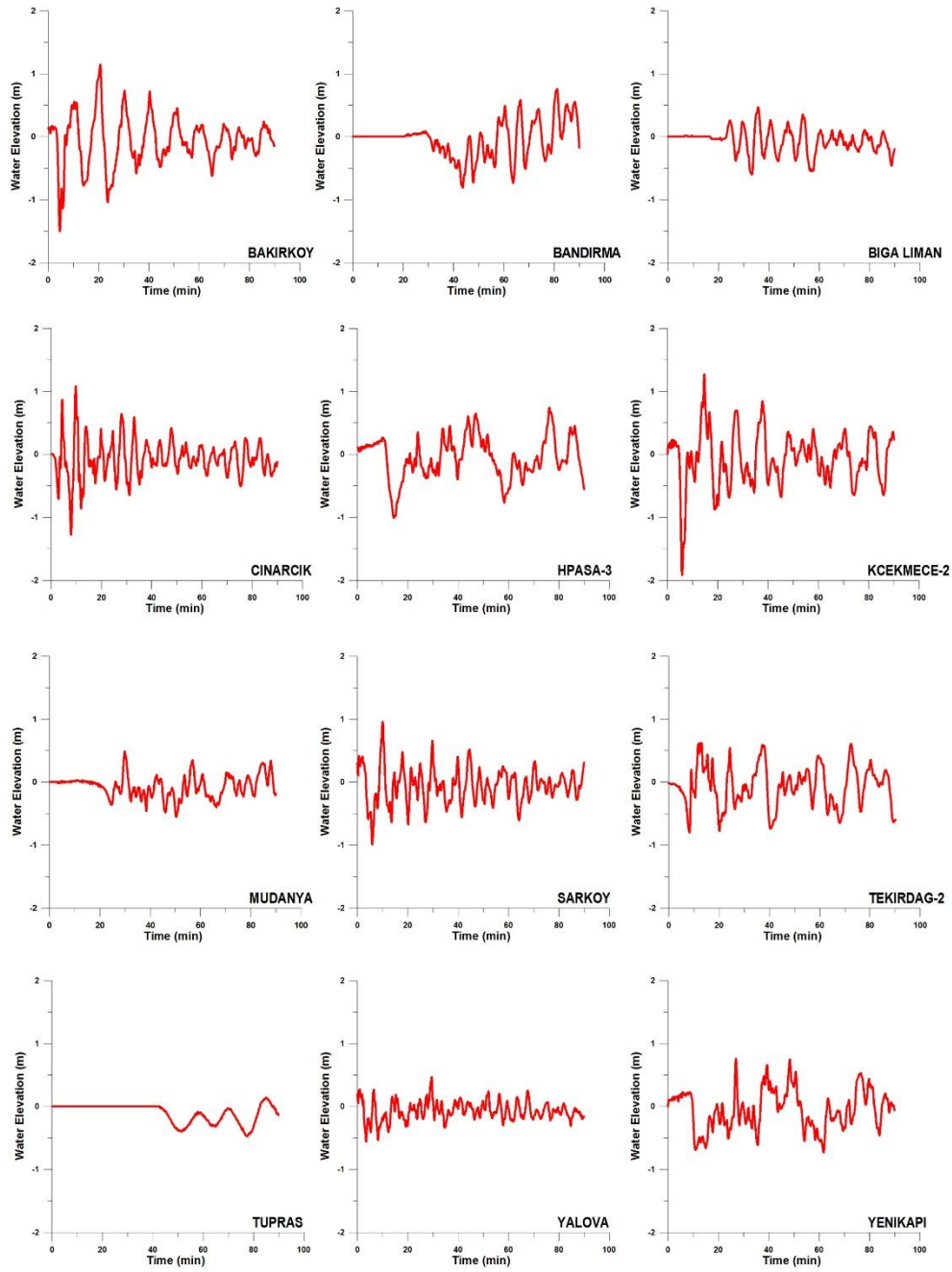


Figure 3.19 Time Histories of Water Surface Fluctuations at the Selected Gauge Locations for PI-GA

From Table 3.8 and Figure 3.19 it is seen that the first wave arrives at İstanbul coasts immediately with amplitude less than 0.5m. A maximum amplitude of 1.3m and a maximum negative amplitude of -1.4m at Küçükçekmece gauge is observed (Kcekmece2)

PI+GA source also produces rather small amplitudes in eastern coasts of the Marmara Sea. In western Marmara Sea, the amplitudes are a little bit larger than former simulations. At Sarkoy gauge a maximum positive amplitude of 1.0m and a maximum negative amplitude of -1.0m are observed. Since the İzmit Bay is naturally protected the amplitudes are not high. However, further studies of wave oscillation should be conducted for this area.

3.2.2.4 Simulation of Source GA

In GA scenario, nine segments of the fault are assumed to be ruptured to see the worst case scenario. Four normal segments of the fault are essential in this scenario since they are considered to be more influential on the results. The source is shown in Figure 3.20.

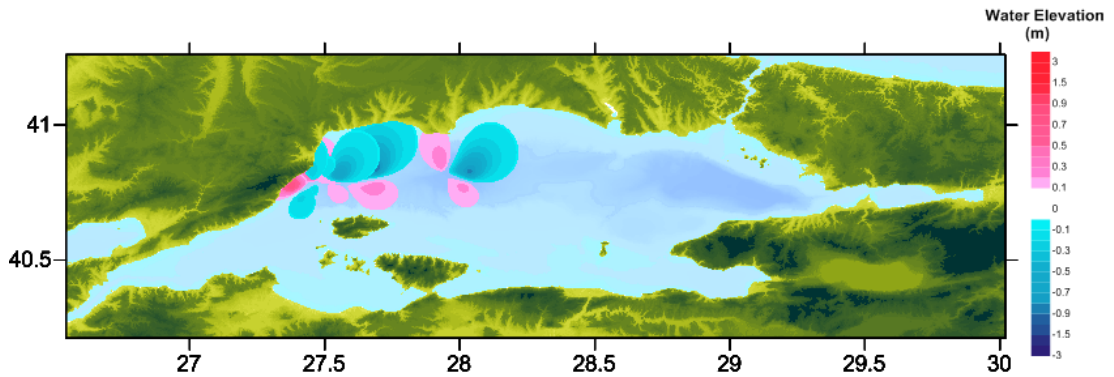


Figure 3.20 Tsunami Source for GA

Sea states for 10, 30, 60 and 90 minutes are given in Figure 3.21 for GA source. Figure 3.22 shows the maximum positive and maximum negative wave amplitudes in the domain. The values for maximum positive and maximum negative tsunami wave amplitudes are +3.5m and -3.3m respectively. Run-up distribution is also presented in Figure 3.23

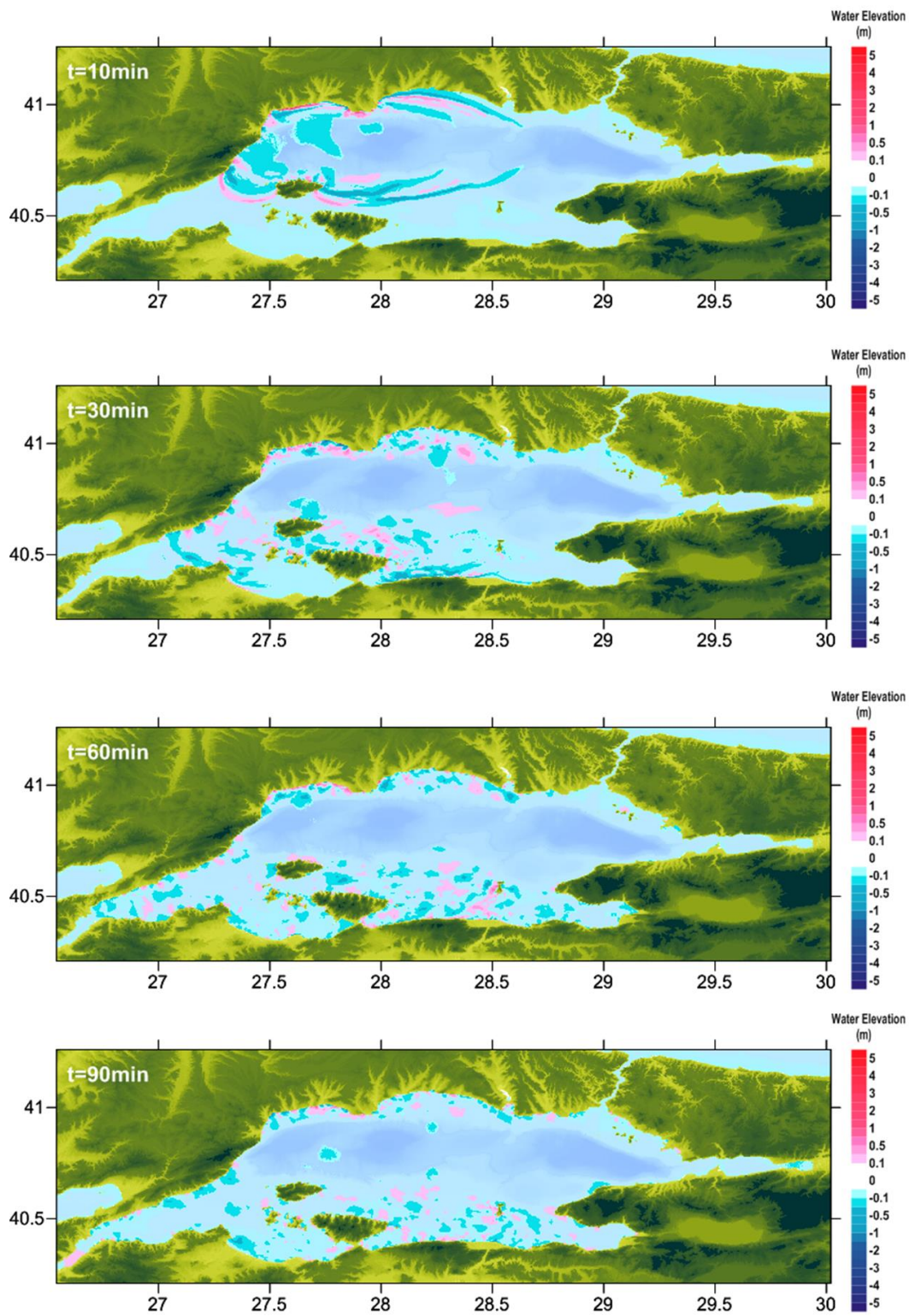


Figure 3.21 Sea states at $t=10, 30, 60$, and 90 min respectively according to the tsunami source GA

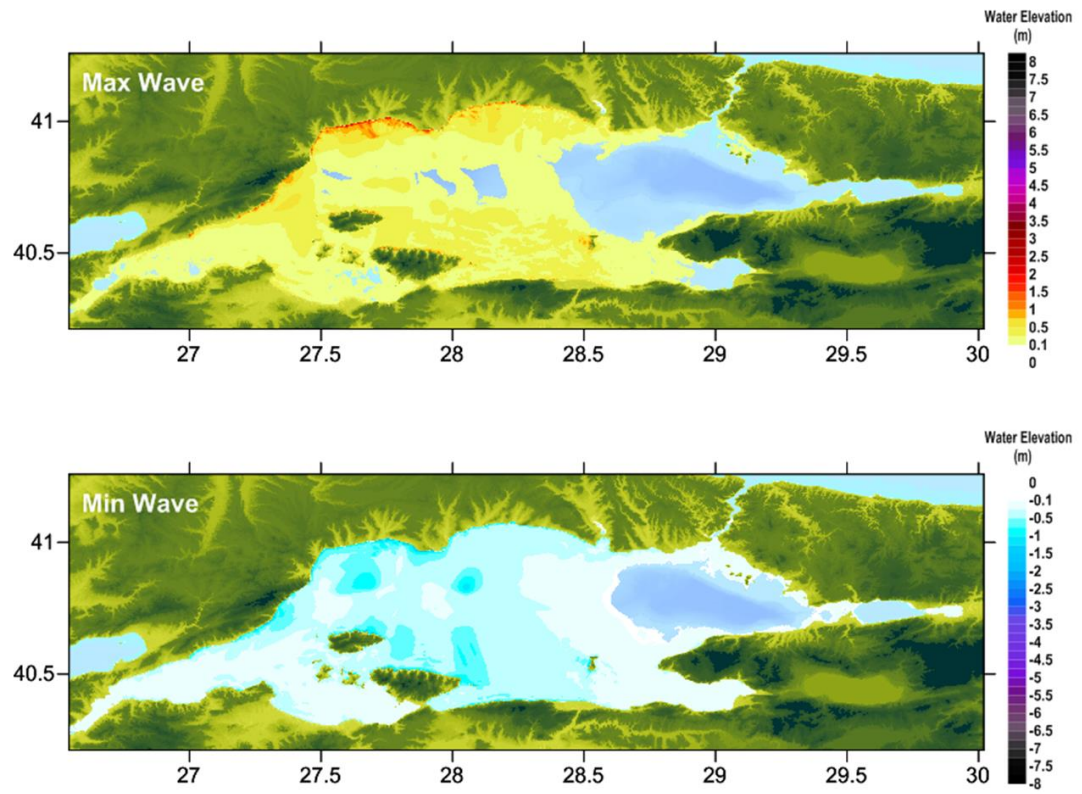


Figure 3.22 Distribution of Maximum (+) Wave Amplitude (top) and Minimum (-) Wave Amplitudes

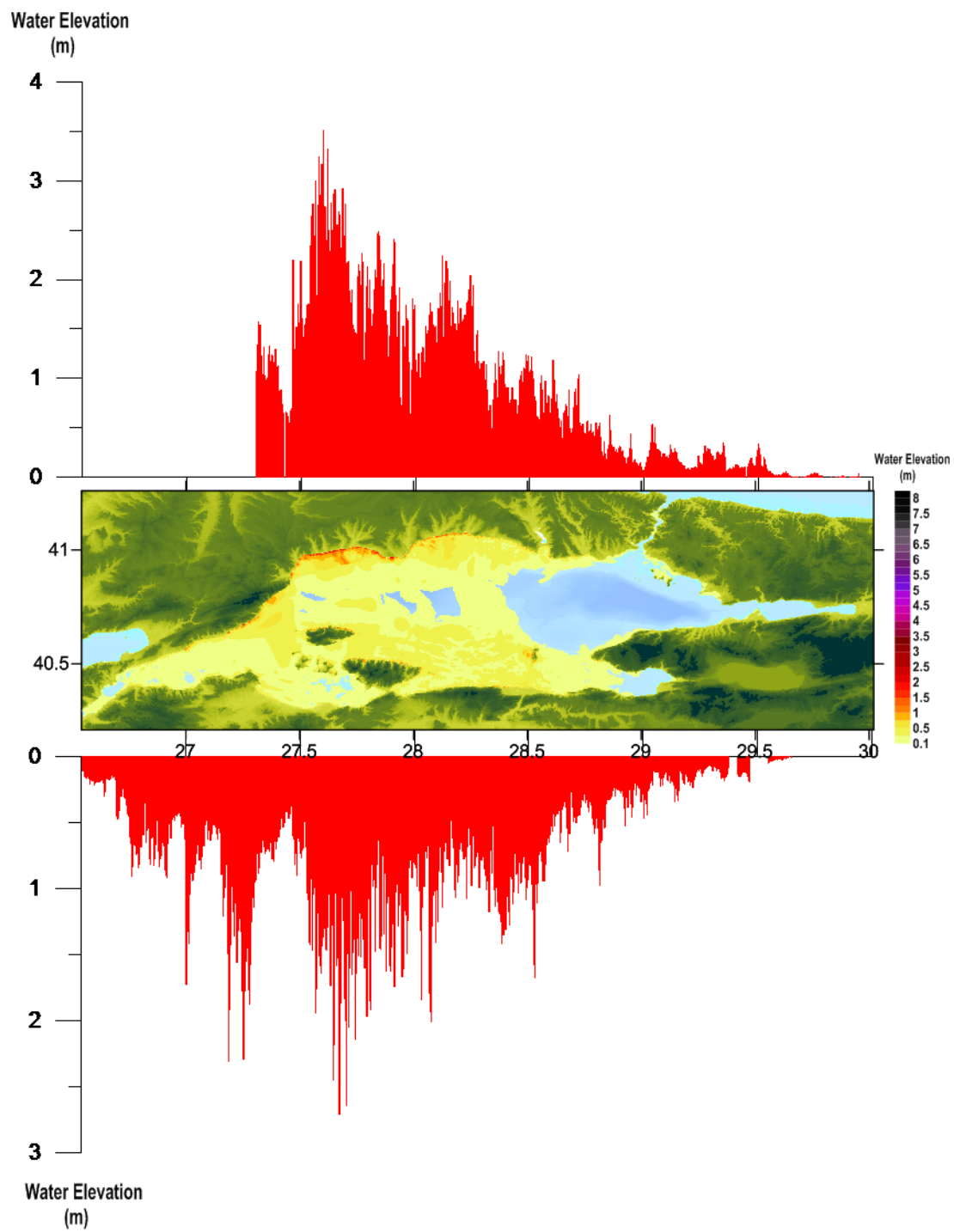


Figure 3.23 Run-up Distribution According to the Tsunami Source GA

Arrival times of the first and the maximum waves, water surface fluctuations measured at the selected gauges are given in Table 3.9. Time history diagrams of the water level fluctuations at the selected gauges are shown in Figure 3.24.

Table 3.9 Results of GA Simulation at the Selected Gauge Points

Name of gauge pt.	Depth at gauge pt.(m)	X	Y	Arrival time of initial wave (min)	Arrival time of max.wave (min)	Maximum (+) wave amp.(m)	Maximum (-) wave amp.(m)
Bakirkoy	9.0	28.826200	40.952800	12	71	0.2	-0.2
Bandirma	6.6	27.968300	40.360600	21	66	0.4	-0.6
BigaLiman	3.9	27.135900	40.451600	7	36	0.5	-0.6
Cinarcik	4.8	29.136000	40.651500	16	84	0.2	-0.2
Hpasa3	9.1	29.014800	40.995700	23	71	0.1	-0.2
Kcekmece2	5.9	28.723800	40.969300	13	72	0.4	-0.4
Mudanya	8.4	28.908900	40.367500	31	89	0.2	-0.3
Sarkoy	5.3	27.336100	40.744900	0	10	1.0	-1.0
Tekirdag2	9.5	27.519700	40.971100	0	24	0.8	-0.8
Tupras	8.3	29.935000	40.737200	59	0	0.0	-0.1
Yalova	8.1	29.276900	40.663400	17	88	0.1	-0.1
Yenikapi	9.7	28.966500	41.001800	21	70	0.1	-0.2

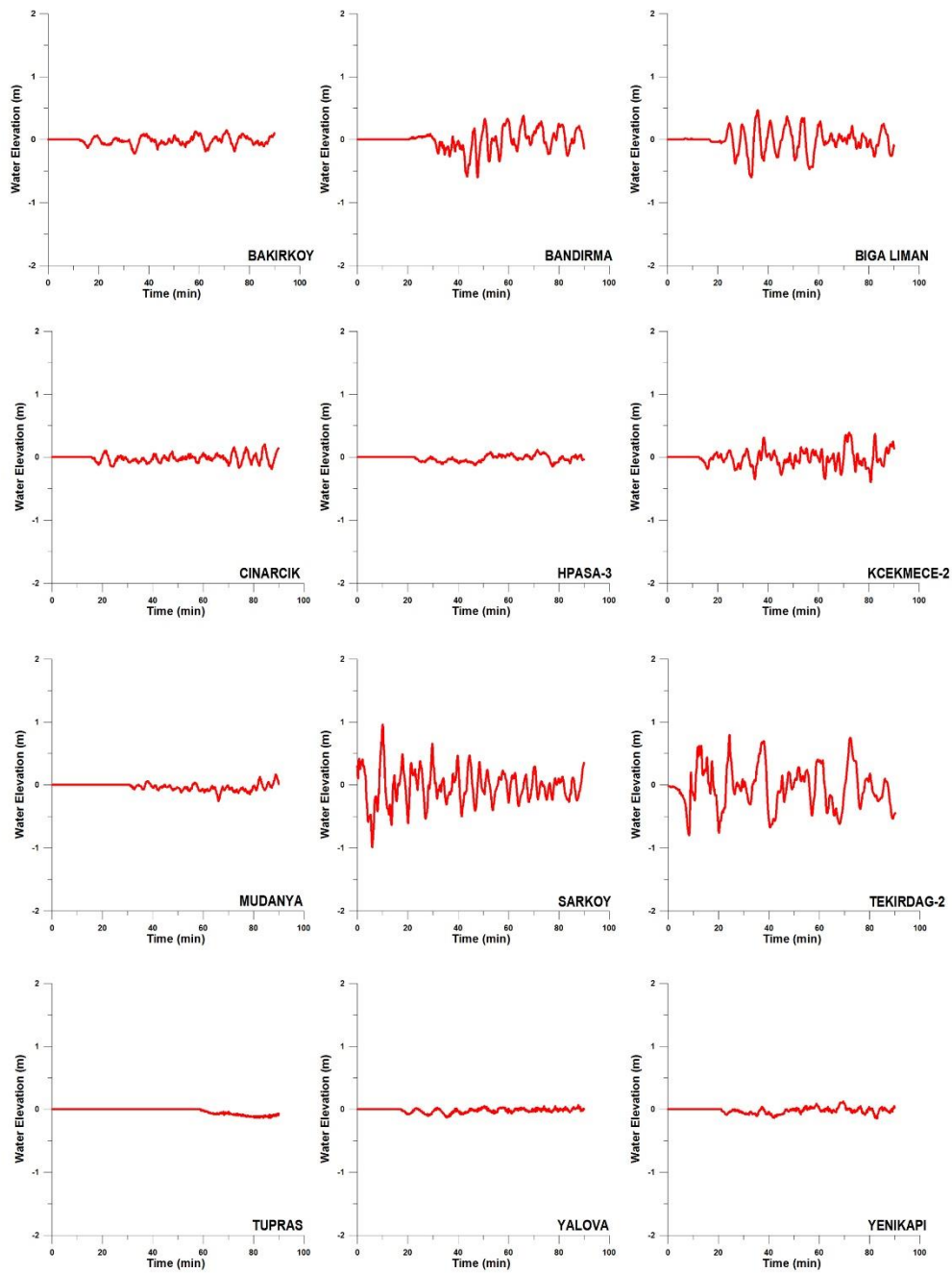


Figure 3.24 Time Histories of Water Surface Fluctuations at the Selected Gauge Locations for GA

From Table 3.9 and Figure 3.24 it is seen that the first wave arrives at İstanbul coasts in 12 minutes at Bakırköy gauge with amplitude less than 0.5m. A maximum amplitude of 0.4m and a maximum negative amplitude of -0.4m at Küçükçekmece gauge is observed (Kcekmece2)

GA source produces rather small amplitudes in İstanbul coasts of the Marmara Sea. The situation is mostly the same for the domain. Just at Sarkoy gauge a maximum positive amplitude of 1.0m and a maximum negative amplitude of -1.0m are observed.

3.2.2.5 Simulation of Source YAN

In YAN scenario, all of the eight segments of the fault are assumed to be ruptured to observe the worst case scenario. The fault consists of five normal and three oblique-normal segments. The source is shown in Figure 3.25.

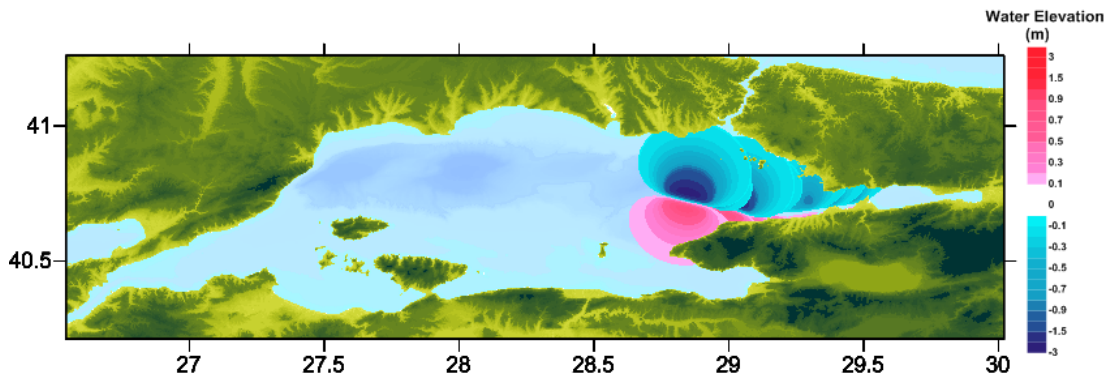


Figure 3.25 Tsunami Source for YAN

Sea states for 10, 30, 60 and 90 minutes are given in Figure 3.26 for GA source. Figure 3.27 shows the maximum positive and maximum negative wave amplitudes in the domain. The values for maximum positive and maximum negative tsunami wave amplitudes are +8.0m and -7.1m respectively. Run-up distribution is also presented in Figure 3.28.

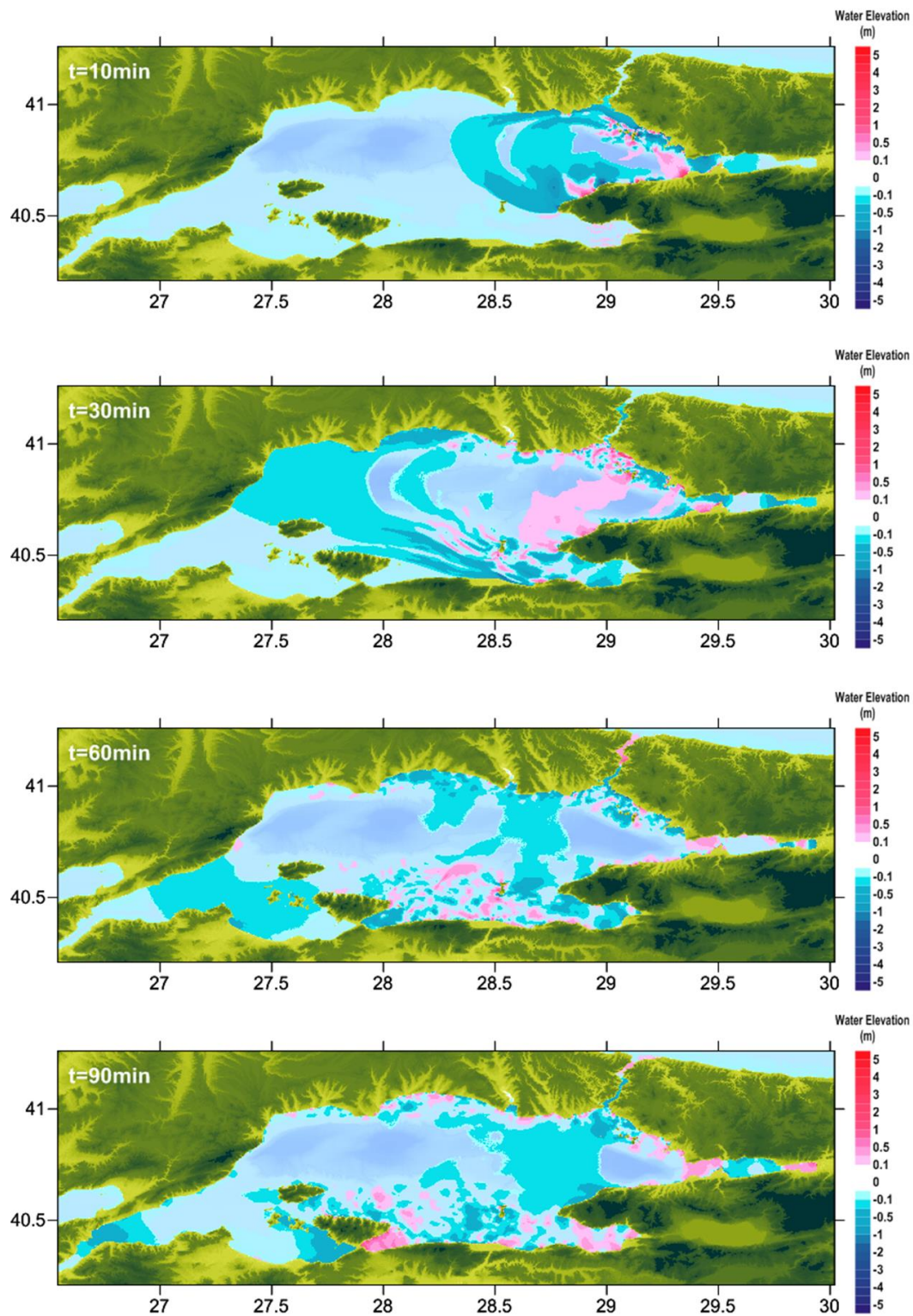


Figure 3.26 Sea states at t=10, 30, 60, and 90 min respectively according to the tsunami source YAN

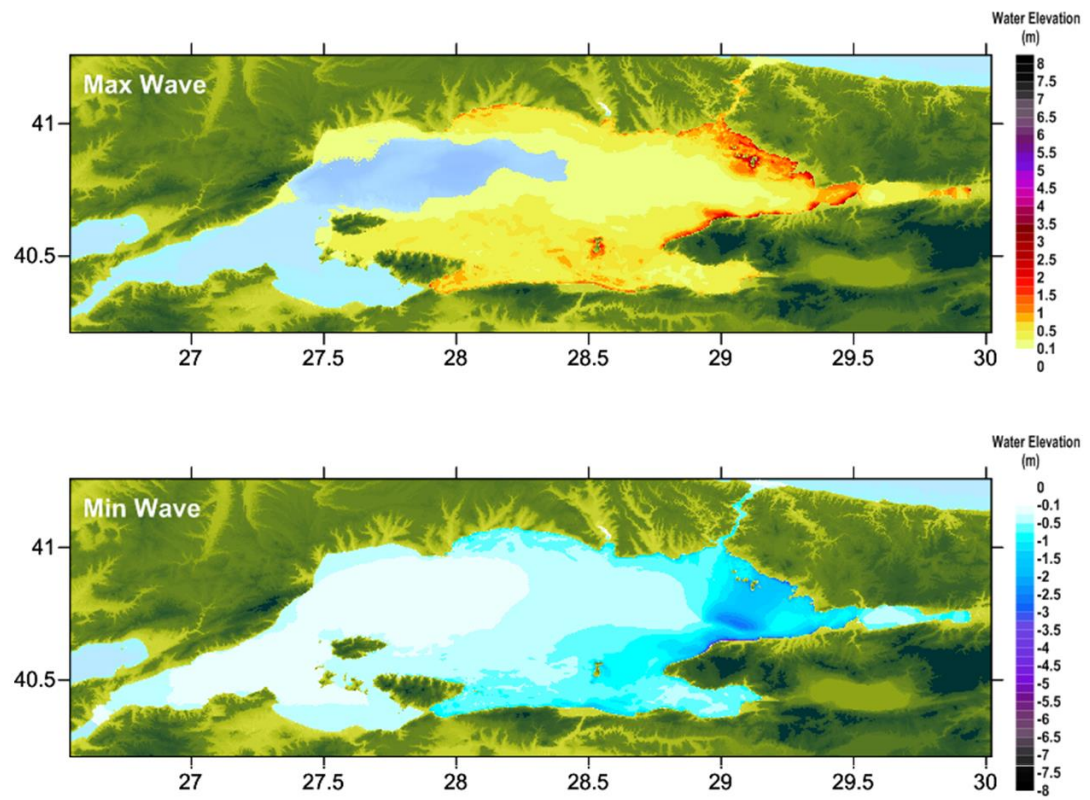


Figure 3.27 Distribution of Maximum (+) Wave Amplitude (top) and Minimum (-) Wave Amplitudes

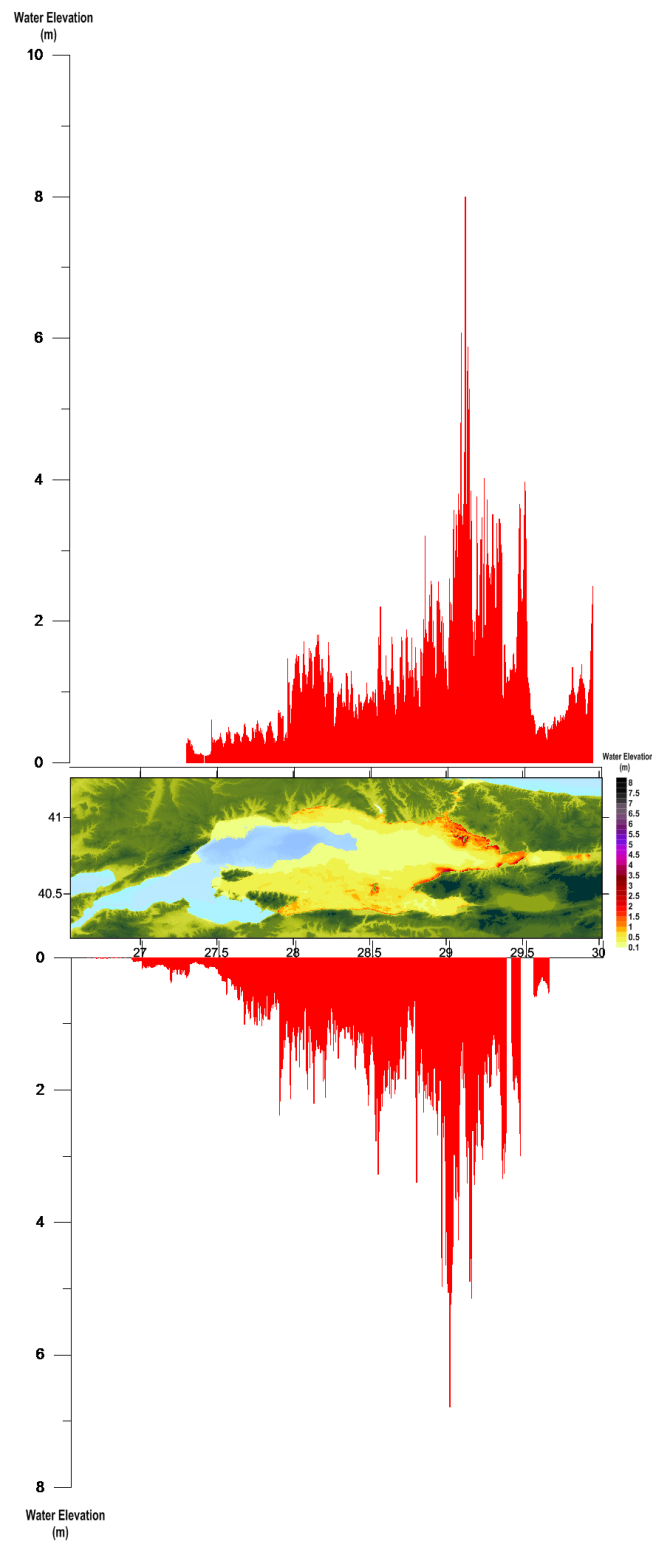


Figure 3.28 Run-up Distribution According to the Tsunami Source YAN

Arrival times of the first and the maximum waves, water surface fluctuations measured at the selected gauges are given in Table 3.10. Time history diagrams of the water level fluctuations at the selected gauges are shown in Figure 3.29.

Table 3.10 Results of YAN Simulation at the Selected Gauge Points

Name of gauge pt.	Depth at gauge pt.(m)	X	Y	Arrival time of initial wave (min)	Arrival time of max.wave (min)	Maximum (+) wave amp.(m)	Maximum (-) wave amp.(m)
Bakirkoy	9.0	28.826200	40.952800	0	20	0.7	-1.2
Bandirma	6.6	27.968300	40.360600	44	85	1.5	-1.0
BigaLiman	3.9	27.135900	40.451600	47	84	0.1	-0.2
Cinarcik	4.8	29.136000	40.651500	0	5	3.2	-4.8
Hpasa3	9.1	29.014800	40.995700	0	32	1.4	-0.9
Kcekmece2	5.9	28.723800	40.969300	6	39	0.8	-1.0
Mudanya	8.4	28.908900	40.367500	0	89	0.5	-0.7
Sarkoy	5.3	27.336100	40.744900	27	83	0.2	-0.3
Tekirdag2	9.5	27.519700	40.971100	28	70	0.2	-0.4
Tupras	8.3	29.935000	40.737200	24	78	1.0	-0.9
Yalova	8.1	29.276900	40.663400	0	7	1.0	-2.0
Yenikapi	9.7	28.966500	41.001800	0	33	1.4	-1.1

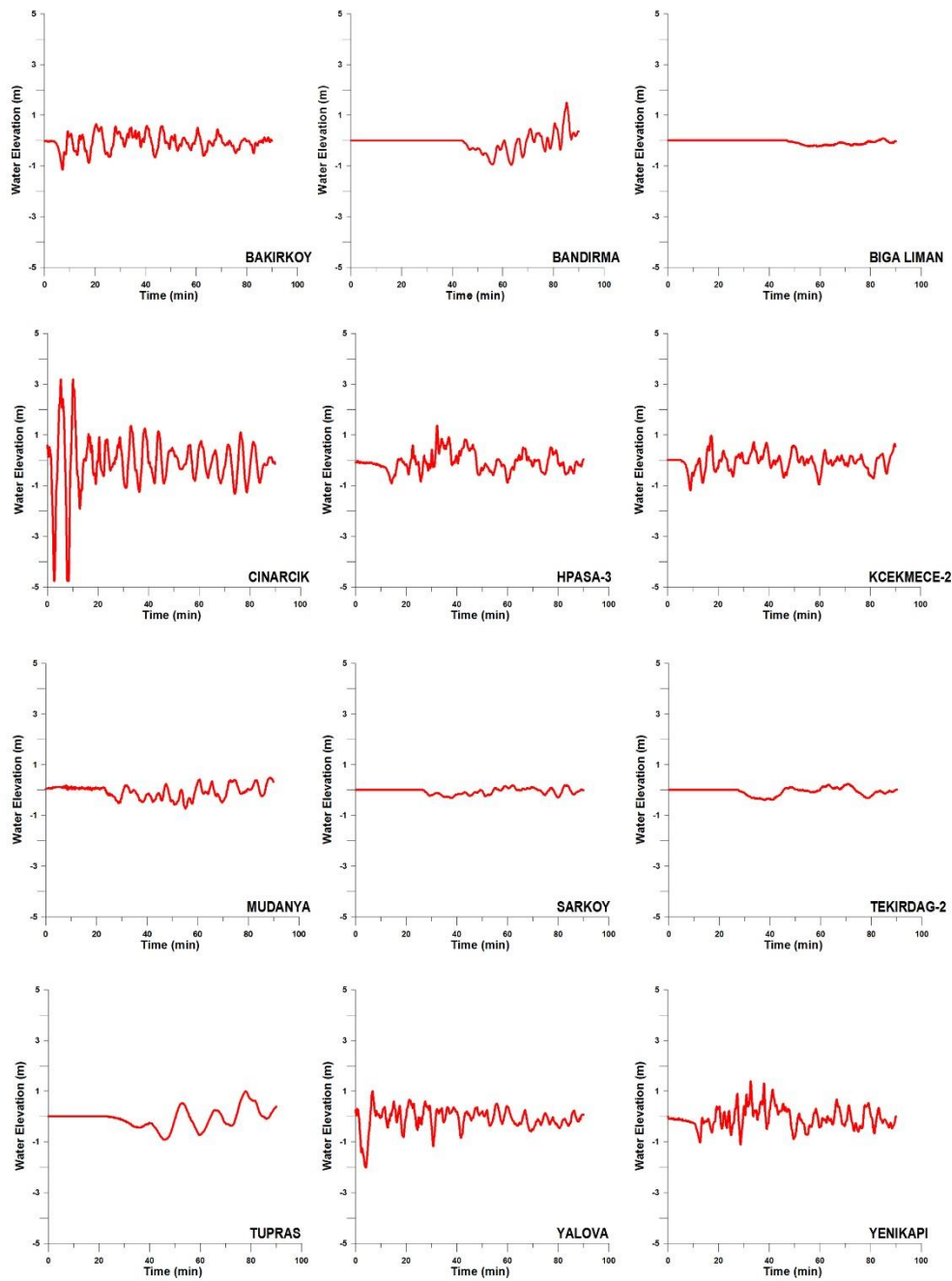


Figure 3.29 Time Histories of Water Surface Fluctuations at the Selected Gauge Locations for YAN

From Table 3.10 and Figure 3.29 it is seen that the first wave arrives at İstanbul coasts immediately at Haydarpaşa and Yenikapi gauges with amplitude than -1.00m. A maximum amplitude of 1.4m and a maximum negative amplitude of -1.1m at Yenikapi gauge is observed (Yenikapi)

YAN source has an influence on İzmit Bay and a maximum positive amplitude of 1.0m and a maximum negative amplitude of -1.0m are observed in the gulf. Also in Çınarcık a maximum positive amplitude of 3.2m and a maximum negative amplitude of -4.8m are observed.

3.2.2.6 Simulation of Source CMN

In CMN scenario, five normal fault segments are assumed to be ruptured to observe the worst case scenario. The fault consists of five normal and three oblique-normal segments. The source is shown in Figure 3.30.

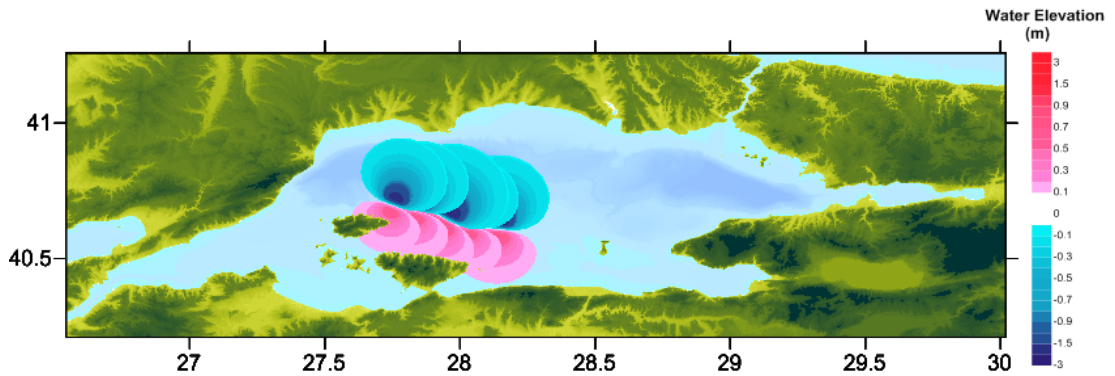


Figure 3.30 Tsunami Source for CMN

Sea states for 10, 30, 60 and 90 minutes are given in Figure 3.31 for CMN source. Figure 3.32 shows the maximum positive and maximum negative wave amplitudes in the domain. The values for maximum positive and maximum negative tsunami wave amplitudes are +5.4m and -8.3m respectively. Run-up distribution is also presented in Figure 3.33.

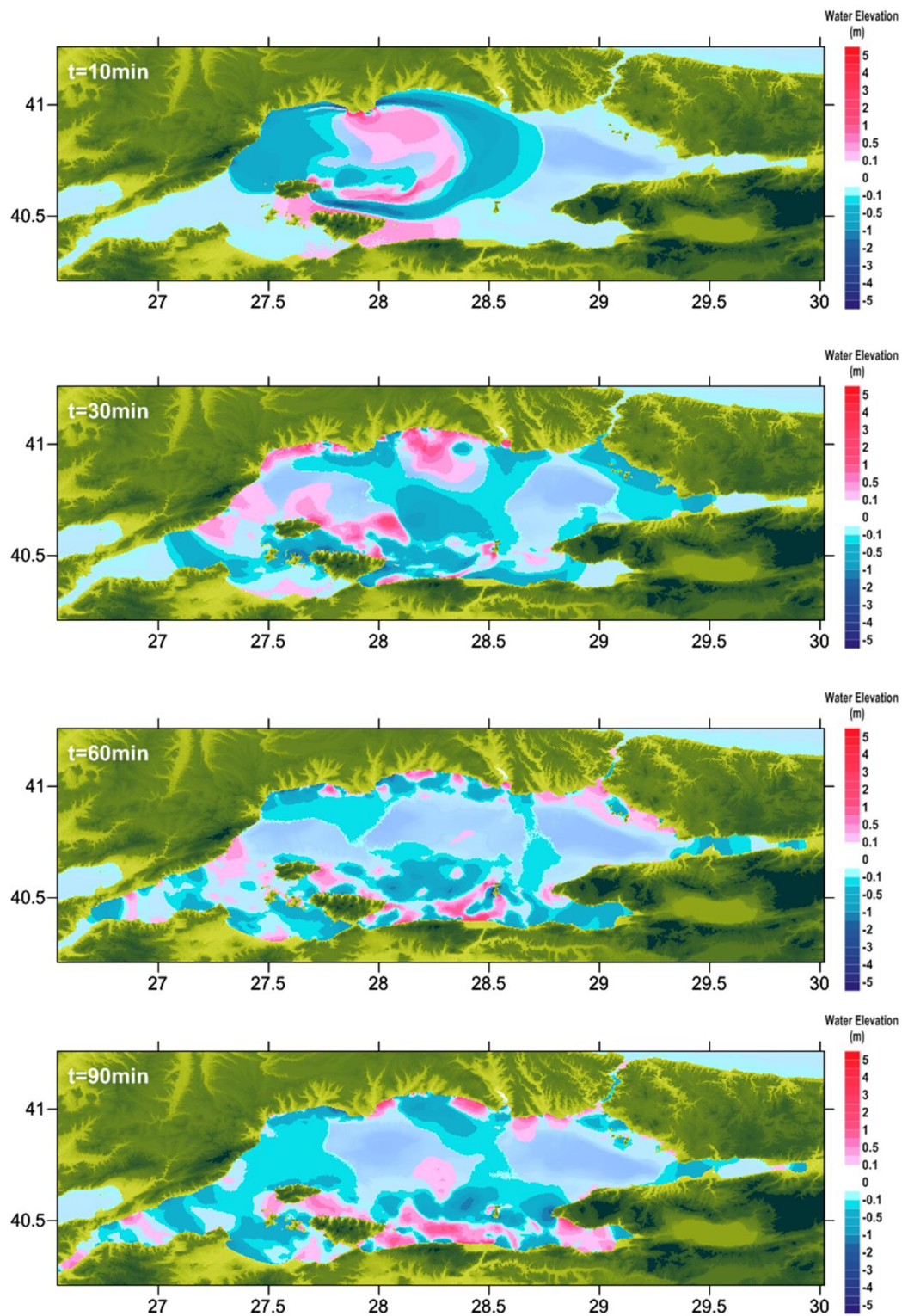


Figure 3.31 Sea states at $t=10, 30, 60$, and 90 min respectively according to the tsunami source CMN

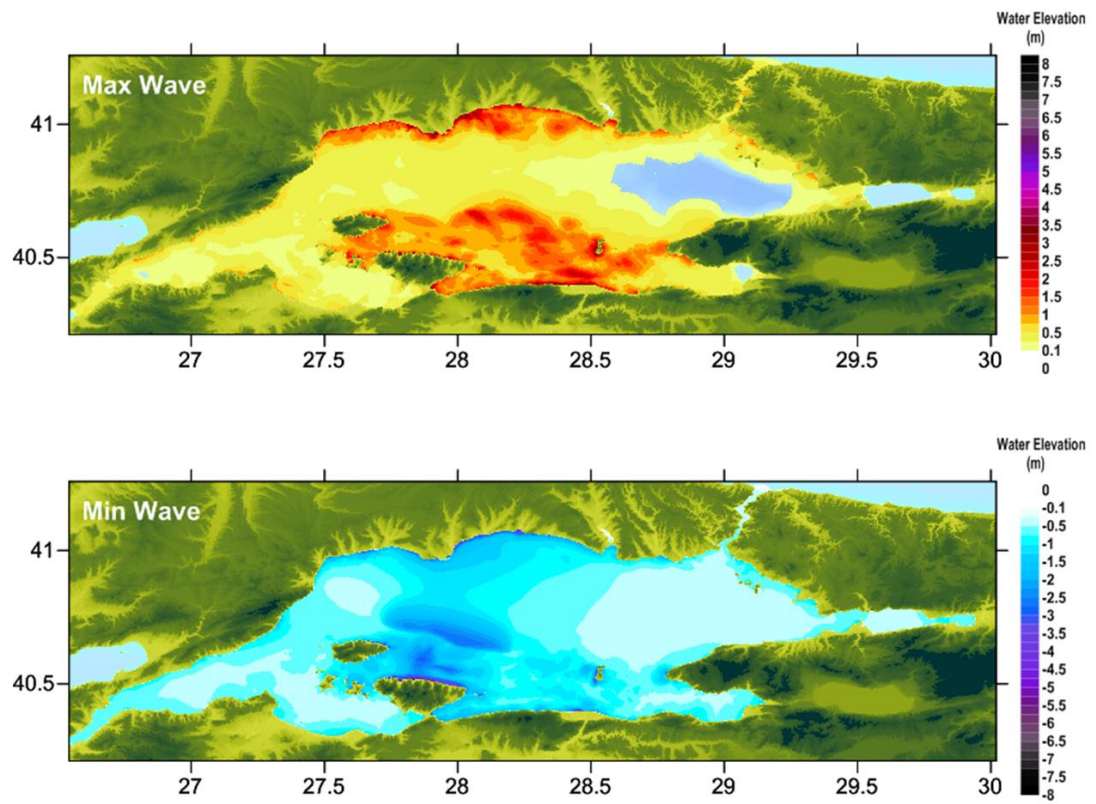


Figure 3.32 Distribution of Maximum (+) Wave Amplitude (top) and Minimum (-) Wave Amplitudes

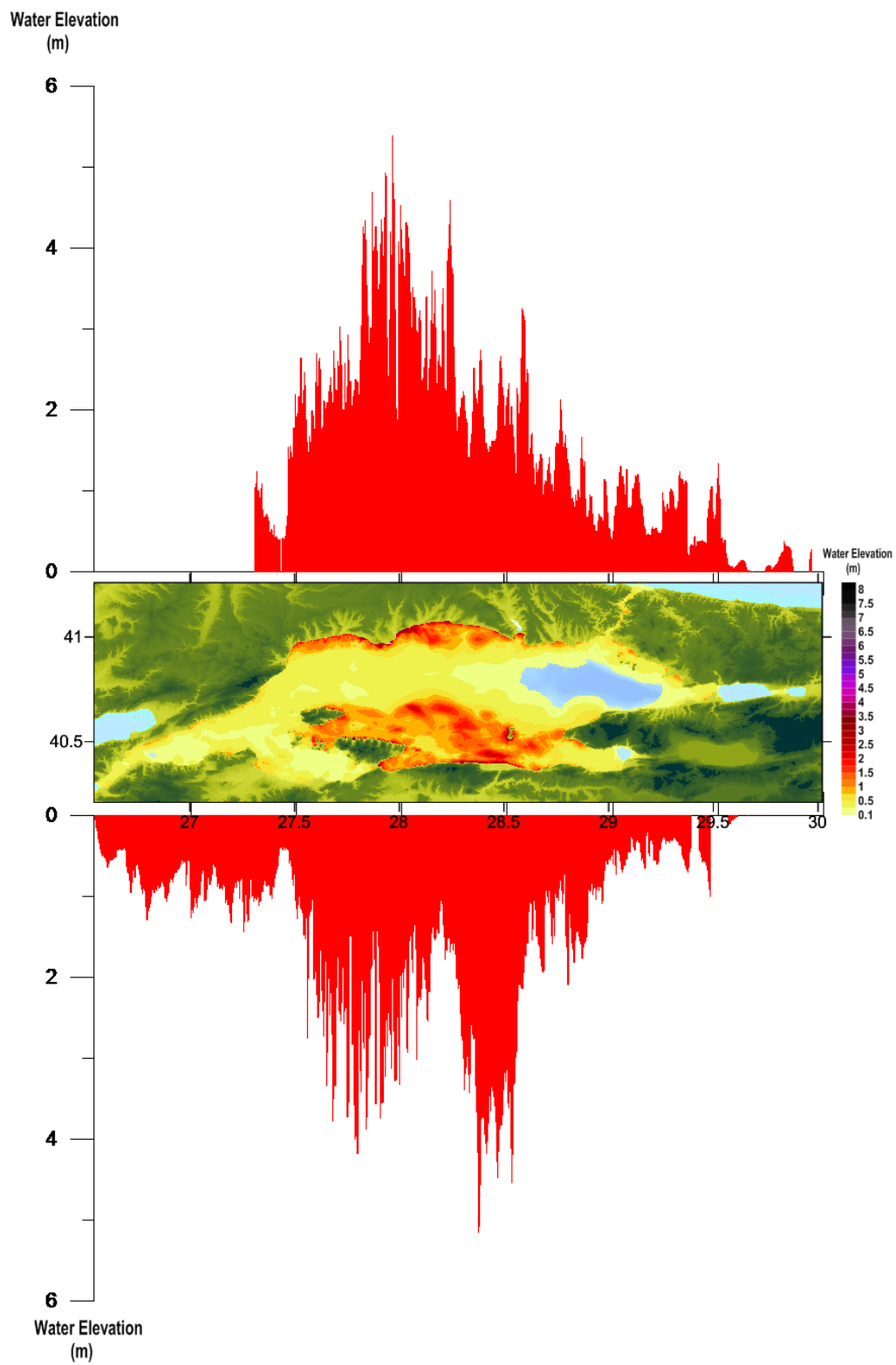


Figure 3.33 Run-up Distribution According to the Tsunami Source CMN

Arrival times of the first and the maximum waves, water surface fluctuations measured at the selected gauges are given in Table 3.11. Time history diagrams of the water level fluctuations at the selected gauges are shown in Figure 3.34.

Table 3.11 Results of CMN Simulation at the Selected Gauge Points

Name of gauge pt.	Depth at gauge pt.(m)	X	Y	Arrival time of initial wave (min)	Arrival time of max.wave (min)	Maximum (+) wave amp.(m)	Maximum (-) wave amp.(m)
Bakirkoy	9.0	28.826200	40.952800	11	71	0.7	-0.9
Bandirma	6.6	27.968300	40.360600	0	70	1.6	-1.8
BigaLiman	3.9	27.135900	40.451600	19	42	0.8	-0.7
Cinarcik	4.8	29.136000	40.651500	14	85	0.4	-0.5
Hpasa3	9.1	29.014800	40.995700	21	60	0.6	-0.7
Kcekmece2	5.9	28.723800	40.969300	11	88	1.0	-1.2
Mudanya	8.4	28.908900	40.367500	28	84	0.8	-1.0
Sarkoy	5.3	27.336100	40.744900	2	23	0.7	-1.4
Tekirdag2	9.5	27.519700	40.971100	6	46	1.6	-2.0
Tupras	8.3	29.935000	40.737200	56	0	0.0	-0.7
Yalova	8.1	29.276900	40.663400	15	54	0.3	-0.6
Yenikapi	9.7	28.966500	41.001800	19	61	0.4	-0.6

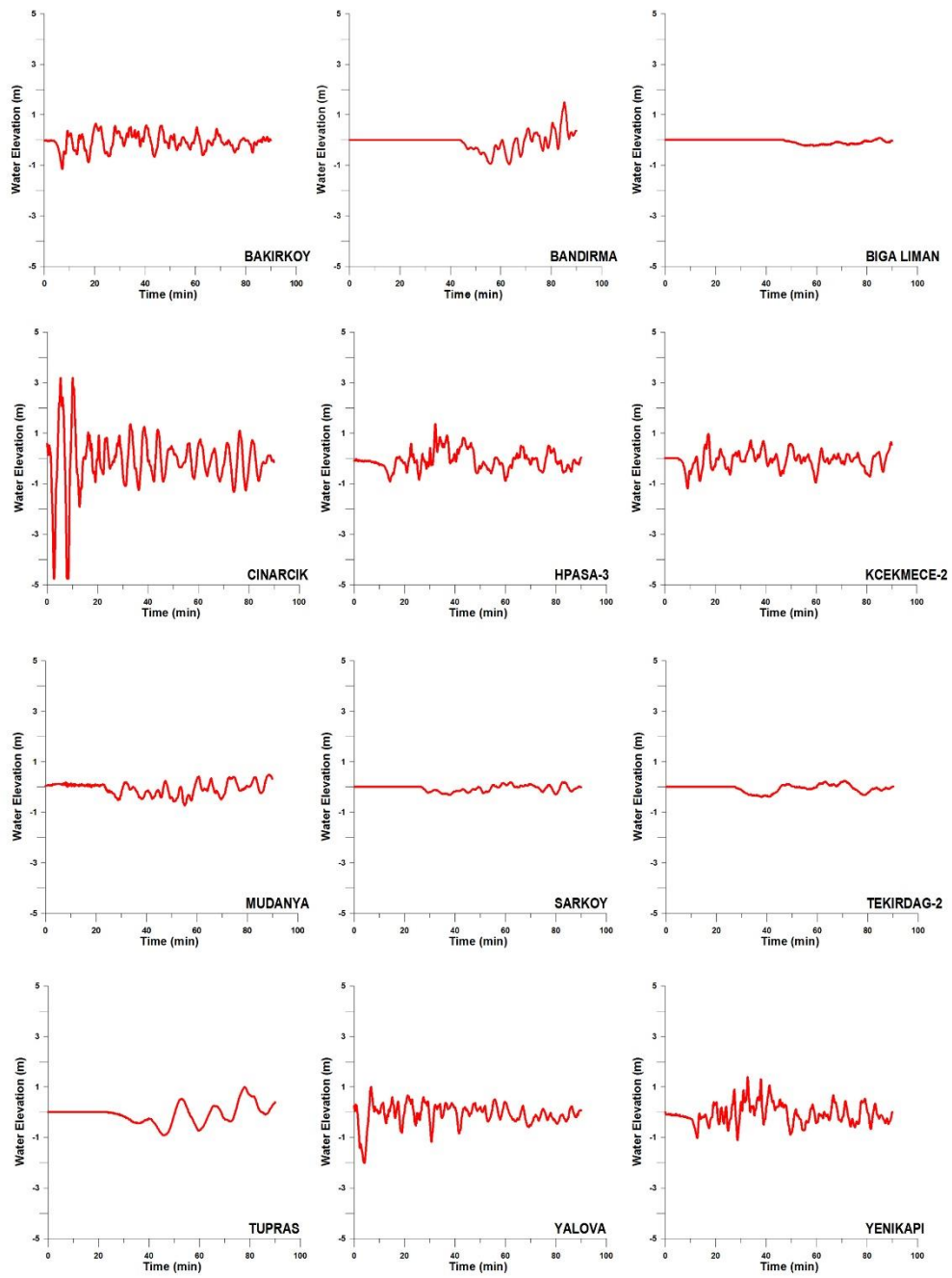


Figure 3.34 Time Histories of Water Surface Fluctuations at the Selected Gauge Locations for CMN

From Table 3.11 and Figure 3.34 it is seen that the first wave arrives at İstanbul coasts in 11 minutes at Bakırköy and Küçükçekmece gauges with amplitude than 0.5m. A maximum amplitude of 1.0m and a maximum negative amplitude of -1.2m at Küçükçekmece gauge is observed (Kcekmece2)

YAN source has an influence on western coasts of the Marmara Sea such as Tekirdağ and also southern parts like Mudanya and Bandırma. At Bandırma gauge a maximum positive amplitude of 1.6m and a maximum negative amplitude of -1.8m are observed in the gulf.

CHAPTER 4

DATABASE FOR THE WARNING SYSTEM IN THE SEA OF MARMARA

This chapter focuses on how to use the simulation results and construct a code, a simple early warning system. A preliminary design of the system uses the set of results obtained in Chapter 3 is given in this part.

4.1 Idea and Method

The idea of a need for a simple early warning system is based on modelling a tsunami genic event in real time as the event happens. To simulate a tsunami model with reliable parameters and to receive an accurate result takes at least couple of hours considering one domain in Marmara Sea region. To decrease computational time, low resolution simulation should be conducted which is unacceptable to develop emergency evacuation measures. In other words, it is needed to use high resolution data to some extent to safely evacuate people in the dangerous regions.

Since the area of the Sea of Marmara is considerably smaller than the Mediterranean and the Black Sea, tsunami waves are expected to hit the coasts in a shorter period. In average, 15 minutes is an essential period for the Marmara Sea (OYO – IMM, 2007); therefore, an early warning system that gives results as quickly as possible is a solid need in this region.

In this study, a simple code is developed to provide an early warning system that uses results previously simulated tsunamis using high resolution data. The idea behind this system is to develop a code which would be initiated with the input parameters that

can be quickly obtained from the authorities after an earthquake. These parameters are coordinates, magnitude and focal depth of the earthquake. After getting the necessary inputs, the code chooses and outputs results of one of the previously simulated tsunamis.

This system shows the possible arrival period of tsunami waves at the selected gauge points and wave amplitudes. Without waiting for an accurate simulation, this simple system gives an early warning in just a couple of seconds. It should be noted that this system is as accurate as the previous simulations.

4.2 Formation of the Database

In order to form a meaningful database, a good knowledge of the seismic events in the region and active fault lines in the Sea of Marmara should be existent. In Chapter 3, the possible fault lines are discussed, the simulations of the tsunamis are conducted and the results are presented.

In this thesis, a database is formed by simulating the tsunamis that are given in Chapter 3. In addition to the simulations given in Chapter 3, simulations given in Appendix are considered where focal depth parameter changed from 2 to 5 km. A positive side feature of this system is modifiable characteristic of the database. Whenever a new simulation is prepared and processed, results can be added in the database easily. Current database with the focal depth of 2 km is presented in Table 4.1.

In Table 4.1, it can be seen that all of the sources that are simulated are given a number which are stated below;

- PI : 1
- PIN : 2
- PI+GA : 3
- GA : 4
- YAN : 5
- CMN : 6

Any additional sources can be added to the database by assigning a new number. The second column of the database is the number that are assigned to each segment. For instance when the code processes a calculation on PI source 12nd in the database it refers to 'faultNum' 1, 'faultSegNum' 12.

Table 4.1 Database

1: PJ	2: PIN	3: PI+GA	4: GA	5: YAN	6: CMN	dip(deg)	rake(deg)	length(m)	width(m)	slip(m)
faultNum	faultSegNum	lat(decDeg)	lon(decDeg)	depth(m)	strike(deg)	dip(deg)	rake(deg)	length(m)	width(m)	slip(m)
1	1	40.727930	29.473130	2000	84.44	90	180	4717	16000	0
1	2	40.733309	29.235720	2000	92.06	90	180	20066	16000	0
1	3	40.733306	29.228180	2000	90.20	90	180	636	16000	0
1	4	40.756910	29.129420	2000	108.15	70	195	8753	17027	5
1	5	40.786100	29.069280	2000	123.15	70	195	6024	17027	5
1	6	40.816530	28.994650	2000	118.85	70	195	7148	17027	5
1	7	40.872510	28.904320	2000	129.90	70	195	9834	17027	5
1	8	40.873760	28.878430	2000	94.37	70	195	2187	17027	5
1	9	40.880330	28.750890	2000	94.66	70	195	10777	17027	5
1	10	40.878430	28.705950	2000	87.64	70	195	3795	18027	5
1	11	40.873280	28.644660	2000	84.56	70	195	5199	17027	5
1	12	40.869710	28.560060	2000	87.73	70	195	7144	17027	5
1	13	40.873010	28.517660	2000	96.80	90	180	3593	16000	0
1	14	40.872980	28.471600	2000	90.93	90	180	3884	16000	0
1	15	40.865800	28.418440	2000	80.93	90	180	4553	16000	0
1	16	40.847610	28.268010	2000	82.03	90	180	12847	16000	0
1	17	40.804200	28.061590	2000	75.73	90	180	18074	16000	0
2	1	40.756910	29.129420	2000	108.15	70	270	8753	17027	5
2	2	40.786100	29.069280	2000	123.15	70	270	6024	17027	5
2	3	40.816530	28.994650	2000	118.85	70	270	7148	17027	5
2	4	40.872510	28.904320	2000	129.90	70	270	9834	17027	5

Table 4.1 (Continued)

3	1	40.727930	29.473130	2000	84.44	90	180	4717	16000	0
3	2	10.733090	29.235720	2000	92.06	90	180	20066	16000	0
3	3	40.733060	29.228180	2000	90.20	90	180	636	16000	0
3	4	40.756910	29.129420	2000	108.15	70	195	8753	17027	5
3	5	40.786100	29.069280	2000	123.15	70	195	6024	17027	5
3	6	40.816530	28.994650	2000	118.85	70	195	7148	17027	5
3	7	40.872510	28.904320	2000	129.90	70	195	9834	17027	5
3	8	40.873760	28.878430	2000	94.37	70	195	2187	17027	5
3	9	40.880330	28.750890	2000	94.66	70	198	10777	17027	5
3	10	40.878430	28.705950	2000	87.64	70	195	3795	17027	5
3	11	40.873280	28.644660	2000	84.56	70	195	5199	17027	5
3	12	40.869710	28.560060	2000	87.73	70	195	7144	17027	5
3	13	40.873010	28.517660	2000	96.80	90	180	3593	16000	0
3	14	40.872980	28.471600	2000	90.93	90	180	3884	16000	0
3	15	40.865800	28.418440	2000	80.93	90	180	4553	16000	0
3	16	40.847610	28.268010	2000	82.03	90	180	12847	16000	0
3	17	40.804200	28.061590	2000	75.73	90	180	18074	16000	0
3	18	40.804200	28.061590	2000	263.30	70	195	2143	17027	5
3	19	40.801520	28.036440	2000	286.31	70	195	8664	17027	5
3	20	40.821700	27.937290	2000	266.61	90	180	9516	16000	0
3	21	40.714580	27.824940	2000	271.96	90	180	10494	16000	0
3	22	40.815400	27.700620	2000	260.87	70	195	12441	17027	5
3	23	40.794640	27.555820	2000	278.58	70	195	5660	17027	5

Table 4.1 (Continued)

3	24	40.800810	27.489290	2000	258.14	70	165	3046	17027	5
3	25	40.794410	27.454220	2000	238.95	70	165	6945	17027	5
3	26	40.760610	27.385060	2000	257.18	90	180	4519	16000	0
4	1	40.804200	28.061590	2000	263.30	70	195	2143	17027	5
4	2	40.801520	28.036440	2000	286.31	70	195	8664	17027	5
4	3	40.821700	27.937290	2000	266.61	90	180	9516	16000	0
4	4	40.714580	27.824940	2000	271.96	90	180	10494	16000	0
4	5	40.815400	27.700620	2000	260.87	70	195	12441	17027	5
4	6	40.794640	27.555820	2000	278.58	70	195	5660	17027	5
4	7	40.800810	27.489290	2000	258.14	70	165	3046	17027	5
4	8	40.794410	27.454220	2000	238.95	70	165	6945	17027	5
4	9	40.760610	27.385060	2000	257.18	90	180	4519	16000	0
5	1	40.721150	29.471030	2000	257.96	70	195	7058	17027	5
5	2	40.707500	29.389460	2000	261.14	70	195	6873	17027	5
5	3	40.697510	29.309200	2000	260.98	70	195	10952	17027	5
5	4	40.681210	29.181430	2000	262.35	70	270	4448	17027	5
5	5	40.675500	29.129360	2000	273.96	70	270	4562	17027	5
5	6	40.677910	29.075510	2000	283.78	70	270	10021	17027	5
5	7	40.698430	28.960070	2000	294.84	70	270	3154	17027	5
5	8	40.710050	28.926020	2000	284.90	70	270	14043	17027	5
6	1	40.612610	28.193940	2000	276.59	70	270	9505	17027	5
6	2	40.620630	28.082150	2000	279.18	70	270	7069	17027	5

Table 4.1 (Continued)

6	3	40.629380	27.999430	2000	299.07	70	270	10705	17027	5
6	4	40.674210	27.887440	2000	283.92	70	270	7850	17027	5
6	5	40.689520	27.796830	2000	291.38	70	270	7269	17027	5
1	1	40.727930	29.473130	5000	84.44	90	180	4717	16000	0
1	2	40.733309	29.235720	5000	92.06	90	180	20066	16000	0
1	3	40.733306	29.228180	5000	90.20	90	180	636	16000	0
1	4	40.756910	29.129420	5000	108.15	70	195	8753	17027	5
1	5	40.786100	29.069280	5000	123.15	70	195	6024	17027	5
1	6	40.816530	28.994650	5000	118.85	70	195	7148	17027	5
1	7	40.872510	28.904320	5000	129.90	70	195	9834	17027	5
1	8	40.873760	28.878430	5000	94.37	70	195	2187	17027	5
1	9	40.880330	28.750890	5000	94.66	70	195	10777	17027	5
1	10	40.878430	28.705950	5000	87.64	70	195	3795	18027	5
1	11	40.873280	28.644660	5000	84.56	70	195	5199	17027	5
1	12	40.869710	28.560060	5000	87.73	70	195	7144	17027	5
1	13	40.873010	28.517660	5000	96.80	90	180	3593	16000	0
1	14	40.872980	28.471600	5000	90.93	90	180	3884	16000	0
1	15	40.865800	28.418440	5000	80.93	90	180	4553	16000	0
1	16	40.847610	28.268010	5000	82.03	90	180	12847	16000	0
1	17	40.804200	28.061590	5000	75.73	90	180	18074	16000	0
2	1	40.756910	29.129420	5000	108.15	70	270	8753	17027	5
2	2	40.786100	29.069280	5000	123.15	70	270	6024	17027	5
2	3	40.816530	28.994650	5000	118.85	70	270	7148	17027	5

Table 4.1 (Continued)

2	4	40.872510	28.904320	5000	129.90	70	270	9834	17027	5
3	1	40.727930	29.473130	5000	84.44	90	180	4717	16000	0
3	2	10.733090	29.235720	5000	92.06	90	180	20066	16000	0
3	3	40.733060	29.228180	5000	90.20	90	180	636	16000	0
3	4	40.756910	29.129420	5000	108.15	70	195	8753	17027	5
3	5	40.786100	29.069280	5000	123.15	70	195	6024	17027	5
3	6	40.816530	28.994650	5000	118.85	70	195	7148	17027	5
3	7	40.872510	28.904320	5000	129.90	70	195	9834	17027	5
3	8	40.873760	28.878430	5000	94.37	70	195	2187	17027	5
3	9	40.880330	28.750890	5000	94.66	70	198	10777	17027	5
3	10	40.878430	28.705950	5000	87.64	70	195	3795	17027	5
3	11	40.873280	28.644660	5000	84.56	70	195	5199	17027	5
3	12	40.869710	28.560060	5000	87.73	70	195	7144	17027	5
3	13	40.873010	28.517660	5000	96.80	90	180	3593	16000	0
3	14	40.872980	28.471600	5000	90.93	90	180	3884	16000	0
3	15	40.865800	28.418440	5000	80.93	90	180	4553	16000	0
3	16	40.847610	28.268010	5000	82.03	90	180	12847	16000	0
3	17	40.804200	28.061590	5000	75.73	90	180	18074	16000	0
3	18	40.804200	28.061590	5000	263.30	70	195	2143	17027	5
3	19	40.801520	28.036440	5000	286.31	70	195	8664	17027	5
3	20	40.821700	27.937290	5000	266.61	90	180	9516	16000	0
3	21	40.714580	27.824940	5000	271.96	90	180	10494	16000	0
3	22	40.815400	27.700620	5000	260.87	70	195	12441	17027	5

Table 4.1 (Continued)

3	23	40.794640	27.555820	5000	278.58	70	195	5660	17027	5
3	24	40.800810	27.489290	5000	258.14	70	165	3046	17027	5
3	25	40.794410	27.454220	5000	238.95	70	165	6945	17027	5
3	26	40.760610	27.385060	5000	257.18	90	180	4519	16000	0
4	1	40.804200	28.061590	5000	263.30	70	195	2143	17027	5
4	2	40.801520	28.036440	5000	286.31	70	195	8664	17027	5
4	3	40.821700	27.937290	5000	266.61	90	180	9516	16000	0
4	4	40.714580	27.824940	5000	271.96	90	180	10494	16000	0
4	5	40.815400	27.700620	5000	260.87	70	195	12441	17027	5
4	6	40.794640	27.555820	5000	278.58	70	195	5660	17027	5
4	7	40.800810	27.489290	5000	258.14	70	165	3046	17027	5
4	8	40.794410	27.454220	5000	238.95	70	165	6945	17027	5
4	9	40.760610	27.385060	5000	257.18	90	180	4519	16000	0
5	1	40.721150	29.471030	5000	257.96	70	195	7058	17027	5
5	2	40.707500	29.389460	5000	261.14	70	195	6873	17027	5
5	3	40.697510	29.309200	5000	260.98	70	195	10952	17027	5
5	4	40.681210	29.181430	5000	262.35	70	270	4448	17027	5
5	5	40.675500	29.129360	5000	273.96	70	270	4562	17027	5
5	6	40.677910	29.075510	5000	283.78	70	270	10021	17027	5
5	7	40.698430	28.960070	5000	294.84	70	270	3154	17027	5
5	8	40.710050	28.926020	5000	284.90	70	270	14043	17027	5
6	1	40.612610	28.193940	5000	276.59	70	270	9505	17027	5
6	2	40.620630	28.082150	5000	279.18	70	270	7069	17027	5

Table 4.1 (Continued)

6	3	40.629380	27.999430	5000	299.07	70	270	10705	17027	5
6	4	40.674210	27.887440	5000	283.92	70	270	7850	17027	5
6	5	40.689520	27.796830	5000	291.38	70	270	7269	17027	5

4.3 Working Stages of Tsunami Warning System

Working stages of the tsunami early warning system developed in MATLAB environment can be summarized in three steps

- Input Stage
- Processing Stage
- Output Stage

4.3.1 Input Stage

As mentioned before, the system asks user to input the basic parameters that are acquired after a possible earthquake which are listed below. Input screenshot is also given in Figure 4.1.

- Longitude and latitude (decimal degrees, ED50)
- Magnitude of the earthquake (Richter Scale)
- Focal depth of the earthquake (km)

```
%% INPUTS
lon=27.50; % Longitude Coordinate (Decimal Degrees)
lat=41.12; % Latitude Coordinate (Decimal Degrees)
depth=2000; % Depth of Fault (meters)
magnitude=6.8; % Magnitude
```

Figure 4.1 Screenshot of the Input Screen

4.3.2 Processing Stage

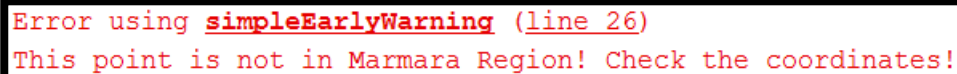
4.3.2.1 First Checks

After obtaining the input from the user, code first checks whether the given coordinates are in the domain. If the coordinates are in the limits of the domain, code continues running. Corner coordinates of the domain are given in Table 4.2.

Table 4.2 Corner Coordinates of the Domain

Spatial Reference	Coordinates (WGS84)	
Longitude	26.542°	30.020°
Latitude	40.210°	41.260°

If the entered coordinates are out of border, code outputs a warning message as shown in Figure 4.2.



```
Error using simpleEarlyWarning (line 26)
This point is not in Marmara Region! Check the coordinates!
```

Figure 4.2 Coordinate Warning Message

Second check is made for the magnitude of the earthquake. Indian Ocean tsunami in 2004, increased the public awareness that a tsunami can cause devastating events very far from its source. In case of a tsunami generation a main challenge is to decide whether an earthquake is capable of generate a tsunami or not. The challenge can be managed by using a decision matrix (DM). (Tinti, et al., 2012)

An efficient DM depends strongly on the tsunamigenic peculiarities of the area. Thus, in 2005 Intergovernmental Coordination's Groups (ICGs) of North Eastern Atlantic, the Mediterranean and Connected Seas (NEAMTWS) developed two different DMs. First of them shown in Table 4.3 is developed for the NE Atlantic and the one presented in Table 4.4 is developed for the Mediterranean Basin. (Tinti, et al.,2012)

In this thesis, with respect to the DM presented in Table 4.4, the limitation of the magnitude is chosen to be 6.5. It can be concluded that magnitudes of less than 6.5 in Richter scale can be neglected for tsunami formation.

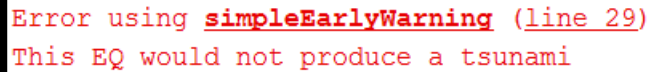
Table 4.3 Decision Matrix for the Atlantic (Tinti, et al., 2012)

Decision Matrix for the NE Atlantic							
Depth	Epicenter Location	M_w	Tsunami Potential	Tsunami Message Type			
				Local	Regional	Basin	
<100 km	Offshore or close to the coast (≤ 40 km inland)	>5.5 and ≤ 7.0	Weak potential for local tsunami	Advisory	Information	Information	
		>7.0 and ≤ 7.5	Potential for a destructive local tsunami (<100 km)	Watch	Advisory	Information	
	Offshore or close to the coast (≤ 100 km inland)	>7.5 and ≤ 7.9	Potential for a destructive regional tsunami (<400 km)	Watch	Watch	Advisory	
		>7.9	Potential for a destructive basin-wide tsunami	Watch	Watch	Watch	
≥ 100 km	Offshore or inland ≤ 100 km	>5.5	Nil	Information	Information	Information	

Table 4.4 Decision Matrix for the Mediterranean (Tinti, et al., 2012)

Decision Matrix for the Mediterranean						
Depth	Epicenter Location	M_w	Tsunami Potential	Tsunami Message Type		
				Local	Regional	Basin
<100 km	Offshore or close to the coast (≤ 40 km inland)	>5.5 and ≤ 6.0	Weak potential for local tsunami	Advisory	Information	Information
		>6.0 and ≤ 6.5	Potential for a destructive local tsunami (<100 km)	Watch	Advisory	Information
	Offshore or close to the coast (≤ 100 km inland)	>6.5 and ≤ 7.0	Potential for a destructive regional tsunami (<400 km)	Watch	Watch	Advisory
		>7.0	Potential for a destructive basin-wide tsunami	Watch	Watch	Watch
≥ 100 km	Offshore or inland ≤ 100 km	>5.5	Nil	Information	Information	Information

When a magnitude less than 6.5 is entered, the code outputs another warning message as shown in Figure 4.3.



```
Error using simpleEarlyWarning (line 29)
This EQ would not produce a tsunami
```

Figure 4.3 Magnitude Warning Message

4.3.2.2 Reading the Database

As mentioned before a database is constructed with respect to the fault parameters that are given in Table 4.1.

The code reads the database considering all faults, all fault segments and corresponding fault segment parameters. In this thesis study, simulations are conducted with both 2 and 5 kilometers of focal depths for each earthquake source as mentioned above.

4.3.2.3 Calculating the Geographical Distance between Coordinates and the Haversine Formula

The next step is the calculation of geographical distance between the entered coordinates and coordinates of the faults that are listed in the database. Haversine formula which is also known as Half Versine formula is used for this calculation.

The haversine formula is a fundamental equation used in navigation in determining great-circle distances between two points on a sphere from their latitudes and longitudes. The law of haversines which relates the sides and angles of spherical triangles is the basis of this formula. Prof. James Inman coined the term haversine in 1835.

➤ Law of Haversines

A unit sphere is assumed as in Figure 4.4 having a spherical triangle on its surface.

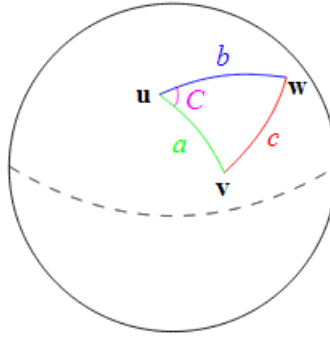


Figure 4.4 Spherical Triangle Solved by the Law of Haversines

In Figure 4.4 there are three points which are **u**, **v** and **w**, on the sphere. They are connected by great circles. The lengths of the sides are **a**, **b** and **c**. The angle of the corner opposite to **c** is **C**. In this case the law of haversines states:

$$\text{haversin}(c) = \text{haversin}(a - b) + \sin(a) \sin(b) \text{haversin}(C) \quad (\text{Eqn.4.1})$$

The lengths *a*, *b*, and *c* are in radians and are equal to the angles subtended by those sides from the center of the sphere. To derive the law of haversines, spherical law of cosines is the starting point.

$$\cos(c) = \cos(a) \cos(b) + \sin(a) \sin(b) \cos(C) \quad (\text{Eqn.4.2})$$

Spherical law of cosines is a right however not an accurate formula for small distances. Thus obtaining the haversines law by substituting Eqn.3 and adding the identity stated by Eqn.4 is a more accurate way.

$$\cos(\theta) = 1 - 2\text{haversin}(\theta) \quad (\text{Eqn.4.3})$$

$$\cos(a - b) = \cos(a) \cos(b) + \sin(a) \sin(b) \quad (\text{Eqn.4.4})$$

➤ The Haversine Formula

For any points on a sphere, the haversine of the central angle between them is given by

$$hav\sin\left(\frac{d}{r}\right) = hav\sin(\varphi_2 - \varphi_1) + \cos(\varphi_1) \cos(\varphi_2) hav\sin(\lambda_2 - \lambda_1) \quad (\text{Eqn.4.5})$$

Where haversin is the haversine function

$$hav\sin(\theta) = \sin^2\left(\frac{\theta}{2}\right) = \frac{1 - \cos(\theta)}{2} \quad (\text{Eqn.4.6})$$

- d: distance between two points on a great circle of the sphere
- r: the radius of the sphere
- φ_1, φ_2 : latitude of 1st and 2nd points
- λ_1, λ_2 : longitude of 1st and 2nd points

The Eqn.5 is solved for d ,

$$\begin{aligned} d &= 2r \arcsin\left(\sqrt{hav\sin(\varphi_2 - \varphi_1) + \cos(\varphi_1) \cos(\varphi_2) hav\sin(\lambda_2 - \lambda_1)}\right) \\ &= 2r \arcsin\left(\sqrt{\sin^2\left(\frac{\varphi_2 - \varphi_1}{2}\right) + \cos(\varphi_1) \cos(\varphi_2) \sin^2\left(\frac{\lambda_2 - \lambda_1}{2}\right)}\right) \quad (\text{Eqn.4.7}) \end{aligned}$$

Is obtained.

4.3.2.4 Sorting Results and Choosing the Right Source

The code calculates the distances between the segments and the entered point for all sources and sorts the distances as indices. Code selects the source at the shortest distance to the entered point.

In this thesis focal depths of 2 and 5 km are studied. Thus, a depth check should also be conducted in order to obtain the relevant results. If the entered depth value is up to 4 km, the code uses the sources simulated for 2 km focal depth. If the entered depth value is higher than 4km, the code uses the sources simulated for 5km focal depth.

4.3.3 Output Stage

After selecting the tsunami source and segment, the code chooses the relevant results for that source as shown in

```
Nearest EQ source is PIN. Fault Number: 2 Fault Segment Number: 4
```

Figure 4.5 Selection of the Source as Output

The code also calls the visual results (tables and graphs) which are discussed in Chapter 3. The images are output in just a few seconds. A sample output of the images are shown in Figure 4.6 and Figure 4.7. Finally, the code outputs the elapsed time to show how fast the processing is. The maximum duration of the process in construction phase is read to be 8.5 seconds. The screenshot is shown in Figure 4.8.

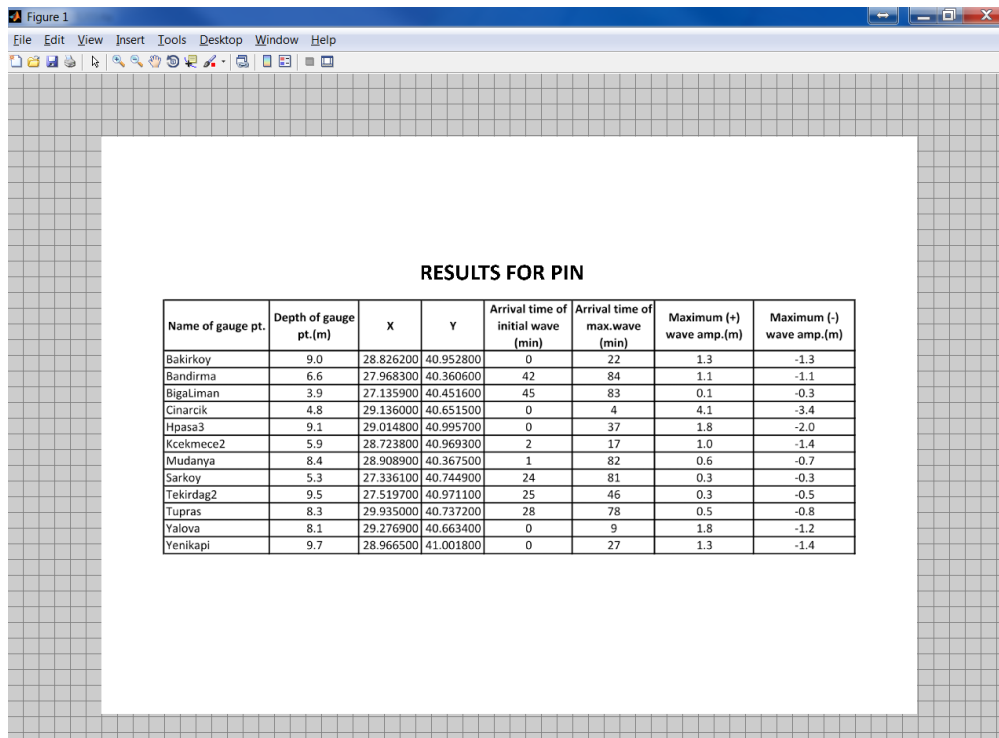


Figure 4.6 Visual Outputs of the Code

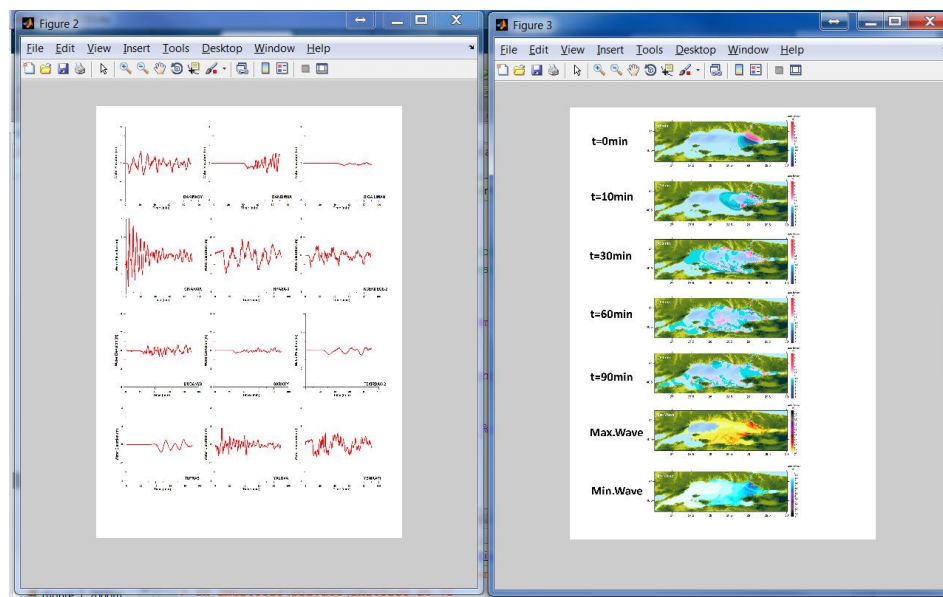


Figure 4.7 Visual Outputs of the Code

Elapsed time is 1.815484 seconds.

Figure 4.8 Sample Output of Elapsed Time Message

CHAPTER 5

CONCLUSIONS and FURTHER RECOMMENDATIONS

The aim of this research is to develop a database for possible tsunamis and construct an informative tsunami warning system in the Marmara Region.

A database of tsunami sources is constructed by researching the active fault lines passing beneath the Sea of Marmara. By studying the rupture parameters of the sources, several tsunami sources are created. While creating these sources, informative data from the historical tsunamis in the region are used.

5.1 Conclusions on Tsunami Simulations

There is not an exact procedure to estimate magnitudes and return periods of tsunami sources, since the knowledge in this area is still grey.

Therefore, in this study a deterministic approach is followed to find the possible maximum extent of tsunami inundations. Following results are obtained from the tsunami simulations for Sea of Marmara;

- Six different scenarios were studied namely Prince's Islands (PI), Prince's Islands Normal (PIN), Ganos Fault (GA), Prince's Islands Fault and Ganos Fault (PI + GA), Yalova Fault (YAN) and Central Marmara Fault (CMN).
- PI Scenario is not affective in the region. Only some coastal parts of İstanbul and Prince's Islands are under the effect the generated waves with run up values of 3 meters.

- PIN Scenario rises as the most critical among other scenarios for Istanbul and Yalova. Run-up of 9-10 meters is observed in this case. PIN source also does not show a potential danger in the western Marmara.
- GA and PI + GA scenarios are important since they have the potential to influence the western coasts unlike the first two sources. In GA scenario, run-up heights reach up to 3-4 m around Tekirdag.
- YAN scenario shows a considerable impact on the İzmit Gulf. In the other cases, İzmit Gulf is protected against the waves by the geographical characteristics. However, the proximity of the source shows influence on the generated waves towards the gulf. This scenarios shows run up in range of 3-4 meters.
- CMN scenario shows run up around 5-6 meters and affects all the region in a considerably especially western İstanbul and south Marmara coasts.
- In this thesis, seismic sources are determined with deterministic approach. Source parameters can differ in reality.
- Local tsunamis can happen at local coastal regions. Main sources stated in the study can trigger local and small fault lines. Moreover landslide tsunamis might take place in the region.
- It is not guaranteed to attain stated wave height and run-up values in a real tsunami event.

5.2 Conclusions on Software for Database

In this thesis a simple informative tsunami warning system for the Sea of Marmara is constructed. Below are the main conclusions for this system;

- The code, written in MATLAB language, uses database which consists of already simulated tsunami sources in the region.
- The system is constructed with the aim of obtaining informative results in a short period of time. Thus, the code should be kept as simple as possible.
- A numerous historical tsunamis and the same amount of factual simulations should be performed to obtain more accurate results

- Input values are the first earthquake information that are heard from the authorities which are namely coordinates, magnitude and depth. These values are entered to initiate the code.
- The code compares the entered coordinates with the coordinates of tsunami sources in the database. The source with the smallest distance to the database is selected. The distance is calculated by using the Haversine Formula which is used to obtain the geographical distance of two points on the great circle.
- After selecting the source, the code determines the depth to be used in the simulations. In this thesis focal depths of 2 and 5 km are studied.
- The code outputs the results of the relevant source with the relevant focal depth. Sea states of the domain at 10th, 30th, 60th and 90th minutes, maximum positive and maximum negative wave amplitudes in the domain, time histories of the water surface fluctuations and results at the selected gauges are presented as image files.

5.3 Recommended Future Studies

- Database shall be extended by adding more sources by studying the domain and historical tsunamis.
- Simulations of the models with different focal depths, displacements and coordinates shall be conducted in order to extend the database.
- The code shall be developed as an application or browser based program since this code needs MATLAB software to be run.
- If the database is extended, input values such as slip, dip, rake, strike angles, length and width of the fault, displacement of the fault can be added to obtain more accurate results in a massive database.

REFERENCES

- Alpar, B., Gazioglu, C., Altinok, Y., Yucel, Z. Y., & Dengiz, S. (2004).
Tsunami Hazard Assessment in Istanbul Using By High Resolution
Satellite Data (Ikonos) and Dtm. 4 pages.
- Altinok, Y., Alpar, B., Ozer, N., & Akyurt, H. (2011). Revision of the Tsunami
Catalogue Affecting Turkish Coasts and Surrounding Regions. *Natural
Hazards and Earth System Sciences*, 11, 273-291.
- Altinok, Y., Ersoy, S., Yalciner, A. C., Alpar, B., & Kuran, U. (2001). Historical
Tsunamis in the Sea of Marmara. ITS 2001, Session 4, pp. 527-534.
- Ambraseys, N. N. (2002). The Seismic Activity of the Marmara Sea Region over the
Last 2000 Years. *Bulletin of the Seismology Society of America*, 92(1), 1-18.
- Armijo, R. N., Pondard, B., Meyer, B., Ucar, G., Lepinay, B. m., Malavieille, J.,
et al. (2005). Submarine Fault Scarps in the Sea of Marmara Pull-Apart
(North Anatolian Fault): Implications for Seismic Hazard in Istanbul. *An
Electronic Journal of the Earth Sciences*, 6(6), 1-29.
- Barka, A. A., & Kandinsky-Cade, K. (1988). Strike-Slip Fault Geometry In Turkey
and Its Influence on Earthquake Activity. *Tectonics*, 7(3), 663-684.
- Borrero, J. C., Sieh, K., Chlieh, M., & Synolakis, C. E. (2006). Tsunami Inundation
Modeling for Western Sumatra. *PNAS*, 103, 19673-19677.
- Hebert, H., Schindele, F., Altinok, Y., Alpar, B., & Gazioglu, C. (2005). "Tsunami
Hazard in the Marmara Sea (Turkey): a Numerical Approach to Discuss
Active Faulting and Impact on the Istanbul Coastal Areas. *Marine Geology*,
215, 23-43.
- IMM, O. a. (2007). Project report on simulation and vulnerability analysis of
Tsunamis Affecting the Istanbul Coasts. Istanbul: OYO Int. Co (Japan) for
Istanbul Metropolitan Municipality (IMM).

- Leone, F., Lavigne, F., Paris, R., Denain, J.-C., & Vinet, F. (2011). A Spatial Analysis of The December 26th, 2004 Tsunami-Induced Damages: Lessons Learned For A Better Risk Assessment Integrating Buildings Vulnerability. *Applied Geography*, 31, 363-375.
- Okada, Y. (1985). Surface Deformation Due To Shear and Tensile Faults in a Half-Space. *Bulletin of the Seismology Society of America*, 75(4), 150-173.
- Straub, C., Kahle, H. G., & Schindler, C. (1997). GPS and Geological Estimates of the Tectonic Activity in the Marmara Sea Region, NW Anatolia. *Journal of Geophysical Research*, 102(B12), 27,587-27,601.
- Strunz, G., Post, J., Zosseder, K., Wegscheider, S., Mück, M., Reidlinger, T., et al. (2011). Tsunami Risk Assessment in Indonesia. *Natural Hazards and Earth Sciences*, 11, 67-82.
- Tinti, S., Graziani, L., Brizuela, B., Maramai, A., Gallazzi, S., et al. (2012). Applicability of the Decision Matrix of North Eastern Atlantic, Mediterranean and connected seas Tsunami Warning System to the Italian Tsunamis. *Natural Hazards and Earth Sciences*, 12, 843-857.

APPENDIX A

TSUNAMI CATALOGUE FOR TURKISH COASTS

Altinok et al., 2011 created a database that contains the data for 134 tsunami genic events that have occurred near the Turkish coasts.

Table A.1 Tsunamis Occurred on and Near Turkish Coasts (Altinok, 2011)

1.	1410±100 BC: 1700–1380 BC (54), 1600–1500 BC (56); SA; VA; 36.5_ N–25.5_ E (55); IO: X–XII (55); TI1: 6? (11), Rel: 3. Earthquakes and a tsunami accompanied the eruption of the Santorini volcano. The Minoan Kingdom ceased to exist on the Aegean islands (2, 17, 41, 53, 54, 56).
2.	1365±5 BC: _1365 BC (52), 1356BC (23); EM; ER; 35.68_ N–35.8_ E (23); I : VIII–IX in Ugharit (52, 67); AA: half of the Ugharit burnt (52); Rel: 2. Tsunami at Syrian coast (23).
3.	1300 BC: NA; ER; TI1: 6? (11, 41), 5 (54); Rel: 2. Tsunami along the shore of the Ionian Sea and in Asia Minor, Dardanelles, Troy (2, 11, 17, 41, 56).
4.	590 BC: EM; EA; I: Tyre VII? (52); ML: 6.8 (67); Rel: 2. Tsunami at Tyre and on the Lebanese coast (52, 67).
5.	525 BC: EM; EA; I: Tyre VIII–IX (52); ML: 7.5 (67); Rel: 2. Tsunami at Bisri and on the Lebanese coast (52, 67).
6.	330 BC: NA; ER; 40.1_ N–25.25_ E (55); IO _IX (53); Rel: 3. An underground shock near the western shore of Lemnos island generated a strong tsunami (2, 11, 17, 41, 53, 54, 55).
7.	227 BC: 222 BC (2, 55), 220/222/227 BC (54); SA; ER; 36.6–28.25 (43); IO:(IX); M: (7.5) (45); AA: Rhodes Cyprus, Corinth (2, 10, 11, 21, 41, 53); TI1: 3 (54); Rel: 3. Tsunami associated with a large shock in Rhodes (43); originated on the northern shore of the islands of Rhodes and Tilos; many ships were destroyed (54).
8.	140 BC: 138 BC (11, 54); EM; ER; 33.0N–35.0E (55); IO: VIII (55); Rel: 2–3. Silifke region in Turkey was affected by the tsunami (2, 55); tsunami between Akka and Sur (21, 23, 54).
9.	92 BC: EM; EA; I: Syria III–IV, Egypt III–IV (52); ML: 7.1 (67); Rel: 2. Tsunami hit Levantine coastal cities, mostly Syrian-Lebanese coast (52, 67).
10.	26 BC: 23 BC (23); EM; ER; 34.75N–32.4E (55); IO: VII (55); TI1:3 (11, 23), TI2:5 (23); Rel: 2. Tsunami at Pelusium-Egypt (23); tsunami at Paphos- Cyprus (2, 11, 17, 55).
11.	20±20: 50 (55); BS; EA; 43.0_ N–41.0_ E (33); IO: VIII (55); M_6.5 (33); h: 20 (33); AA: Colchis Shore, Sukhumi Bay, the submersion of the ancient town of Dioscuria on the coast of the Sukhumi Bay, Colchis, can be inferred both from local legend and from the archeological remains at the sea bottom (8, 33, 65); TI1: 4–5 (33), TI2: 4–6 (65); Wr: _2.5 (33); Rel: 3–4. The waves were more than 2.5m high in Sukhumi and were associated with an M= 6.5 earthquake (8).
12.	46: SA; VA; 36.4_ N–25.4_ E (45); IO: VIII (55); M: (6.5) (45); AA: North east of Crete, Santorini Isl. (2, 11, 17, 41, 53, 55), south coast of Crete (11); eruption of Santorini Volcano (41); TI1: 3 (54); Rel: 3. Tsunami observed in Crete (45).

Table A.2 (Continued)

13.	62: 66 (41, 53), 53/62/66 (2, 24), 46/62/66 (54); at noon (55); SA; ER; 34.8_ N–25.0_ E (45); IO: IX (55); M: (7.0) (45); AA: Southern coasts of Crete, Lebena (2, 11, 17, 54) and northern coast of Crete (55); TI1: 3 (11, 54); Rel: 4. The sea receded about 1300m (45); the sea in Lebena retreated about 100m from the waterline (54).
14.	68: EM; ER; AA: Demre and Patara region of Lycia (2, 24); Rel: 2. The sea retreated along the coast of Alexandria, Egypt and covered the coast of Lycia; the dark waters of the sea spread sand over Patara (24)
15.	76: 77–78 (21), 76/77 (54); EM; ER; IO: X (55); AA: Larnaka, Paphos, Salamis-Cyprus (2, 10, 11, 17, 55, 56); TI1: 4 (54); Rel: 2. The earthquake was accompanied by tsunami waves seen mostly in Kition, Paphos, Salamis (54).
16.	13 December 115: at night (23); EM; ER/EL; 36.25_ N–36.10_ E (55); IO: (IX) (55); ML: 7.4 (67); AA: Antioch region, Mt. Casius (24, 55); probably triggered by an earthquake generated on the Cyprian Arc fault system (49); Rel: 3. Possible landslide (24); tsunami waves hit Caesaria, the Lebanese coast and Yavne (52, 67).
17.	10 October 123: 120 (54, 55), 10 October 120 (45), 120/128 (24); SM; EA; 40.7_ N–29.1_ E (45, 54); I: IX–XI (24); M: (7.2) (45); AA: Kapıdağ Peninsula (Cyzicus), Iznik and Izmit (24, 55); TI1: 2 (54); Rel: 3. The sea flooded into the Orhaneli (Rhyndacus) River (6, 24).Tsunami in Izmit (54).
18.	142: 144 (55); 148 (41, 43, 44), 142/144 (24); SA; ER; 36.3_ N–28.6_ E (45); I: Rhodes IX (45); M: 7.6 (45); TI1: 3 (11, 41, 44), 3 (43, 54), TI2: 6 (43); Rel: 3–4. A destructive shock caused a strong tsunami in Rhodes, Fethiye Gulf, Kos, Seriphos, Syme, Caria, Lycia (2, 11, 17, 24, 41, 44, 56); destructive sea inundation (43); the sea water penetrated deep into dry land for several miles (54).
19.	262: 261–262 (2, 56); SA; ER; 36.5_ N–27.8_ E (43); IO: IX (55); AA: South coast of Anatolia (2, 11, 17, 24), west Anatolia (54); TI1: 4? (11), 4 (54); 4 (54); Rel: 2. Sea inundation (43); many cities were flooded by the sea, possibly tsunami (54).
20.	300: 293–306 (2, 24); EM; ER; 35.2_ N–33.9_ E (23); I: IX–XI (24); Rel: 1. Great part of Salamis-Cyprus was plunged into the sea by the earthquake (23, 24).
21.	2 April 303: 303/304 (24), 303–304 (52, 67), 306 (55); EM; ER; 33.8_ N–34.3_ E (52); IO: VIII–IX (52); ML: 7.1 (67), MS: 7.1 (52); h: 20 (52); AA: Sidon, Tyre- Syrian (24, 55); Rel: 2. Tsunami in Caesaria in Palestine (52, 67).
22.	342: EM; ER; (34.75_ N–32.4_ E) (55); I: IX–XI (24); AA: Paphos, Famagusta, Salamis, Larnaka-Cyprus (2, 11, 17, 24, 54, 55, 56); TI1: 3 (54); Rel: 4. The harbour of Paphos slid down into sea (54); the tsunami waves were observed on the SW, S and SE shores of Cyprus and in the Bay of Famagusta (54).
23.	344: NA; EA; 40.3_ N–26.5_ E (GITEC); AA: Canakkale region, Thracian coasts (2, 11, 17, 56); TI1: Dardanelles 3, Thrace coasts 4 (11); Rel: 1.
24.	348: 348/349 (24), 348–349 (52, 67); 349 (55); EM; EA/ER; 33.8_ N–33.5_ E (55); IO: (IX) (55); ML: 7.0 (67); AA: Beirut-Leban (24, 55); Rel: 2. Possible tsunami (52); a tsunami was observed on the Arwad island, the Syrian coast and in Beirut (54).
25.	24 August 358: SM; EL; 40.75_ N–29.96_ E (55); IO: (IX) (55); M: 7.4 (15); AA: Izmit Gulf, Iznik, Istanbul (2, 15, 18, 21, 55, 56); Rel: 4. The damaging waves in Izmit could have been generated by coastal landslides (15).
26.	21 July 365: In the morning (24); SA; ER; 35.2_ N– 23.4_ E (45); I: X–XI (24); Mw: 8.5+ (57); AA: East Mediterranean, Crete, Greece, Adriatic coasts, Alexandria, West Anatolia (2, 10, 11, 17, 24, 26, 41, 44, 53, 55); TI1: Methoni, Epidaurus, Crete 4, Adriatic coasts, Alexandria, Sicily 3+ (11), Epidaurus, Crete 4, Alexandria, Albania, Sicily 4 (41), Crete 6, Epidaurus 4+, Methoni 4, Alexandria 3+ (44); Rel: 4. First the sea was driven back and then huge masses of water flowed back (45); shipwrecks were found 2 km off the coastal line on the southwestern shore of Peloponnessus near Methoni (41, 54); tsunami was observed in Asia Minor; the coast of Sicily was flooded (54).

Table A.3 (Continued)

27.	11 October 368: SM; EA; (40.4_ N–29.7_ E) (55); I: VIII (45); M: (6.4) (45); AA: Iznik and its surroundings (2, 24, 55); Rel: 1–2. Depending on the description given by Guidoboni et al. (1994), the waters of Lake Iznik rose up.
28.	1 April 407: 5 July 408 (55), 20 April 417 (19); at night (24); SM; ER; I: VII–VIII (24); M: (6.6) (45); AA: Istanbul (2, 24); TI1: 3–4 (54); Rel: 2. Many ships were wrecked, many corpses carried out to the coast of Hebdoman (Bakirköy-Istanbul) (24, 45). The Ottoman archives confirm that many ships sunk because of a tsunami caused by an earthquake (19).
29.	6 November 447: November 447 (11, 17, 56), 8 November 447 (2, 54), 8 December 447 (55), 447 (GITEC); 26 January 447 at night (9, 24, 45); SM; ER; (40.7_ N–28.2_ E) (4); I: IX–XI (24); M: 7.2 (15); AA: Istanbul, Gulf of Izmit, Marmara Islands, Sea of Marmara and Canakkale coasts (2, 9, 15, 24, 45); TI1: 4- (11), Istanbul 3 (11, 41, 44), Erdek Gulf 4, Marmara Islands 4- (44); Rel: 4. The sea cast up dead fish; many islands were submerged; ships were stranded by the retreat of waters (9, 15, 24, 54).
30.	25 September 478: 24/25/26 September 477/480 (2, 24); SM; EA; (40.8_ N–29.0_ E) (55); IO: IX (55); M: 7.3 (15); AA: Sea of Marmara, Yalova, Izmit, Hersek, Canakkale Region, Bozcaada (Tenedos), Istanbul (2, 15, 24, 55); Rel: 4. In Istanbul the sea became very wild, rushed right in, engulfed a part of what had formerly been land, and destroyed several houses (15, 24, 45).
31.	26 September 488: SM; EA; (40.8_ N–29.6_ E) (55); IO: VIII (55); AA: Izmit Gulf (2, 56), Istanbul (55); Rel: 1. It might be identical with 25 September 478 (55).
32.	524: 523–525 (24), 524/525 (2); EM; EA; (37.2_ N–35.9_ E) (55); IO: (VIII) (55); AA: Southern coasts of Anatolia, Anazarba-Adana (2, 55, 56); Rel: 1.
33.	542: 16 August 542 (24, 45), 6 September 542/543 (54), 16 August 541 (55); winter time (54, 56); SM; I: VIII (24); M: 6.8 (54), M: (6.5) (45); AA: West coasts of Thrace, Bandırma Gulf (2, 56), Edremit Gulf (2, 11, 17); TI1: 4 (11, 54); Rel: 1.
34.	6 September 543: SM; ER; (40.35_ N–27.8_ E) (55); IO: IX (55); M: (6.6) (45); AA: Kapıdağ Peninsula, Erdek, Bandırma (2, 6, 10, 21, 24, 41, 53, 55), Gulf of Edremit (56); TI1: 4 (54); Rel: 3. Tsunami waves were reported (6, 24).
35.	August 545: 543±1 (33), 543 (65); BS; ER; IO: IX (33); M: 7.5±0.5 (33); h: 20±10 (33); AA: Thrace, vicinity of Varna (24, 33); TI1: 5 (33); TI2: 8–10 (65); Wr: 2.0–4.0 (33); Rel: 4. Sea covered the territories of Varna and Balchik (33). In the year 544/545, the sea advanced in the territories of Odessa and Thrace, with a maximum inundation of 6 km on Thrace. Many were drowned in Odessa and Balchik (24). Many people were drowned by the waves along the Bosphorus shores (19). The accompanying earthquake may have been related to the one in Balcik-Bulgaria in 544/545 (8, 9).
36.	January 549: SM; ER; AA: Istanbul; Rel: 2–3. Massive waves were created by the earthquake and a huge fish (porphyron) was thrown on shore (9, 19).
37.	9 July 551: EM; ER+EL; 34.0_ N–35.5_ E (52); IO: IX – X (52); MS: 7.2 (52); h: 28 (52); AA: Lebanese coast (24, 35, 52, 55); TI1: 5 (23), TI2: 8 (23); Rel: 4. Tsunami along Lebanese coast (24, 35, 52, 55, 67); in Botrys Mt. Lithoprosopon broke off and fell in to the sea, and formed a new harbour (24, 35); the sea retreated for a mile and then was restored to its original bed, many ships were destroyed (24, 35); the sea retreating by 1000 m, tsunami waves destroyed many houses (54). Receding distance was 1800m in Botrys (24, 35).
38.	15 August 553: 15 August 554 (24, 45); at night (24); SM; ER; (40.75_ N–29.10_ E) (55); IO: X (55); M: (7.0) (45); AA: Istanbul, Izmit Gulf (2, 24, 55, 56); Rel: 4. Inundation distance about 3000m (56).

Table A.4 (Continued)

39.	15 August 554: 554–558 (24), 554 (21, 53, 55), 556 (43), 558 (GITEC), August 556 (45); SA; ER; 36.8_ N–27.3_ E (43, 45); I: X (45); M: (7.0) (45); AA: The southwest coast of Anatolia, Kos Island, Gulf of Gulluk (2, 10, 11, 17, 24, 41, 44, 45, 55, 56); TI1: 4 (54); Rel: 4. The sea rose up to a fantastic height and engulfed all the buildings near shore in the Island of Kos (43, 45); the sea receded at least 2 km and then flooded a 1-km-wide coastal area; many ships were wrecked; many sea animals and fish perished; waves were possibly observed on the Syrian coast (54).
40.	15 August 555: 15/16 August 555 (2, 18, 53, 56), 11 July 555 (24); SM; EA; AA: Istanbul, Izmit Gulf (2, 18, 21, 53, 56); Rel: 1.
41.	14 December 557: 14/23 December 557 (24) towards midnight (24, 55), 11 October/14 December 558 (54); SM; ER; 40.9_ N–28.8_ E (45, 54); I: IX (45); M: (7.0) (45); AA: Lake Iznik region (9), Gulf of Izmit, Istanbul (2, 21, 24, 55, 56); Many houses and churches were destroyed, particularly in the district Kucukcekmece (Regium, Rhegium or Rhegion) which was an outlying port of Istanbul (45); TI1: 4 (54); Rel: 4. Inundation distance about 5000m (56). Depending on recent archaeological findings this place should be the ancient Theodosian Harbor in Yenikapi, Istanbul.
42.	26 October 740: Early afternoon (24); 08.00 (55); SM; ER; 40.7_ N–28.7_ E (15, 16); I: IX–XI (24); MS: 7.1 (16); AA: Sea of Marmara, Istanbul, Izmit, Iznik, southern coasts of Thrace, Mudanya (2, 9, 10, 11, 15, 17, 24, 26, 41, 55, 56); TI1: 3 (54), 4- (44); Rel: 4. In some places, the sea receded from its shores, without returning to flood the coast (15, 24, 45). The sea retreated behind its usual boundaries and was intense enough to change the frontiers of some cities (9, 15).
43.	18 January 747: 18 January 749 (23, 24, 67), 18 January 743/745/746 (54); in the morning (24), 10:00 (23); EM; EA/EL; 32.50_ N–35.60 (52); IO: (IX) (55); MS: 7.2 (52); h: 25 (52); TI1: 5 (23), TI2: 8 (23); Rel: 4. Waves were observed in Lebanon and Egypt (54); the sea boiled and overflowed and it destroyed most of the cities and villages along the coast (24); surface faulting and liquefaction in Mesopotamia, landslide at Mt. Tabor, many ships sank (52); a village near Mt. Tabor moved 6000m from its original position; Moab fortress, then situated on the coast when the flood of the sea struck was uprooted from its foundations and set down 4500m away (24).
44.	19 December 803: 803 (47); EM; AA: Gulf of Iskenderun (2, 17, 56); TI1: 3 (11); Rel: 1.
45.	30 December 859: 8 April 859 (55), 8 April 859–27 March 860 (24), 30 December 859–29 January 860 (52), November 859/861 (54), 859 (47); EM; EA/EL; 35.7_ N–36.4_ E (52); IO: VIII–IX (52); MS: 7.4 (52); h: 33 (52); AA: Syrian coasts, Adana, Antakya, Samandag, Akka (2, 17, 24, 54); Rel: 4. A landslide on Mt. Casius, rocks fell into the sea (24); a part of Jabal Al-Akraa (Mt. Casius) was split and sank into the sea generating high waves (52); in the region of Samandag the sea receded and then flooded the coast (54).
46.	25 October 989: 26 October 989 (24, 45), evening (24); 19:00 (16); SM; ER; 40.8_ N–28.7_ E (15, 16); I: VIII (24); MS: 7.2 (16); AA: Istanbul, coasts of Sea of Marmara, Gulf of Izmit (2, 18, 21, 24, 56); Rel: 4. The earthquake set up waves in the sea between the provinces of Thrace from Bythia that reached into Istanbul (9, 15, 18).
47.	5 April 991: in the night (24, 52); EM; EA/EL; 33.7_ N–36.4_ E (52); IO: IX (52); MS: 7.1 (52), ML: 6.5 (67); h: 22 (52); AA: Damascus, Baalbek (24, 52, 55); Rel: 2–3. Landslide; tsunami at Syria (52, 67).
48.	5 December 1033: 17 February 1033 (55), 4 January 1034, 6 March 1032, 1039, May 1035 (54); before sunset (25); EM; EA/ER; 32.4_ N–35.5_ E (23); IO: IX (25); M: 6.9 (54); AA: Israel-Palestinian, Syria, Telaviv, Gaza with 70 000 casualties (25, 55); TI1: 3 (23, 54), TI2: 5 (23); Rel: 4. Tsunami and subsidence, a tsunami on the coast of Palestine, causing the water of Akka to recede at night (23, 25); tsunami at Balash (55); the sea port of Akka went dry for a long time, and then it was half destroyed by a wave (54).
49.	12 March 1036/11 March 1037: EM; EA/ER; AA: Cilicia (?), Southern Turkey; mountains were severely shaken and some landslides (25, 67); Rel: 2–3. There was a strong tsunami in relation to this earthquake (25, 67).

Table A.5 (Continued)

50.	2 February 1039: January 1039 (11, 17, 56), 2 January/ February 1039 (54), 1 September 1038–31 August 1039 (25); SM; EA; 41.02_ N–28.5_ E (25); AA: Istanbul and other coastal region of the Sea of Marmara (2, 11, 17, 41, 56); TI1: 4 (54); Rel: 1.
51.	23 September 1064: 23 September 1063 (16, 25, 45), 23 September 1065 (54); at night (25); 22:00 (16); SM; ER; 40.8_ N–27.4_ E (16); IO: (IX) (55); MS: 7.4 (16); AA: Iznik, Bandırma, Murefte and Istanbul (2, 21, 55, 56); Rel: 1.
52.	29 May 1068: 18 March 1068/1067/1069 (54); 08:30 (23); EM; EA/ER; 32.0_ N–34.83_ E (23); IO: IX (25); M: 7.0 (23); AA: Yavne-South Israel, Jerusalem, coast of Palestine (23, 25, 54); TI1: 4 (54), 5 (23), TI2: 8 (23); Rel: 3–4. Tsunami in Holon, Ashdod and Yavne (23, 54); the sea retreated from the coast of Palestine, and then flowed back, engulfing many people, the banks of the river Euphrates overflowed (25, 54).
53.	20 November 1114: 1114 (54), 10 August 1114 (55), November 1114 (52, 67); EM; ER; 36.5_ N–36.0_ E (54); IO: VIII–IX (52); MS: 7.4 (52); h: 40 (52); AA: Ceyhan, Antakya, Maras, Samandag (2, 29, 47, 54, 55); TI1: 3 (54); Rel: 2–3. Landslide (52, 67); tsunami in Palestine (67).
54.	12 August 1157: 15 July 1157 (2, 55); EM; EA; 35.4_ N–36.6_ E (52); IO: IX–X (52); MS: 7.4 (52); h: 15 (52); AA: Hama-Homs, Shaizar region (2, 55), Western Syria including Damascus (52); Rel: 1.
55.	29 June 1170: 03:45 (25); EM; ER; 34.4_ N–35.8_ E (55); IO: X (25); MS: 7.7 (52); h: 35 (52); AA: Trablus, Antakya, Aleppo, Damascus region (52, 55), felt in Cyprus (55); Rel: 2. Tsunami is reported without any location (52, 67).
56.	20 May 1202: 2 June 1201 (47), 21 May 1201 (23), early morning (52), 22 May 1202/1222 (54); EM; EA/ER; 33:43_ N–35.72_ E (25); IO: X (25); MS: 7.6 (52); h: 30 (52); AA: Cyprus, Syrian coasts, Egypt, Nablus, Lebanon (2, 11, 17, 29, 47, 55, 67); TI1: 5 (54), 4 (23), TI2: 7 (23); Rel: 4. Damaging sea wave on Levantine coast (23); the sea withdrew from the coast, ships were hurled onto the eastern coast of Cyprus, fish were thrown onto the shore, and lighthouses were severely damaged (67); Paphos harbour in Cyprus dried (54).
57.	11 May 1222: 25 December 1222, 06:15 (10, 21), May 1222 (2, 10, 11, 17); EM; ER; 34.7_ N–32.8_ E (67); IO: IX (25, 55); M: 7.0–7.5 (67); AA: Baf, Limassol - Cyprus, Nicosia (2, 23, 55, 56, 67); TI1: 3 (23), TI2: 5 (23); Rel: 4. Tsunami flooding in Paphos and Limasol (23); the harbour at Paphos was left completely without water (25, 67).
58.	11 August 1265: 10/11/12 August 1265, at midnight (6); SM; EL; 40.7_ N–27.4_ E (6, 45); I: VIII (13); M: (A big piece of mountain breaks off and tumbles into the sea at Cınarli, Marmara Island, creating huge waves that hit the shore and swallow up the area (6, 25, 45).
59.	8 August 1303: 8/12 August 1303/1304 (54), August 1304 (44), 8 August 1304 (2, 41, 55); 03:30 (25), at 6 a.m. (43); SA; ER; 35.0_ N–27.0_ E (43); IO: X (25, 43, 55, 67); M: 8.0 (43, 45, 54); AA: Crete, Peloponnesus, Dodecanesse Island, Rhodes, Antalya, Cyprus, Akka, Alexandria – Nile Delta, Lebanon, Palastine, Syria (23, 54, 67); TI1: 4 (54), 5 (43), TI2: 10 (43); Rel: 4. Destructive inundation (43); the sea wave drowned many people and threw European ships on land (45); tsunami (25); landslide, the tsunami struck Crete, the coast of Egypt and part of Palestine, and fewer effects were observed in the Adriatic (67); in Egypt, ships sailing in the middle of the Nile and lying at anchor were thrown up into the banks 15m inland (54).
60.	12 February 1332: 16 January 1332 (9, 19, 51), 12 February 1332/1331 (54), 17 January 1332 (25), 12 February 1331 (45); SM; ER; 40.9_ N–28.9_ E (45, 54); IO: VIII (45); M: (6.8) (45, 54); AA: Marmara Sea, Istanbul (2, 9, 11, 17, 54, 56); TI1: 3+ (54); Rel: 3. The waves beat the city walls of Istanbul, seriously damaging many of the dwellings therein (9); huge waves not necessarily of a tsunami but a by the product of the storm in Istanbul (54); a large sea wave covered and destroyed the coastal walls of Byzantium up to their foundation (45).

Table A.6 (Continued)

61.	18 October 1343: 12 February 1331/1332/1334/ 1342/1343/1344 (54), 14 October 1344 (2, 10, 11, 17, 26, 41, 55, 56), 1343.10.18 at 21:00 (16), 16:15 (25, 67); SM; ER; 40.9_N–28.0_E (16); I: VIII (45, 67); MS: 7.0 (16); AA: Sea of Marmara, Istanbul, Marmara Ereglisi (Heraclea), Gelibolu (2, 15, 16, 45, 54, 55); TI1: 4 (54); Rel: 4.Huge waves flooded the shore of Thrace at a great distance, for a mile in some place (54). The sea rushed on land and plains, reaching up to 2000 m. In some places it took off some ships at harbour and crushed them (9, 11, 36, 41, 45); the large sea wave caused great destructions in Istanbul and in several other cities of Thrace in the Marmara (45); the sea receded, leaving mud and dead fish on land behind (9, 25, 36, 67); tsunami waves reached the Strait of Istanbul and affected Beylerbeyi (9, 36).
62.	20 March 1389: 12:30 (25); CA; ER; 38.4N–26.3E (45, 54); IO: VIII–IX (25, 67); M: 6.8 (54); AA: Izmir, Chios (2, 5, 10, 11, 17, 41, 44, 53, 55, 56, 67); TI1: 3 (54); Rel: 4.Tsunami penetrated as far as the market place in Chios (25, 45). The waves caused destruction in Izmir and Yeni Foca (54).
63.	16 November 1403: 1402 (21, 26, 55), 16 November 1402/1403 (54), 18 December 1403 (25, 52); EM; ER; IO: (VIII) (55); AA: Aleppo (25, 52), southern coasts of Anatolia, Syrian coasts (2, 11, 17, 54, 56); mountains collapsed (54); TI1: 3 (54); Rel: 4.Near the shore of Syria and Palestine, the sea receded by more than one mile and then returned to its usual limits (54).
64.	20 February 1404: EM; EA+EL; 35.7_N–36.2_E (52); IO: VIII–IX (52); MS: 7.4 (52); h: 30 (52); AA: Aleppo (52, 67); Rel: 2–3.Landslide with damage in a few cities and tsunami in the Syrian coast (52).
65.	29 December 1408: 30 December 1408 (47), 1408 (23); EM; EA+EL; 35.8_N–36.1_E (52); Imax: X (25); MS: 7.4 (52); h: 25 (52); AA: Western Syria-Cyprus (67); TI1:3 (23), TI2: 5 (23); Rel: 3–4.Landslide in Sfuhen and tsunami in Lattakia (52); tsunami threw the boats onto the shore (25, 67); strong tsunami in Syrian coasts (23); faulting between Sfuhen and Al-Quseir (52); faulting along at least 20 km from Quasr along Dead Sea Fault (25, 67).
66.	18 December 1419: 25 May 1419 (45), 19 December 1419/16 January 1420 (67); SM; ER; 40.9_N–28.9_E (45); M: (6.6) (45); AA: Istanbul (45); Rel: 2.The earthquake caused tsunami (45); the sea became very rough and flooded the land, which was unusual (15).
67.	3 May 1481: 06:30 (25); SA; ER; 36.2_N–28.5_E (54); I: IX (45); M: 7.2 (45); AA: Rhodes, southwestern coasts of Anatolia, Crete (2, 25, 56); TI1:3 (54), TI2:8 (43); Wr: 1.8 (11, 41); Rp: 3 (43, 60); Rel: 4.The largest shock accompanied by a sea wave of 3 m height (43, 45, 54, 60); the wave flooded the land and a ship in the harbour was whisked away, the damage done by the tsunami waves was greater than the damage caused by the earthquake (45, 54). In Rhodes the inundation distance was 60m (11, 41).
68.	1489: 1481/1505–1510 (30); SA; ER; AA: Southern coasts of Anatolia, Antalya (2, 56); Rel: 2–3.Submarine earthquake and strong withdrawal (43); the sea receded for three hours in Antalya (30); a tsunami was described by Leonardo da Vinci to have occurred in 1489 in the sea of Antalya (17, 43)
69.	1 July 1494: Evening time (41, 55); 10:10 (25); SA; ER; 35.5_N–25.5_E (54, 55); Imax: VIII–IX (25); M: 7.2 (54); AA: Heraklion-Crete (2, 11, 17, 25, 44, 55); TI1: 2+ (54); Rel: 4.In the Candia (Heraklion) harbour, large waves caused violent collisions of anchored ships (25, 45, 54); a withdrawal of the sea was observed in Israel (45).
70.	10 September 1509: 22:00 (14, 16); SM; ER; 40.75_N–29.0_E (55); IO: IX (55); MS: 7.2 (16); AA: Istanbul and coasts of the Sea of Marmara (2, 10, 11, 17, 21, 26, 38, 41, 44, 53, 55, 56), felt over a large area from Bolu to Edirne with 4000–5000 casualties (9, 14); TI1: 3+ (44), 3- (54); Rp: 6.0 (38); Rel: 4.The shipyard in Izmit collapsed and waves flooded the dockyard (9, 14, 38); In Istanbul tsunami waves overtopped the walls in Galata and flooded the districts of Yenikapı and Aksaray (2, 9, 38); depending on recent archaeological findings in Yenikapı the inundation distance in this region can be estimated as 500–600m along the paleo-Lycus (Bayrampas, a) stream valley.

Table A.7 (Continued)

71.	29 September 1546: 14 January 1546 (23, 54); EM; EA; 32.0 N–35.1 E (23); I: VIII (23); M: 6.0 (23); AA: Nablus, Damascus, Jarusalem, Yafa, Tripoli, Famagusta (52); Israel and Palestine (23); Jerusalem, Damascus, Yafa, Sisem (61); TI1: 3+ (54), 5 (23), TI2: 8(23); Rel: 4.Tsunami at Cyprus (52); tsunami from Yafa to Gaza (23); many people were killed (61); after the storming sea had returned and rolled onto the coast, over 12,000 inhabitants of Gaza and Yafa were drowned (54); tsunami on the coasts of Cyprus and of Asia Minor (54).
72.	717 July 1577: 18:00 (14); SM; ER; AA: Istanbul (2, 14); Rel: 1.Tremors in the sea, causing the sea to swell and engulf the galleys harboured therein (14).
73.	1598: BS; EA; (40.4) N–35.4 E (55); IO: (IX) (55); AA: Amasya, C, orum (14); TI1: (4–5) (34), TI2: 2–4(65); Wr: 1.0 (34); Rel: 4.Tsunami waves at the coastal area between Sinop and Samsun 8, 34). The waves inundated about 1.6 km landward drowning a few thousand people living in the towns and villages (14).due to the Amasya and C, orum earthquake (2,)
74.	April 1609: SA; ER; 36.4 N–28.4 E (45, 54); IO: IX (43); MS: 7.2 (43); AA: Rhodes, Eastern Mediterranean,SE Aegean Sea (2, 14, 67); TI1: 4 (54), TI2: 8 (43); Rel: 4.Over 10 000 people were drowned by the waves (14); tsunami on the eastern part of Rhodes (54). Very strong waves observed in Rhodes and Dalaman (43, 67).
75.	8 November 1612: SA; ER; 35.5 N–25.5 E (54, 55); IO: VIII (55, 67); MS: 7.0 (67); AA: Northern Crete (2,10, 11, 17, 41, 44, 55, 67); TI1: 5- (54); Rel: 4.Many ships sank in the harbour of Heraklion (45, 54).
76.	28 June 1648: 5 April 1641 (56), 5 April 1646 (2, 9, 54), 1646 (44), 21 June 1648 (14, 45), 28 June 1648, just before sunset (51); afternoon (55); SM; ER; IO: (VIII) (55); M: (6.4) (45); AA: Istanbul (2, 9, 10, 11, 14, 17, 26, 44, 55); TI1: 3 (54), 4- (44); Rel: 4.The sea rushed onto the dry land destroying 136 ships (54, 56).
77.	29 September 1650: 9 October 1650 (11, 17, 45), 29 September 1650 (41, 44); SA; VO; 36.4 N–25.4 (44, 54); I: Santorini VIII; M: (7.0) (45); AA: Santorini, Patmos, Sikinos Islands, Northern Crete (2, 10, 11, 17, 41,44); a strong underground volcanic eruption (45, 54); TI1: Sikinos 4+ (44), Heraklion 4 (41, 44); Wr: Western Patmos 30, Eastern Patmos 27, los 18 (11), Eastern Santorini 19, Patmos 30, los 18 (41); Rp:50 (GITEC); Rel: 4.Inundation distances 200 and 100min Eastern Santorini and Sikinos, respectively (41). The generated sea wave reached a height of 30m in the west coast of Patmos and 27m in the east coast. In Sikinos, the sea entered 180 m inland. In Kea, ships drifted onto land and in Crete many ships broke from their anchorage (45).
78.	30 November 1667: 30 November 1667/10 July 1668 (54), 10 July 1668 (18, 21, 41, 56), November 1667 (55); CA; 38.4 N–27.1 E (54); IO: (VIII) (55); M: 6.6 (54); AA: Izmir Gulf (2, 11, 14, 17, 54, 55, 56); TI1: 2 (11, 41, 54); Rel: 1. The sea was stormy in Izmir (54).
79.	14 February 1672: April 1672 (53, 55), 1672 (17), 1672/1673 the middle of April (54); NA; ER; 40.0 N–26.0 E (54, 55); I: IX (54); MS: 6.8 (67); AA: NE Aegean Sea, SE Aegean Sea (43, 67), Santorini, Cyclades, Bozcaada and Kos islands (2, 14, 17, 41, 43, 55), Cyclades and Santorini (17); Rel: 2. Some houses in Bozcaada disappeared in waves (54); abnormal waves in Kos Island (43, 67); the island sank, no tsunami (11).
80.	10 July 1688: 11.00 (55), 11.45 (14, GITEC); CA; ER; 38.4 N–26.9 E (54); IO: X (55); M: 7.0 (54); AA: Izmir Gulf (2, 11, 14, 17, 44, 55); TI1: 3 (44), 2 (54); Rel: 2. A weak tsunami was noted in Izmir (54). Ships in the harbour were disturbed (45).
81.	31 January 1741: 01:15 (14, 43, 45); SA; ER; 36.2 N – 28.5 E (43, 45, 54, 67); I: Rhodes VIII (45); M: 7.3 (43, 45, 54); AA: Rhodes (2, 14, 43, 45, 54); TI1: 5 (43), TI2: 8 (43); Rel: 4. The sea retreated then flooded the coast of Rhodes 12 times with great violence (2, 14, 43, 45, 67); the upper tsunami sediment layer found in Dalaman could be attributed to the 1741 tsunami (43, 67).
82.	14 March 1743: 8–20 March 1743 (14, 43); EM; ER; AA: Antalya, Rel: 2–3. Sea withdrawal in Antalya (43, 67); the port dried up for some time (14, 43).

Table A.8 (Continued)

83.	15 August 1751: SM; ER; AA: Istanbul (2, 14); Rel: 1–2. An earthquake during a thunderstorm; ensuing flood caused considerable damage, carrying away 15 houses; might have been a minor submarine event causing abnormal waves (14).
84.	21 July 1752: EM; ER; (35.6 N–35.75 E) (55); I: X (23); ML: 7.0 (67); AA: Syrian coast (54); TI1: 3? (54), 2 (23), TI2: 3 (23); Rel: 3. Tsunami at Syrian coasts (2, 11, 17, 21, 23, 52, 55, 67); harbour constructions in Syria suffered, possibly from the attack of tsunami waves (54).
85.	2 September 1754: 21:45 (55), 21:30 (16); SM; ER; 40.8 N–29.2 E (15, 16); IO: IX (55); MS: 6.8 (16); AA: Izmit Gulf and Istanbul (2, 14, 15, 55); Rel: 2–3. In places the sea receded from the shore, presumably in Istanbul (15).
86.	30 October 1759: 03:45 (23, 52); EM; EA/EL; 33.1 N–35.6 E (23, 52); IO: VIII–IX (52); MS: 6.6 (23, 52); h: 20 (52); AA: Palestine and Lebanon (54); TI1: 3 (23), TI2: 5 (23); Rp: 2.5 (23); Rel: 4. Landslides at the west of Damascus and Tabariya (52). Tsunami at Akka and Tripoli (23, 52).
87.	25 November 1759: 19:23 (23, 52); EM; EA/EL; 33.7 N–35.9 E (23, 52); I: X (23); MS: 7.4 (23, 52); h: 30 (52); AA: Bekaa-Syria, Antakya (23, 55), faulting along the Bekaa Valley (52); TI1: 4 (23), TI2: 7 (23); Rel: 4. Landslides near Mukhtara and Deir Marjrios (52); tsunami in Akka (23, 52).
88.	22 May 1766: 05:30 (14, 41, 55), 06:00 (51); SM; ER; 40.8 N–29.0 E (15, 16, 54); IO: IX (55); MS: 7.1 (16); AA: Istanbul and Sea of Marmara (2, 11, 14, 17, 41, 53, 54, 55, 56) causing 4000–5000 casualties and heavy damage extended over a large area from Izmit to Tekirdag (14); TI1: 2 (11, 41, 54); Rel: 4. Tsunami waves were recognized in the coastal village Besiktas-Istanbul and the inner parts of the Straits of Istanbul; uninhabited islets in the Sea of Marmara were said to have half-sunk into the sea. Izmit coasts were badly damaged by sea waves (9, 14, 15); strong waves were particularly effective along the Bosphorus and in the Gulf of Mudanya (14).
89.	24 November 1772: 07:45 (2, 5, 14); CA; ER; 38.8 N – 26.7 E (45); I: Foc,a (VIII) (45); M: (6.4) (45); AA: Chios Island and Foc,a (2, 5, 14); Rel: 3. The gates of Foc,a Castle, which were on the edge of the sea, were completely destroyed by the earthquake and tsunami (14).
90.	13 August 1822: 21:50 (52), 20:00 (28); EM; EA; 36.1 N–36.75 E (52); IO: IX (52); MS: 7.0 (52); h: 18 (52); AA: Antakya, Iskenderun, Kilis and Latakia (28, 55) with 20 000 casualties (52, 55); TI1: 3 (54); Rel: 4. Faulting and tsunami in Beirut (52); tsunami in Beirut, Iskenderun, Cyprus and Jerusalem (54, 67).
91.	23 May 1829: 5 May 1829, 09:00 (45); SM; ER/EA; I: Drama X (45); M: 7.3 (45, 54); AA: AA: Istanbul, Gelibolu (2, 55, 56); TI1: 2 (11, 54); Rel: 1. Tsunami in Istanbul (2, 10, 17, 28, 55, 56); a spurious event (15); two shocks in Istanbul, buildings damaged on the Asiatic coast (28). An unusual roughness in the sea was observed (54).
92.	1 January 1837: 03:00 (28, 55), 16:00 (52); EM; EA/ER; (32.9 N–35.4 E) (55); IO: VIII (52); MS:>7.0 (52); AA: Israel and Syria (23) with 5000 casualties (28, 55); Rel: 3. Tsunami on the coasts of Israel and Syria (23); tsunami in Lake Tabariya (28, 52).
93.	18 October 1843: SA; ER; 36.3 N–27.7 E (45); IO: IX (55); M: 6.5 (44, 54); AA: Chalki and Rhodes Islands, 6000 dead (55); Rel: 3. Chalki, tsunami was observed (54). Ships overturned and a mountain collapsed (45).
94.	25 July 1846: 17:30: CA; ER; AA: Izmir, Aegean Sea (54); TI1: 3? (54); Rel: 1. The sea was very turbulent during fine weather (54).
95.	28 February 1851: 15:00 (43, 45, GITEC), 02:58 (54); SA; ER; 36.4 N–28.7 E (67); IO: IX (55, 67); MS: 7.1 (67); AA: Fethiye, Kaya-Muçgla, Rhodes (2, 11, 17, 28, 41, 44, 53, 55, 56, 67); TI1: 3 (11, 41, 54); Rp: 0.6; Rel:4. Tsunami in Fethiye (43, 67); a subsidence on the Fethiye coast and landslides from the Muçgla mountainsides (45). The sea in Fethiye rose approximately 34 cm. The shore in Fethiye sunk 0.5m (54); the coast was flooded about 0.6m above the normal sea level at Fethiye (43, 67).

Table A.9 (Continued)

96.	3 April 1851: 3/23 April/May 1851 (54); 17:00 (54); SA; ER; 36.4 N–28.7 E (43, 67); AA: Gulf of Fethiye (2, 11, 17, 41, 56, 67), Rhodes (54); TI1: 3 (54); Rp: 1.8; Rel: 4. Tsunami in Fethiye (43, 67). The sea rose many meters higher than its level and flooded the coast (54). This event was possibly an aftershock of the 1851.02.28 earthquake; the run-up was 1.8m in the Fethiye region (43, 67).
97.	23 May 1851: 23 April/May 1851 (54); SA; ER; 36.4 N–28.7 E (43, 67); AA: AA: Rhodes, Dodecanese Islands and Chalki (2, 11, 17, 41, 43, 54, 56, 67); possibly an aftershock of the event of 28 February 1851; TI1: 2 (11, 41, 54); Rel: 2. Tsunami waves observed in Rhodes and Chalki, but the reported inundation distances are doubtful (43, 67).
98.	12 May 1852: 5/12 May 1852, 02:00 (54); CA; ES; TI1: 2–3 (54), 3 (11, 41); Rel: 1–2. The day before the earthquake occurred in Izmir (2, 11, 17, 28, 41, 54) the sea receded leaving the sea bottom dry for a distance of many yards (54). Rather strong tsunami at Izmir (28).
99.	8 September 1852: 22:30 (54); CA; AA:Izmir (2, 11, 17, 28, 41, 56), Fethiye Gulf (56); TI1: 3 (54); Rel: 1–2. Rather strong tsunami at Izmir (28); the sea rose, though no slightest breath of wind was to be felt before (54).
100.	13 February 1855: 9/10/13 February 1855 (21, 29), 2 March 1855 (28, 55), 9–13 February 1855 (56); EM; ER; AA: Chios Island (56), Fethiye Gulf (2, 11, 17, 21, 29, 41); Rel: 2. Tsunami waves in Fethiye with doubtful inundation (43, 67). Depending on the definitions given by Karnik (1971), a 32-m-wide coastal strip in Fethiye sank into the sea.
101.	12 October 1856: 00:45 (55), 02:45 (45); CA/SA; ER;(35.5 N–26.0 E) (28, 54); I: Heraklion IX (45); M: 8.2 (45); AA: Crete and Heraklion (45, 54), Rhodes, Crete, Chios, Karpatos (55); TI1: 3+ (54); Rel: 2–3. A tsunami was generated (54).
102.	13 November 1856: 13 December 1856 (56); CA; ER; 38.25 N–26.25 E (55); IO: VIII (5); M: 6.6 (44, 54); AA: Chios Island (2, 5, 11, 17, 28, 41, 44, 45, 53, 54), Rhodes (55); TI1: 3+ (54); Rel: 4. A large tsunami wave was observed (54); the sea rushed on the land and some people were lost in Chios (5, 45).
103.	17 September 1857: 22:00 (28, 54); SM; ER+EL; AA: Istanbul (54); Rel: 1. Houses on the seashore and the cellar of a brewery at Kuruc.es.me, Bosphorus, were flooded by seawater, a consequence of local land subsidence (54).
104.	21 August 1859: 02:00 (45, 55), 11:55 (28, 54), 11:30 (16); NA; ER; 40.3 N–26.1 E (15, 16); IO: IX (55); MS: 6.8 (15, 16); AA: Gokceada (Imbros) Island (45, 54, 55), felt at Enez, Edirne, Istanbul and Gelibolu (28); TI1:3 (54); Rel: 1–2. Some sailors at sea reported the disappearance of Gokceada for a moment. The sea waves observed at the northern approaches of the Strait of Istanbul could not be related with this event (15).
105.	22 March 1863: 22 April 1863, 20:30 (28, 55), 22 April 1863, 21:30 (45); 22:15 (54); SA; ER; 36.5 N – 28.0 E (28, 54, 55); I: Rhodes X (45); M: 7.8 (45); AA: Rhodes (45, 54); Rel: 2–3. The earthquake gave rise to a terrible storm at the sea which resulted in many accidents, several calamities occurred on the Mersin roadstead, the sea near Tripoli (Lebanon) was furrowed by huge waves at midday of 22 March (54).
106.	19 January 1866: 12:30 (5, 54); CA; ER; 38.25 N – 26.2 E (55); IO: VII (54, 55); M: 6.8 (54); AA: Chios Island (5, 54); Rel: 2. Intensive boiling of the sea water was noticed approximately in the middle of the Cesme strait, oscillations of the level were observed (54).
107.	31 January 1866: 28/31 January 1866 (54); at night (45); SA; ER; 36.4 N–25.4 E (44, 45); IO: (VIII) (55); M: 6.1 (28); AA: Santorini Island (2, 28, 44, 45, 54, 55); TI1: Santorini 4, Kythera 3, Chios 3 (44); Rel: 1–2. The sea started to hit the coastal houses causing cracks and submersions (45); some other sources indicate that no tsunami occurred (54).
108.	2 February 1866: CA; ER; 38.25 N–26.25 E (28, 55); IO: VIII (55); M: (6.4) (45); AA: Chios Island (2, 11, 17, 21, 28, 55); TI1: 3 (11, 54); Rel: 2. Tsunami in Chios (28, 54, GITEC). This earthquake was preceded by a strong shock on 19 January (45).

Table A.10 (Continued)

109. 7 March 1867: 06:00 (55), 16:00 (28), 18:00 (45, 54); CA; ER; 39.1 N - 26.6 E (54); I: (X) (45); M: 6.8 (45); AA: Lesvos Island (45, 54, 55), at Mitilini more than 500 casualties (28, 55); TI1: 2 (54); Rel: 4. After the earthquake dead fish were found inside a boat in the Mitilini harbour, the low-lying lands of Mitilini were flooded after the earthquake (45, 54).
110. 3 April 1872: 2 April 1872, 07:45 (55), 07:40 (23); EM; EA; 36.25 N.(36.10) E (55); IO: (IX) (55); MS:7.2 (23, 67), MS:5.9 (52); h: 10 (52); AA: Antakya, Samandag (55), Amik Lake (23); faulting at Baghras, liquefaction (52); TI1: 3 (23), TI2: 6 (23); Rel: 4. Tsunami waves flooded the Samandag (Suaidiya) coast (23).
111. 19 April 1878: 09:00 (55); SM; EA/ER; 40.7 N - 30.2 E (15); I: IX (54); M: 5.9 (15); AA: Izmit (2, 10, 11, 15, 17, 28, 55, 56), Istanbul, Bursa, Sapanca (55); TI1: 3 (11, 54); Rel: 4. In the Gulf of Izmit the shock set up a small tsunami which propagated into the west of the Gulf where the earthquake was also felt on board of ships, causing some concern (15). A rather strong tsunami was supposedly observed in Izmit (54).
112. 3 April 1881: 11:30 (28, 55); CA; ER; 38.3 N - 26.2 E (5); I: Chios IX (5, 45); M: 6.5 (5, 45); AA: Chios Island and C \square C esme (5, 55) with 4000 casualties; TI1: 2+ (54); Rel: 3. On 5 April at 03:10 a.m. a strong vertical shock demolished some city walls. The sea became wavy right away and a mass of smoke was seen rising from sea surface. The aftershocks created waves on the sea surface (5).
113. 9 February 1893: 28 January 1893 (21, 55), 9 February 1893/28 January 1893 (54); 18:00 (41, 45, 55), 17:16 (16); NA; ER; 40.5 N-26.2 E (15; 16); IO: IX (55); MS: 6.9 (15, 16); AA: Northern Aegean Sea, Samothrace Island, Thracian coasts, Alexandroupolis (2, 10, 11, 17, 21, 28, 41, 44, 55); TI1: Alexandroupolis 3 (11, 41, 44); Wr: Samothrace 0.9 (11, 41), Alexandroupolis 0.9 (41), Islet Aghistro and Alexandroupolis 1.0 (28, 54); Rp: 1.0, Saros (15); Rel: 4. Tsunami at Thracian coasts (55); the water rose by 1m near Islet Aghistro and entered the land in a distance of 25.30m and 40m in Aghistro and Alexandroupolis, respectively (28, 41, 45, 54); tsunami flooded the coast on Samothrace and the mainland in Thrace about 15 min after the main shock (15).
114. 10 July 1894: 12:24 (16), 12:30 (55), 12:33 (28, GITEC); SM; ER; 40.6 N - 28.7 E (28, 54); IO: (X) (55); MS: 7.3 (16); AA: Istanbul (2, 11, 17, 22, 28, 29, 38, 39, 41, 44, 55), Izmit (15), Karamursel, Adapazari, Prince Islands off the coast of Istanbul (55); 474 casualties in Istanbul (9, 39); TI1: 3 (54); Wr: \leq 6.0 (38); Rp: 1.5m in Yesilkoy (San Stefano), 4.5m at the Azapkapi Bridge (9, 15); Rel: 4. Tsunami occurred with a receding distance of 50m and a maximum inundation distance of 200m between Buyukcekmece and Kartal (2, 39).
115. 31 March 1901: BS; EL; 43.4 N-28.5 E (GITEC); IO: X (GITEC); AA: Balchik, Bulgaria (27); Wr: 3.0 (20); Rel: 4. At Balchik boats uplifted (GITEC) and landslide occurred (27). The coastal area (0.2 km ²) at Kecikaya District subsided (27). A three-meter-high tsunami washed away the port of Balchik (20).
116. 9 August 1912: 01:29 UTH (4), 01:28 (16); SM; ES; 40.75 N - 27.2 E (EMSC) I: X (12); MS: 7.3 (12, 15, 16, KOERI); h: 16 (4); AA: Sarkoy, Murefte, Istanbul (4), Ganos (15) with 2800 casualties (12); TI1: 3.4; Rp: Yesilkoy 2.7 (4); Rel: 4. A high water occurred within the Bosphorus, demolishing a yacht named "Mahrusa" anchored at Pasabahce (4); the sea receded along the Tekirdag shores (12). The ships anchored offshore Yesilkoy were aground with the recede of the sea after the earthquake and then the sea lifted the fishery boats up to a height of 2.7m (4).
117. 31 March 1928: 00:29:47 (2, 28, 41); CA; EA; (38.2 N - 27.4 E) (EMSC); IO: IX (28); MS: 6.5 (54, KOERI); AA: Izmir (2, 11, 17, 28, 41, 54); TI1: 2 (54); Wr: 0.5 (54); Rel: 2. A weak tsunami (54).
118. 23 April 1933: 05:57:37 (45), 05:58 (54); SA; ER; 36.8 N - 27.3 E (45); IO: IX (28); M: 6.6 (45); h: 50 (28, 54); AA: Kos Island and Nisyros (45, 54); TI1: 2 (54); Rel: 2. An earthquake and tsunami took place (54).

Table A.11 (Continued)

119.	4 January 1935: 14:41:29 (6), 14:41:30.4 (KOERI), 16:41:29 (6); SM; ER+EL; 40.64 N - 27.51E (6); IO: IX (6); MS: 6.4 (6); h: 30 (KOERI); AA: The villages of Marmara Island were totally destroyed; strongly felt in Istanbul, Tekirda.g, Edirne, Izmir and Bursa (6); TI1: 2.3; Rel: 4. The Hayırsız Island collapsed on three sides causing a local tsunami (6).
120.	26 December 1939: 23:57:16 (2); BS; EA; 39.7 N - 39.7 E (2); I: XI (2); MS: 8.0 (2); h: 20 (KOERI); AA: Erzincan (33, 65); TI1: 4 (33), TI2: 3.5 (65); Wr: 1.0 (33); Rel: 4. Fatsa; extraordinary sea disturbances were seen at the time of the Ms = 8.0 Erzincan earthquake (2, 8, 33, 46, 65). The sea receded in Fatsa about 50m and then advanced 20m. In Unye the sea receded about 100m causing some sunken rocks to appear for the first time. The sea also receded in Ordu by about 15m and then returned back. The initial rise of the sea level was recorded at 6 tidal stations (Tuapse, Novorossiysk, Kerch, Feodosia, Yalta, and Sevastopol) on the northern coast of the Black Sea (32).
121.	20 January 1941: 03:37 (23); EM; ER; 35.0 N–34.0 E (28); Imax: IX (28); MS: 5.9 (23); AA: Cyprus and Ammochostos (23); TI1: 2 (23), TI2: 3 (23); Rel: 2. Small tsunami on Palestine coast (23).
122.	6 October 1944: 02:34:48.7 (7); CA; ER; 39.48 N–26.56 E (7); IO: IX (7); MS: 6.8 (7); h: 20 (EMSC); AA: Earthquake in Ayvacik and Edremit Gulf with 30 casualties and 5500 damaged/destroyed houses (7); TI1: 4; Rel: 4. Numerous surface cracks and water gushes reported; coastal neighborhoods of the town of Ayvalik were flooded; inundation distance was 200 m in Ayvalik (7).
123.	9 February 1948: 12:58:13 (2, 41, 43, 45, 67); SA; ER; 35.51 N–27.21 E; IO: IX (67); MS: 7.1 (67); h: 40 (EMSC); AA: Karpathos-Dodecanese (2, 11, 17, 31, 41, 42, 44); TI1: 4 (43, 54), TI2: 7 (43); Rp: 2.5; Rel: 4. Damaging waves in Karpathos (43, 67, GITEC); a destructive tsunami originated and rolled along the eastern shore of the Island of Karpathos (54); tsunami caused damage on the southwest coast of Rhodes (45); the first tsunami wave followed about 5–10 min after the earthquake, many vessels were cast ashore and destroyed (43, 67); the 1948 wave penetrated inland about 250m leaving scores of fish behind to a distance of about 200m from the shore line (43); the first motion of the sea was withdrawal (43, 67); inundation distance of 900m (11, 41, 42); inundation distance of 1000m near Pigadia (45, 54).
124.	23 July 1949: 15:03:30 (42), 15:03:33.2 (KOERI); CA; ER; 38.58 N–26.23 E (5, 45); IO: IX (5, 45); M: 6.7 (5, 45); h: 10 (KOERI); AA: East Aegean Sea, North Chios Island (2, 42, GITEC); TI1: 2 (54); Wr: 0.7/2.0 (2, 42); Rel: 4. In Chios, the port sank 0.35 m; the sea attacked the coast of Cesme town, leaving many dead fish behind after it retreated (5).
125.	10 September 1953: 04:06 (54), 04:06:09 (23); EM; ER; 34.76 N–32.41 E; I: X (54); M: 6.2 (40); h: 30 (KOERI); AA: South coasts of Turkey (2, 31) and Paphos (23); TI1: 2–3 (54), 2 (23), TI2: 3 (23); Rel: 3–4. Series of tsunami waves were noted on the Island of Cyprus (54); small tsunami wave along the coast of Paphos (23).
126.	9 July 1956: 03:11:40 (41, 42, 45, 67); SA; ER; 36.69 N–25.92 E (KOERI); IO: IX (67); MS: 7.5 (67); h: 10 (KOERI); AA: Greek Archipelago, Amargos, Astypalaea Islands, Fethiye (2, 11, 17, 31, 41, 42, 66); 03:12 and 05:24, event associated with two shocks (54); TI1: Amargos 6 (41), Astypalaea 6 (42); Wr: Amargos 30 (11), 20–25 (41, 42); 30 (11), Astypalaea 20 (11, 41, 42), Pholegandros 10 (11, 41), Patmos 4, Kalimnos 3.6, Crete 3, Tinos 3 (11), 5 (41), Fethiye 1 (66); Rel: 4. Huge waves flooded the fields in the islands. The sea rose up 1m and a recorded inundation distance of 250m in Fethiye (66); inundation distance at Amargos 80–100m (41, 42); at Astypalaea 400m (41, 42); at Pholegandros 8m (41), at Tinos ≥700m (41).
127.	23 May 1961: 02:45:20 (45), 02:45:22 (KOERI); SA; ER; 36.6 N–28.3 E (EMSC); I: Rhodes (VII) (45); h: 72 (EMSC); AA: Marmaris, Fethiye, Rhodes, Izmir, Aegean Sea (45, 54, 59); TI1: 3 (54); Rel: 2. A weak wave, the color of the water in the Gulf of Izmir changed after the earthquake and it was filled with algae (54); the sea colour turned red in Fethiye and Izmir after the earthquake (59).

Table A.12 (Continued)

128. 18 September 1963: 16:58:14.8 (2, 37); SM; ER; 40.64 N–29.13 E; IO: VIII (37); MS: 6.3 (2, KOERI); h: 40 (EMSC); AA: Eastern Marmara, Yalova-Cınarcık, Karamursel, Kılıç, Armutlu, Mudanya, Gemlik Gulf (2, 29, 37); Rp: 1.0 (2, 29); Rel: 4. Along the coast of Mudanya a strip of sea shells and molluscs was observed and waves reached a height of 1m (2, 29, 37).
129. 19 February 1968: 22:45:42 (41, 45), 22:57:47 (42); NA; ER; 39.4 N–24.9 E (54); I: Aghios Eustrations IX (45); M: 7.1 (45); AA: North Aegean Sea (2, 17, 31); TI1: 2 (41), 3 (54); Wr: 1.2 in Mirina (41, 45, 54); Rel: 4. A small tsunami originated on the western (54) and southern (45) shore of the Island of Lemnos; the sea penetrated on land by 20m in Moudros and 4m in Kaspakas (45, 54).
130. 3 September 1968: 08:19:52.6 (2); BS; ER; 41.78 N–32.43 E (1); IO: VIII (1); MS: 6.6 (1); h: 4 (1); AA: Bartın and Amasra (1); TI1: 3+ (33), TI2: 3–5 (65); Wr: 3.0 (48); Rel: 4. The Bartın earthquake exhibited the first known seismological evidence of thrust faulting along the southern margin of the Black Sea (1). The coastal hills between Çakraz and Amasra were uplifted. The sea receded 12–15m in Çakraz and never returned entirely to its original level (29). The sea inundated 100m in Amasra and after 14 min the second wave inundated the shore about 50–60m (62). The reason for this progression was most probably the uplifting around Çakraz (2, 8, 65). The sea rose about 3m in Amasra (48).
131. 6 August 1983: 15:43:51.9 (KOERI); 15:43 (45); NA; ER; 40.0 N–24.7 E (45); I: Aghios Dimitrios VI (45); M: 6.8 (45); h: 10 (EMSC); AA: Lemnos Island (45); TI1: 2+ (54); Rel: 3–4. Tsunami on Lemnos Island (54); light tsunami waves in Mirina of Lemnos (54).
132. 4 January 1991: CA; ER; 37.7 N–26.3 E; AA: Ikaria Island (54); TI1: 2; Rel: 1. Weak local sea waves in Ikaria Island; possibly of meteorological origin (54).
133. 7 May 1991: CA; ER; 37.1N–26.8E; AA: Leros Island (54); TI1: 3; Wr: 0.5; Rel: 1. Sudden and intense rise of the sea level by 0.5 m in Leros Island; possibly of meteorological origin (54).
134. 17 August 1999: 00:01:38.6 (KOERI); SM; EA+EL; 40.73 N–29.88 E; MW: 7.4 (2, 3, 50, 58, 63, 64); h: 18 (2); AA: A very strong earthquake with at least 18850 casualties in the Gulf of İzmit was felt over a very large area (9). The earthquake produced at least 120 km of surface rupture and right lateral offsets as large as 4.2m with an average of 2.7m (3, 9); TI1: 3; Wr: Degirmendere≥12 (3); Rp: Degirmendere 4m (50), Yarımca 3.2m (58), generally between 1–2.5m (2, 3); Rel: 4. The runups are more complex along the south coast due to the presence of coastal landslides (2, 3, 9, 50, 63, 64). The period of tsunami was less than 1 min (63). The inundation distance in Kavaklı was more than 300m(3).

APPENDIX B

RESULTS OF SIMULATIONS FOR 5KM FOCAL DEPTH

- PI SOURCE

Table B.1 Results of PI Simulation at the Selected Gauge Points

Name of gauge pt.	Depth of gauge pt.(m)	X	Y	Arrival time of initial wave (min)	Arrival time of max.wave (min)	Maximum (+) wave amp.(m)	Maximum (-) wave amp.(m)
Bakirkoy	9.0	28.826200	40.952800	0	8	0.9	-0.9
Bandirma	6.6	27.968300	40.360600	32	73	0.5	-0.6
BigaLiman	3.9	27.135900	40.451600	39	54	0.2	-0.2
Cinarcik	4.8	29.136000	40.651500	0	12	2.4	-4.3
Hpasa3	9.1	29.014800	40.995700	0	31	1.2	-1.0
Kcekmece2	5.9	28.723800	40.969300	0	80	1.2	-1.3
Mudanya	8.4	28.908900	40.367500	0	85	0.6	-0.5
Sarkoy	5.3	27.336100	40.744900	18	74	0.2	-0.2
Tekirdag2	9.5	27.519700	40.971100	19	33	0.4	-0.3
Tupras	8.3	29.935000	40.737200	31	85	0.6	-0.9
Yalova	8.1	29.276900	40.663400	0	4	0.7	-1.2
Yenikapi	9.7	28.966500	41.001800	0	31	1.1	-0.9

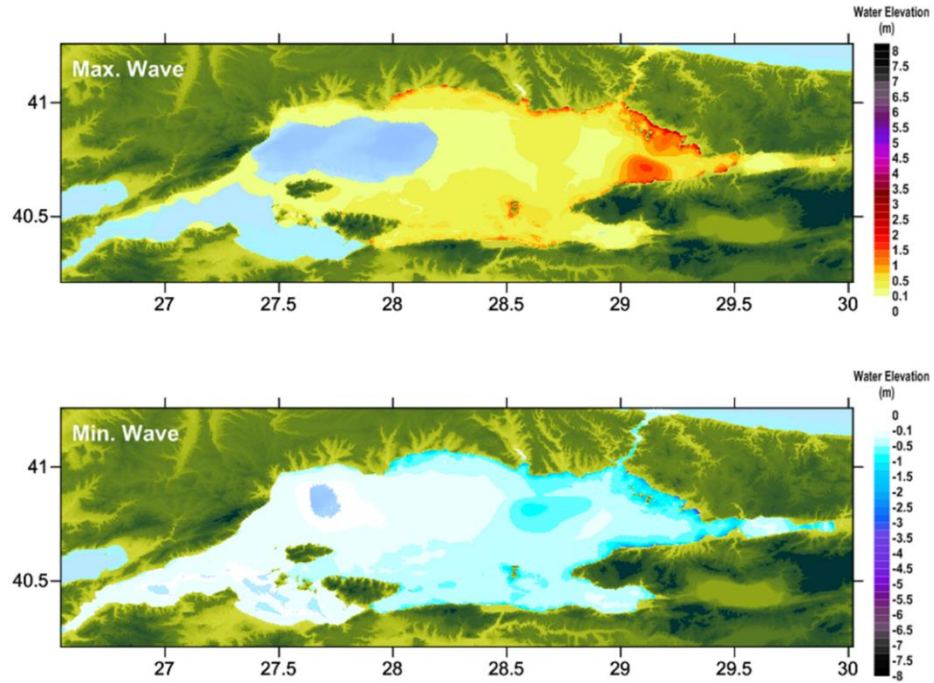


Figure B.1 Distribution of Maximum (+) Wave Amplitude (top) and Minimum (-) Wave Amplitudes

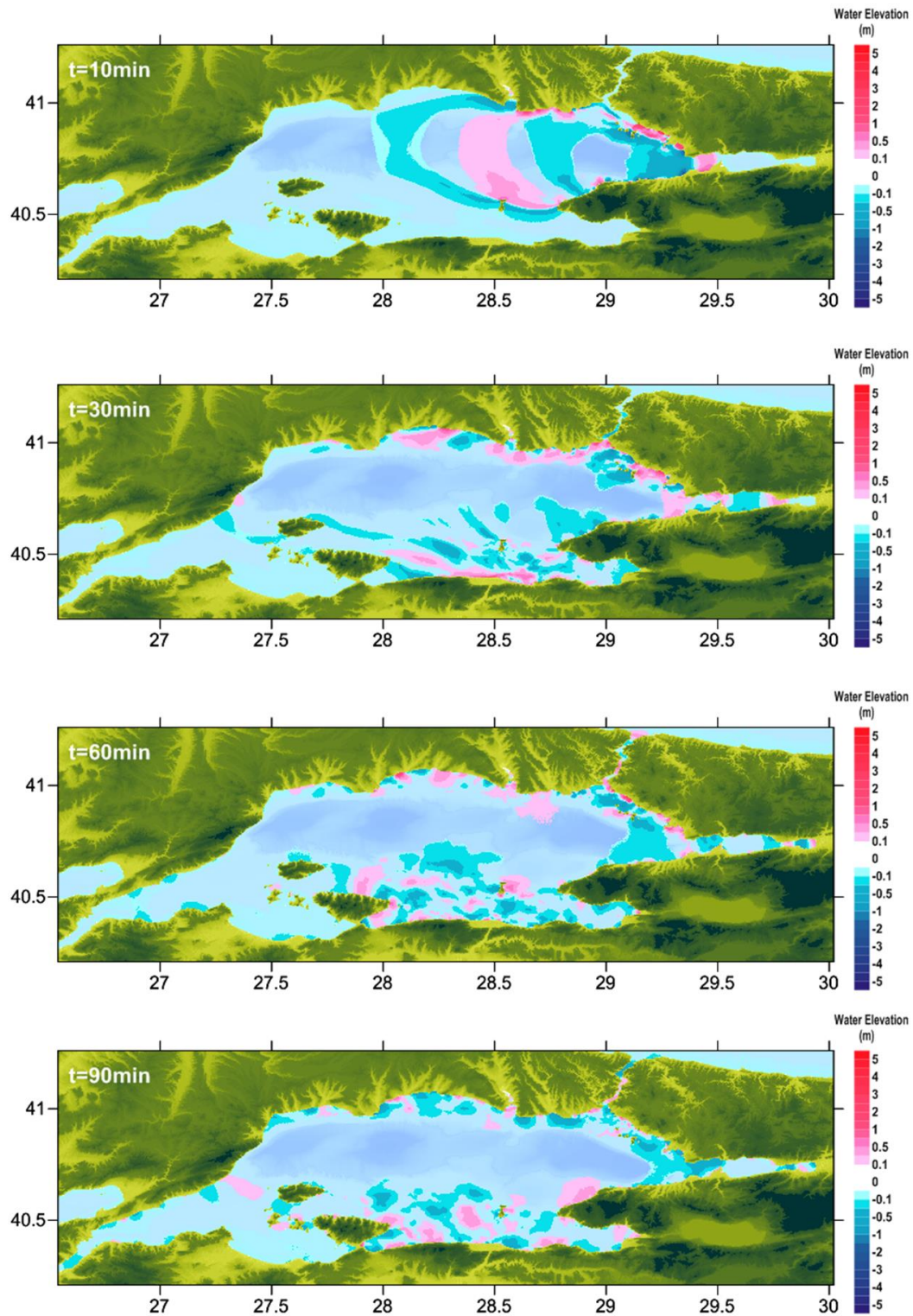


Figure B.2 Sea states at $t=10$, 30, 60, and 90 min respectively according to the tsunami source PI

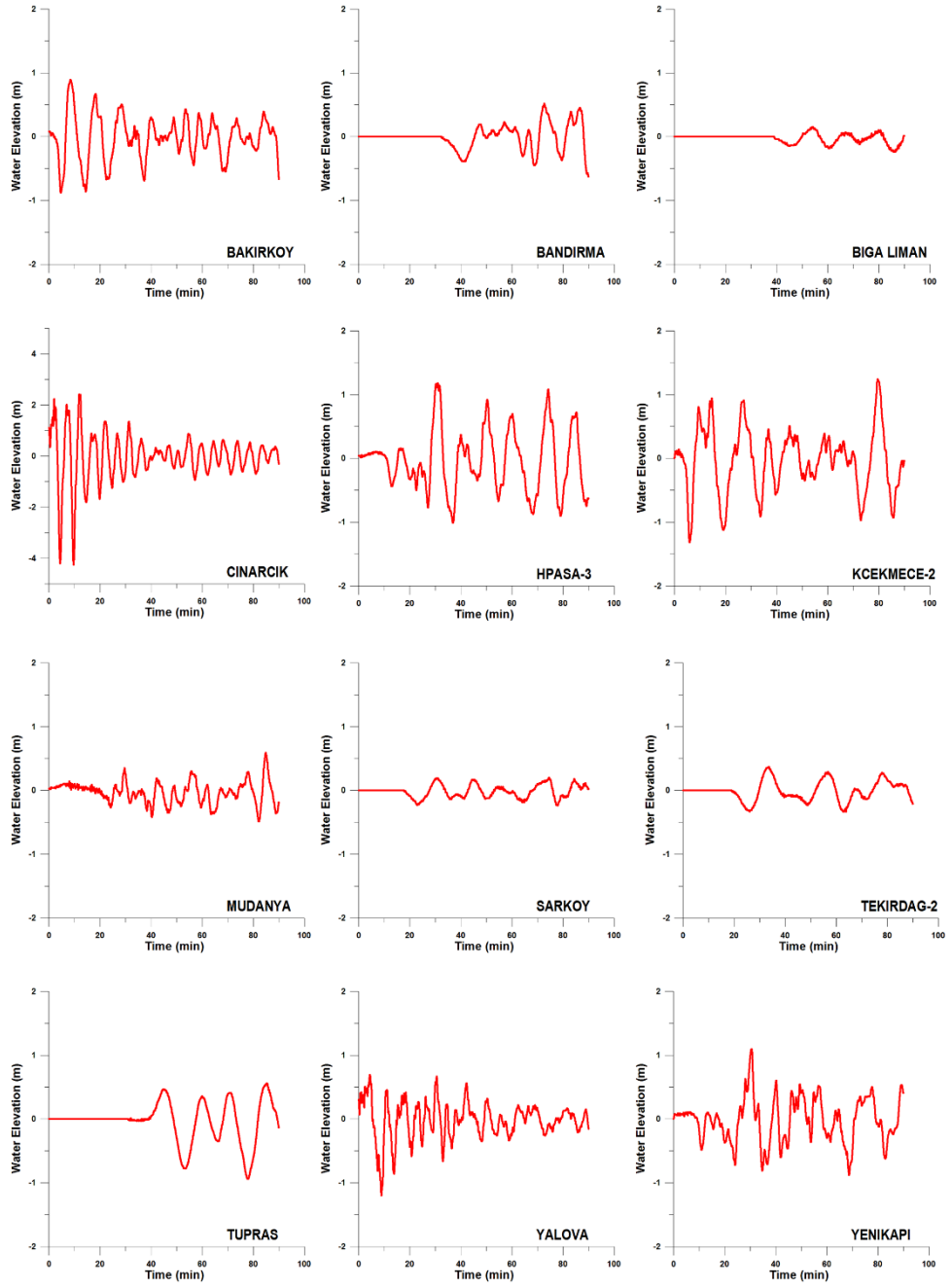


Figure B.3 Time Histories of Water Surface Fluctuations at the Selected Gauge Locations for PI

- PIN SOURCE

Table B.2 Results of PIN Simulation at the Selected Gauge Points

Name of gauge pt.	Depth of gauge pt.(m)	X	Y	Arrival time of initial wave (min)	Arrival time of max.wave (min)	Maximum (+) wave amp.(m)	Maximum (-) wave amp.(m)
Bakirkoy	9.0	28.826200	40.952800	0	21	1.0	-1.2
Bandirma	6.6	27.968300	40.360600	41	90	1.0	-0.8
BigaLiman	3.9	27.135900	40.451600	44	83	0.1	-0.3
Cinarcik	4.8	29.136000	40.651500	0	4	2.8	-2.4
Hpasa3	9.1	29.014800	40.995700	0	37	1.6	-1.6
Kcekmece2	5.9	28.723800	40.969300	0	17	0.9	-1.0
Mudanya	8.4	28.908900	40.367500	0	71	0.5	-0.6
Sarkoy	5.3	27.336100	40.744900	23	82	0.3	-0.3
Tekirdag2	9.5	27.519700	40.971100	25	63	0.3	-0.5
Tupras	8.3	29.935000	40.737200	30	78	0.5	-0.8
Yalova	8.1	29.276900	40.663400	0	9	1.3	-1.0
Yenikapi	9.7	28.966500	41.001800	0	44	1.2	-1.1

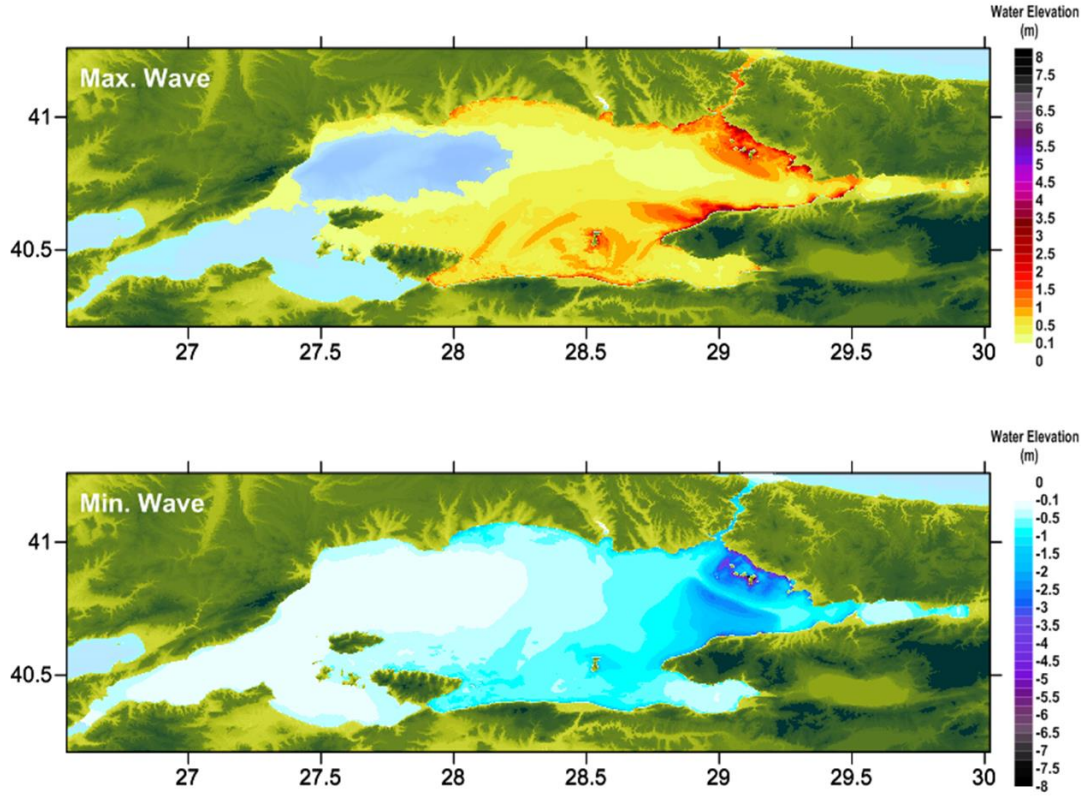


Figure B.4 Distribution of Maximum (+) Wave Amplitude (top) and Minimum (-) Wave Amplitudes

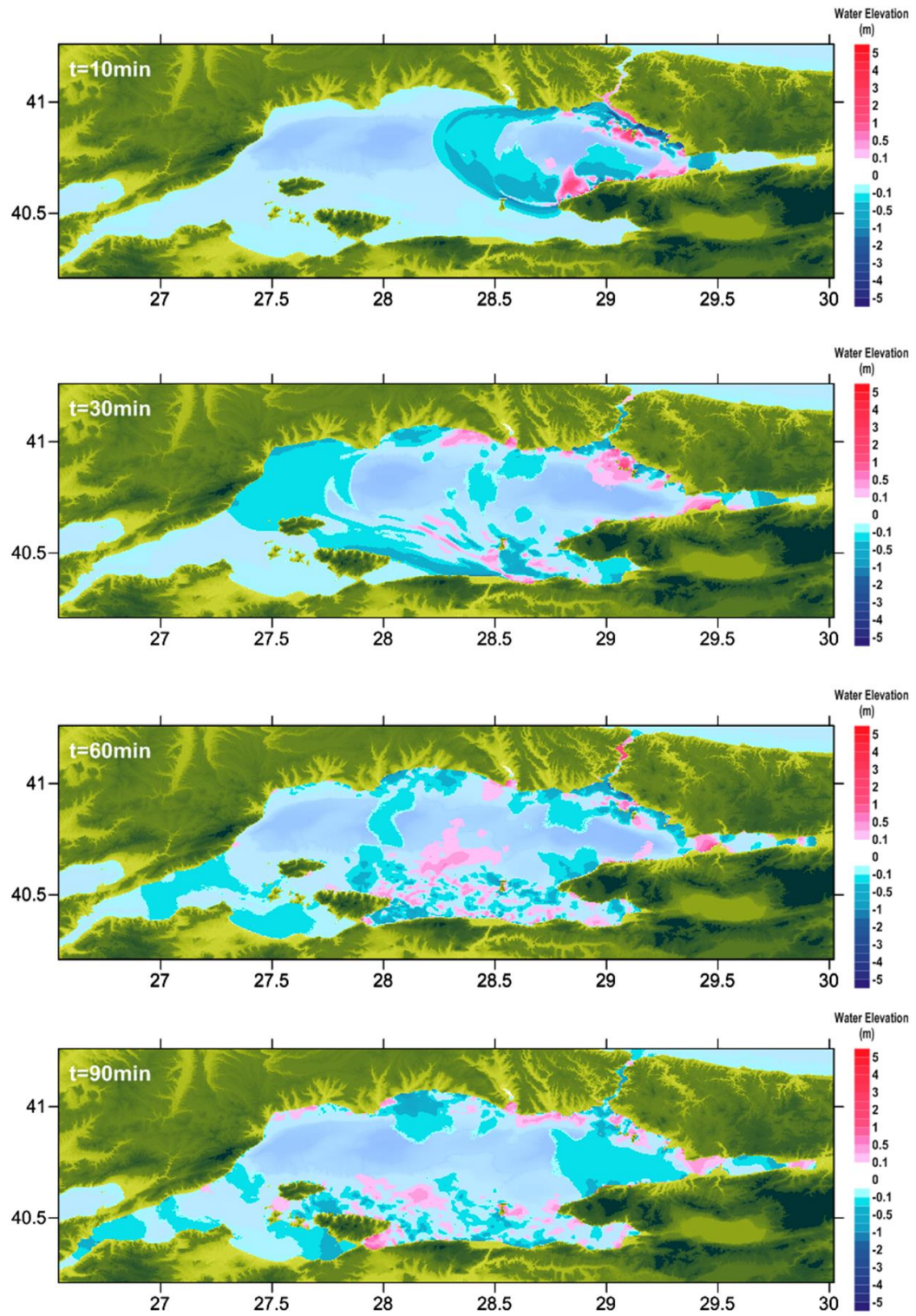


Figure B.5 Sea states at $t=10$, 30, 60, and 90 min respectively according to the tsunami source PIN

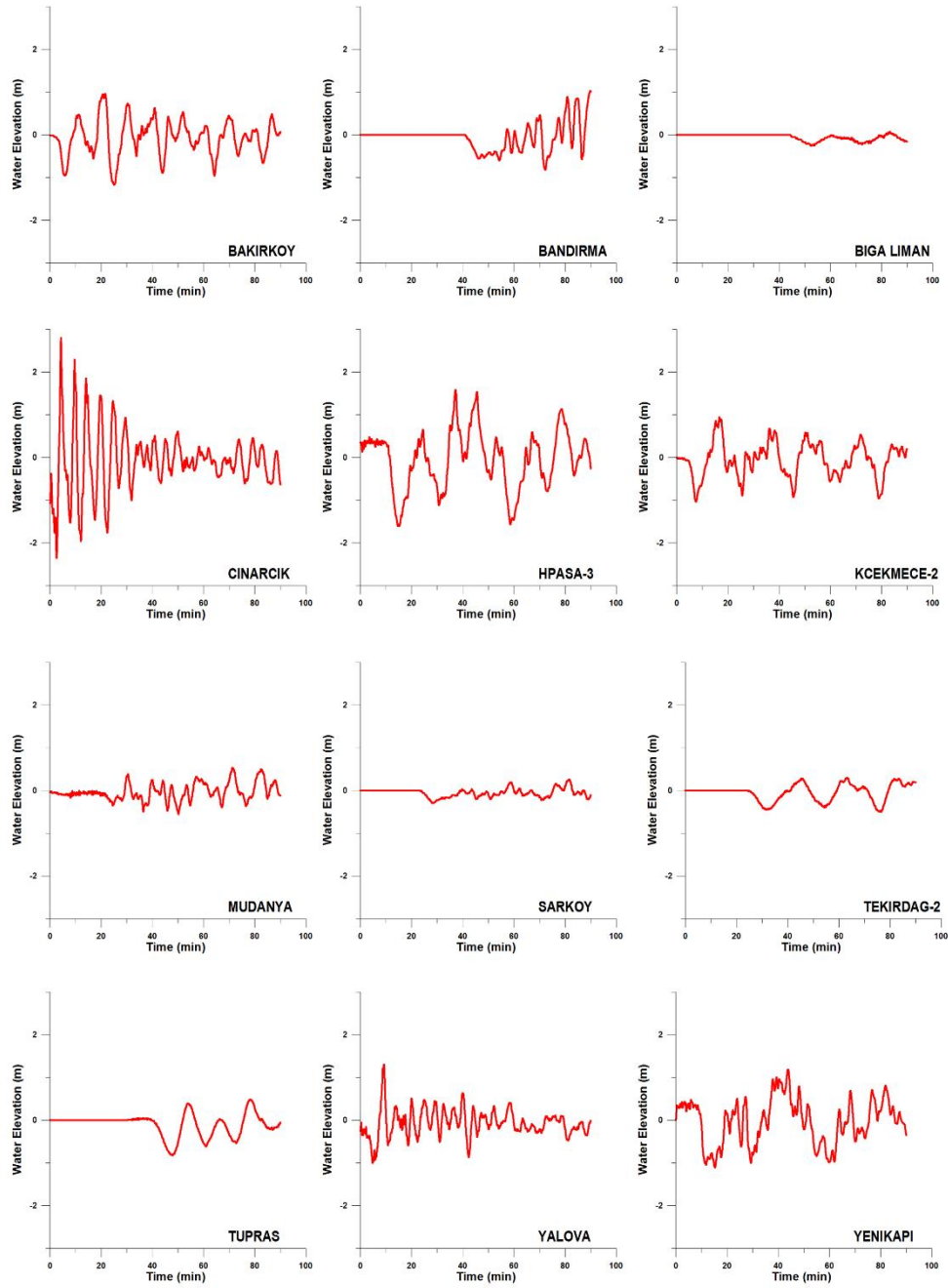


Figure B.6 Time Histories of Water Surface Fluctuations at the Selected Gauge Locations for PIN

- **PI +GA SOURCE**

Table B.3 Results of PI+GA Simulation at the Selected Gauge Points

Name of gauge pt.	Depth of gauge pt.(m)	X	Y	Arrival time of initial wave (min)	Arrival time of max.wave (min)	Maximum (+) wave amp.(m)	Maximum (-) wave amp.(m)
Bakirkoy	9.0	28.826200	40.952800	0	8	0.9	-0.9
Bandirma	6.6	27.968300	40.360600	25	72	0.7	-0.7
BigaLiman	3.9	27.135900	40.451600	21	47	0.3	-0.5
Cinarcik	4.8	29.136000	40.651500	0	12	2.4	-4.3
Hpasa3	9.1	29.014800	40.995700	0	31	1.1	-1.1
Kcekmece2	5.9	28.723800	40.969300	0	80	1.1	-1.3
Mudanya	8.4	28.908900	40.367500	0	85	0.6	-0.5
Sarkoy	5.3	27.336100	40.744900	0	30	0.7	-0.8
Tekirdag2	9.5	27.519700	40.971100	0	13	1.1	-1.0
Tupras	8.3	29.935000	40.737200	31	45	0.5	-1.0
Yalova	8.1	29.276900	40.663400	0	4	0.7	-1.2
Yenikapi	9.7	28.966500	41.001800	0	31	1.0	-0.9

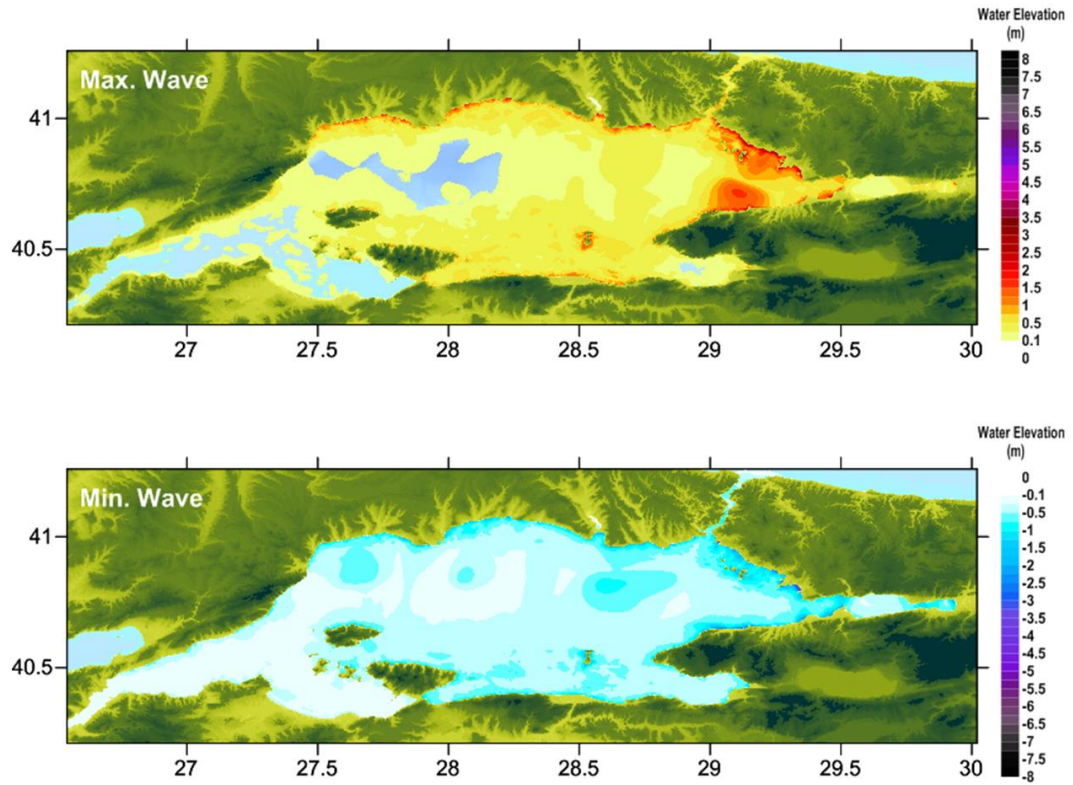


Figure B.7 Distribution of Maximum (+) Wave Amplitude (top) and Minimum (-) Wave Amplitudes

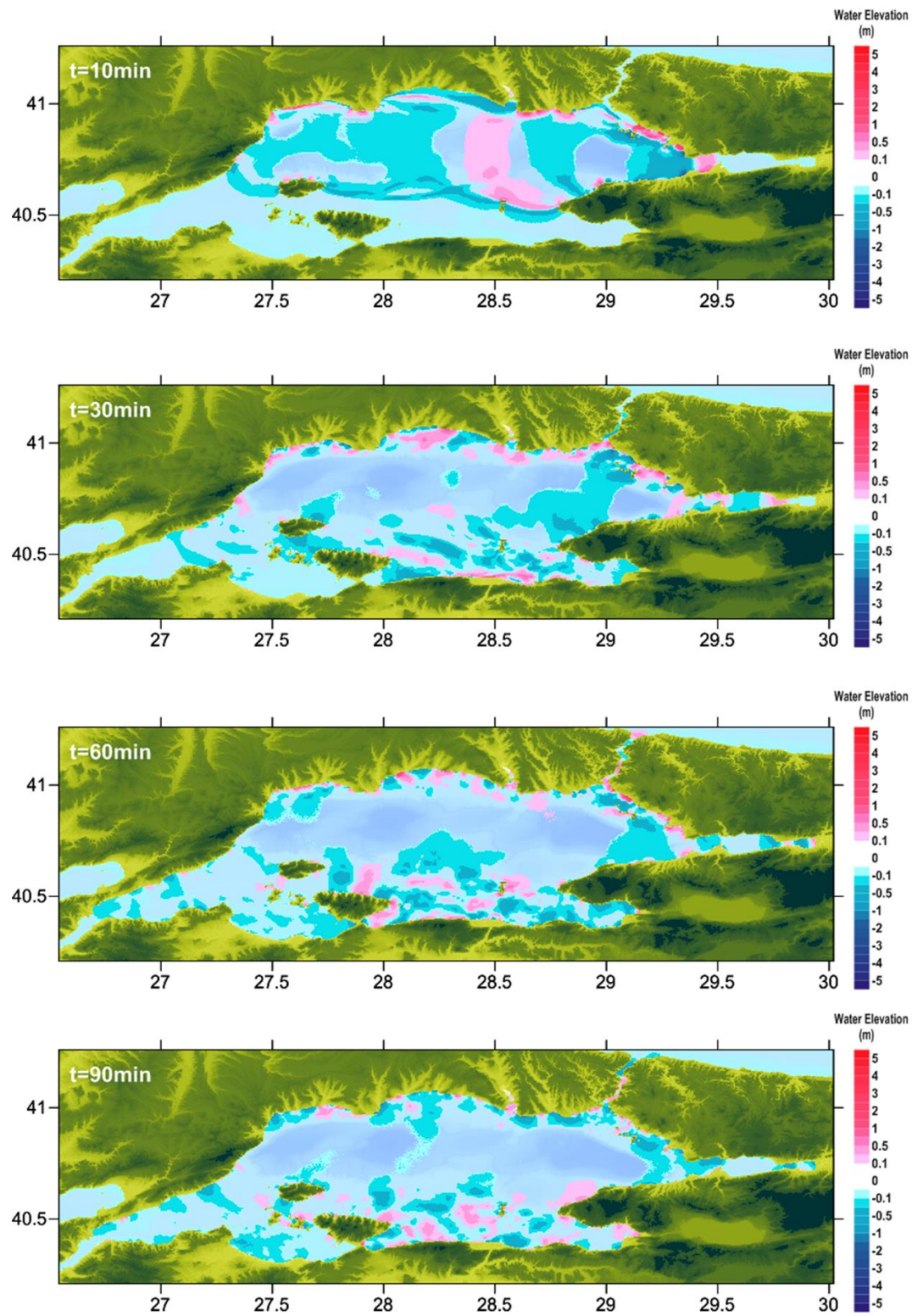


Figure B.8 Sea states at $t=10, 30, 60$, and 90 min respectively according to the tsunami source PI+GA

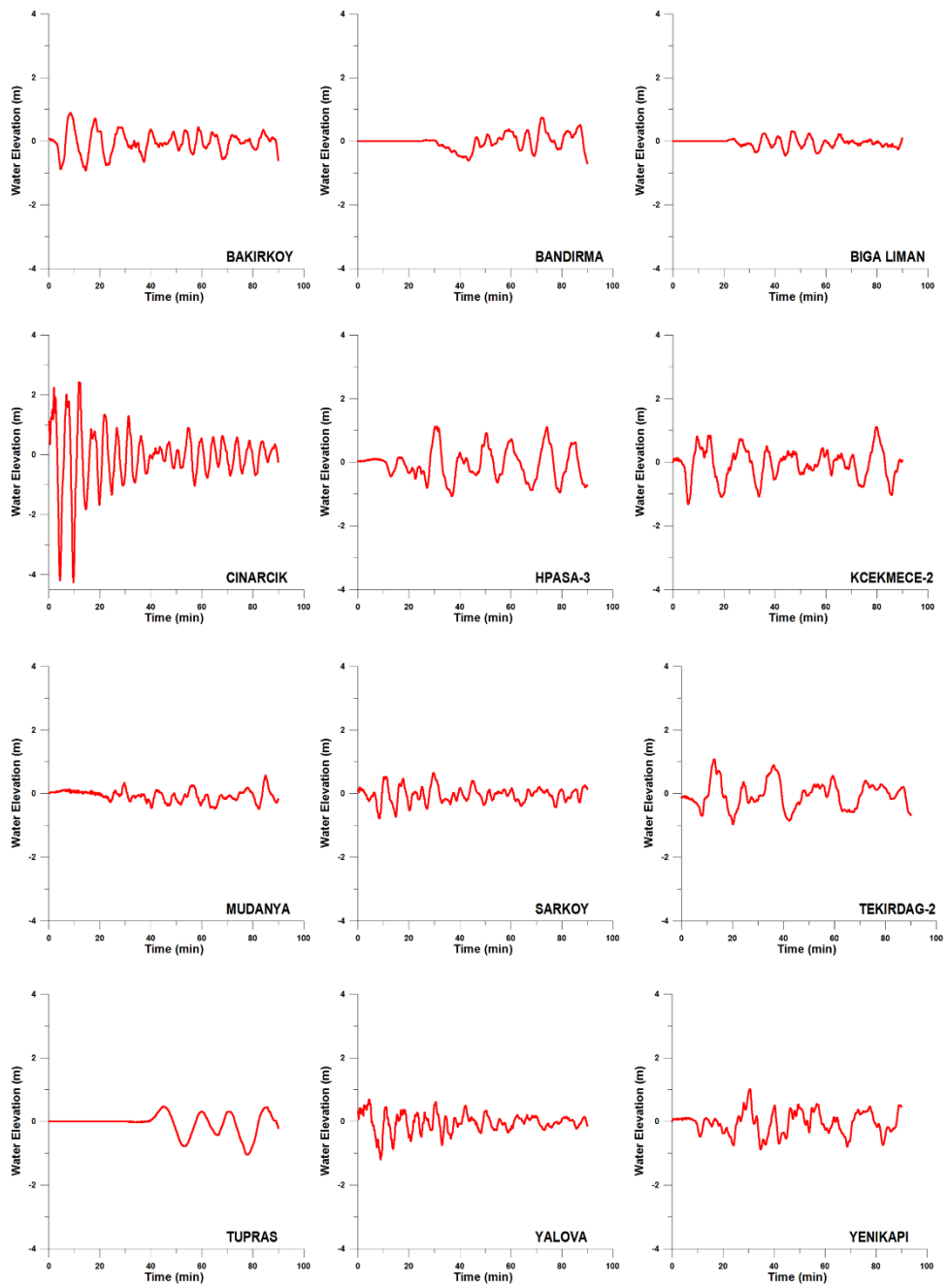


Figure B.9 Time Histories of Water Surface Fluctuations at the Selected Gauge Locations for PI+GA

- GA SOURCE

Table B.4 Results of GA Simulation at the Selected Gauge Points

Name of gauge pt.	Depth of gauge pt.(m)	X	Y	Arrival time of initial wave (min)	Arrival time of max.wave (min)	Maximum (+) wave amp.(m)	Maximum (-) wave amp.(m)
Bakirkoy	9.0	28.826200	40.952800	11	90	0.1	-0.2
Bandirma	6.6	27.968300	40.360600	25	66	0.3	-0.4
BigaLiman	3.9	27.135900	40.451600	21	47	0.5	-0.4
Cinarcik	4.8	29.136000	40.651500	15	84	0.2	-0.2
Hpasa3	9.1	29.014800	40.995700	22	71	0.1	-0.1
Kcekmece2	5.9	28.723800	40.969300	11	71	0.3	-0.3
Mudanya	8.4	28.908900	40.367500	30	89	0.1	-0.2
Sarkoy	5.3	27.336100	40.744900	0	10	0.5	-0.8
Tekirdag2	9.5	27.519700	40.971100	0	13	1.1	-0.9
Tupras	8.3	29.935000	40.737200	59	0	0.0	-0.2
Yalova	8.1	29.276900	40.663400	16	50	0.1	-0.1
Yenikapi	9.7	28.966500	41.001800	20	68	0.1	-0.2

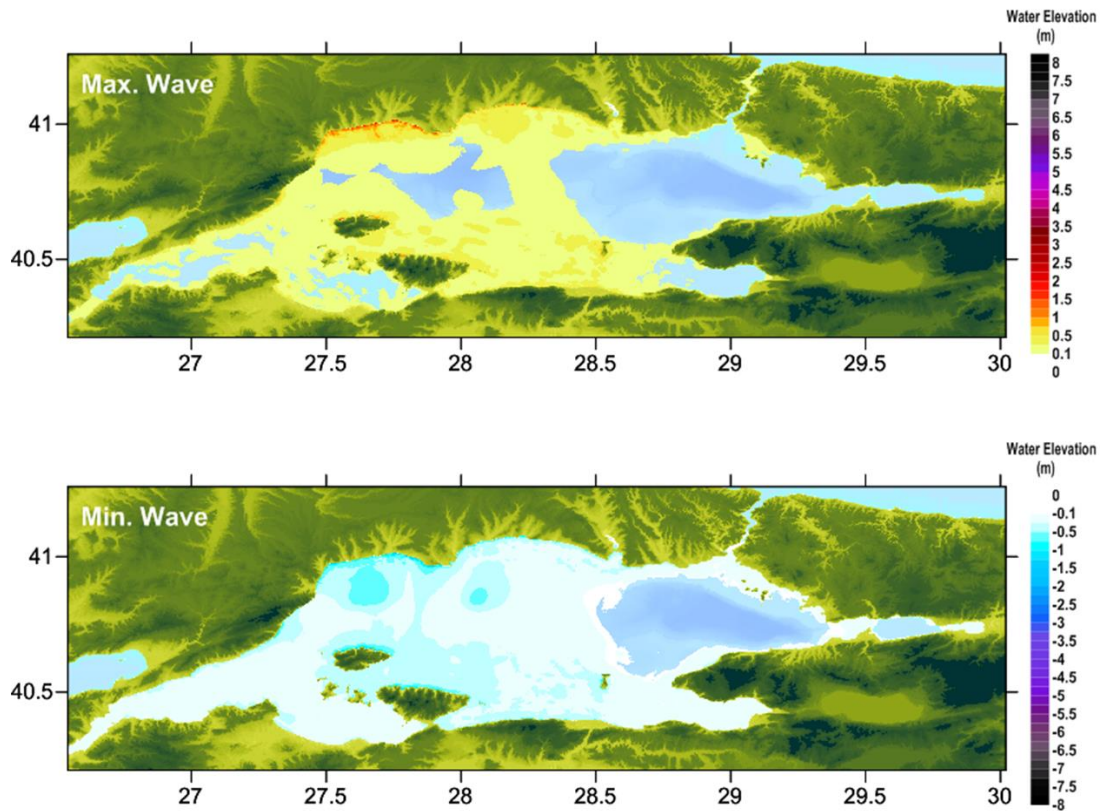


Figure B.10 Distribution of Maximum (+) Wave Amplitude (top) and Minimum (-) Wave Amplitudes

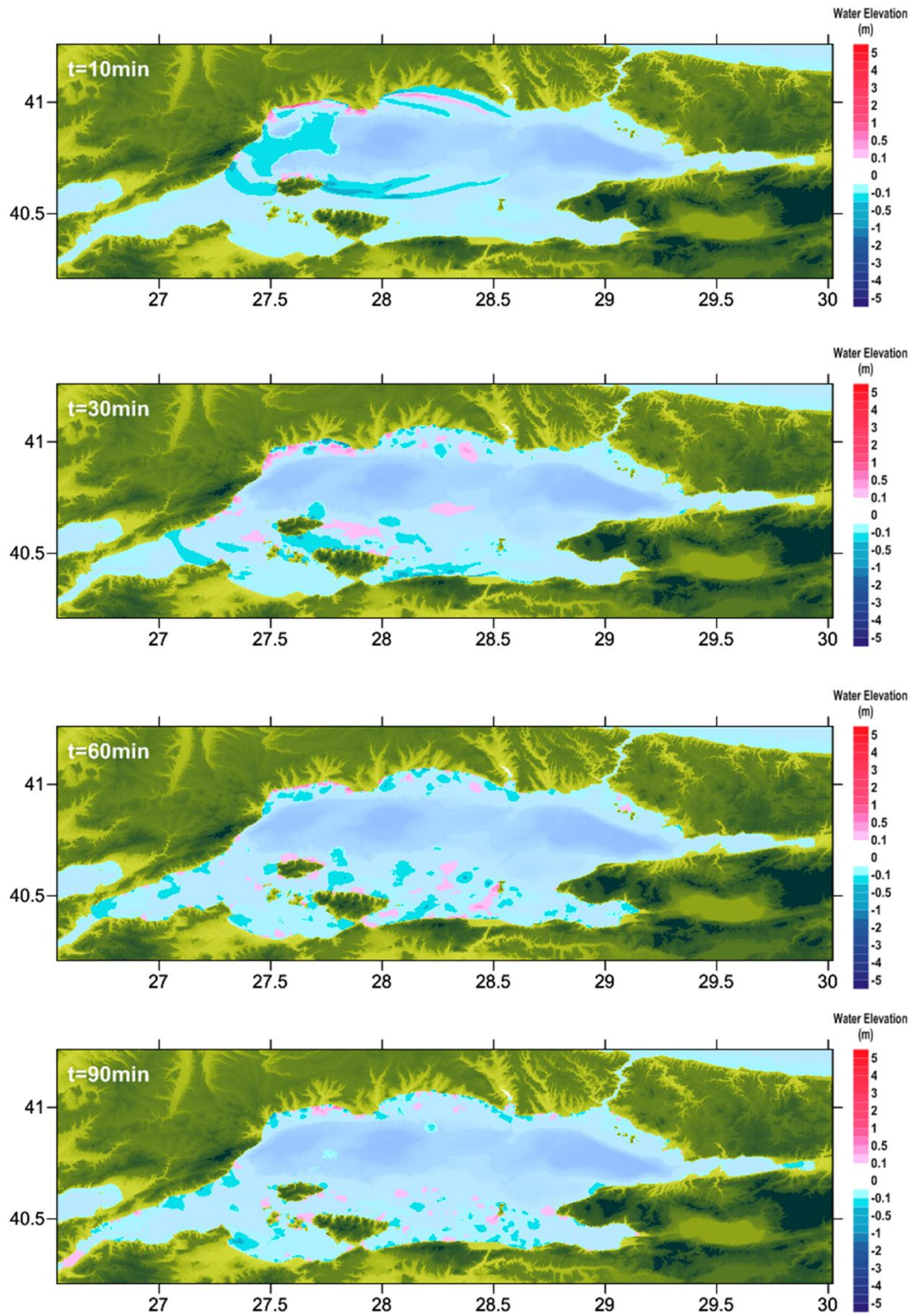


Figure B.11 Sea states at $t=10, 30, 60$, and 90 min respectively according to the tsunami source GA

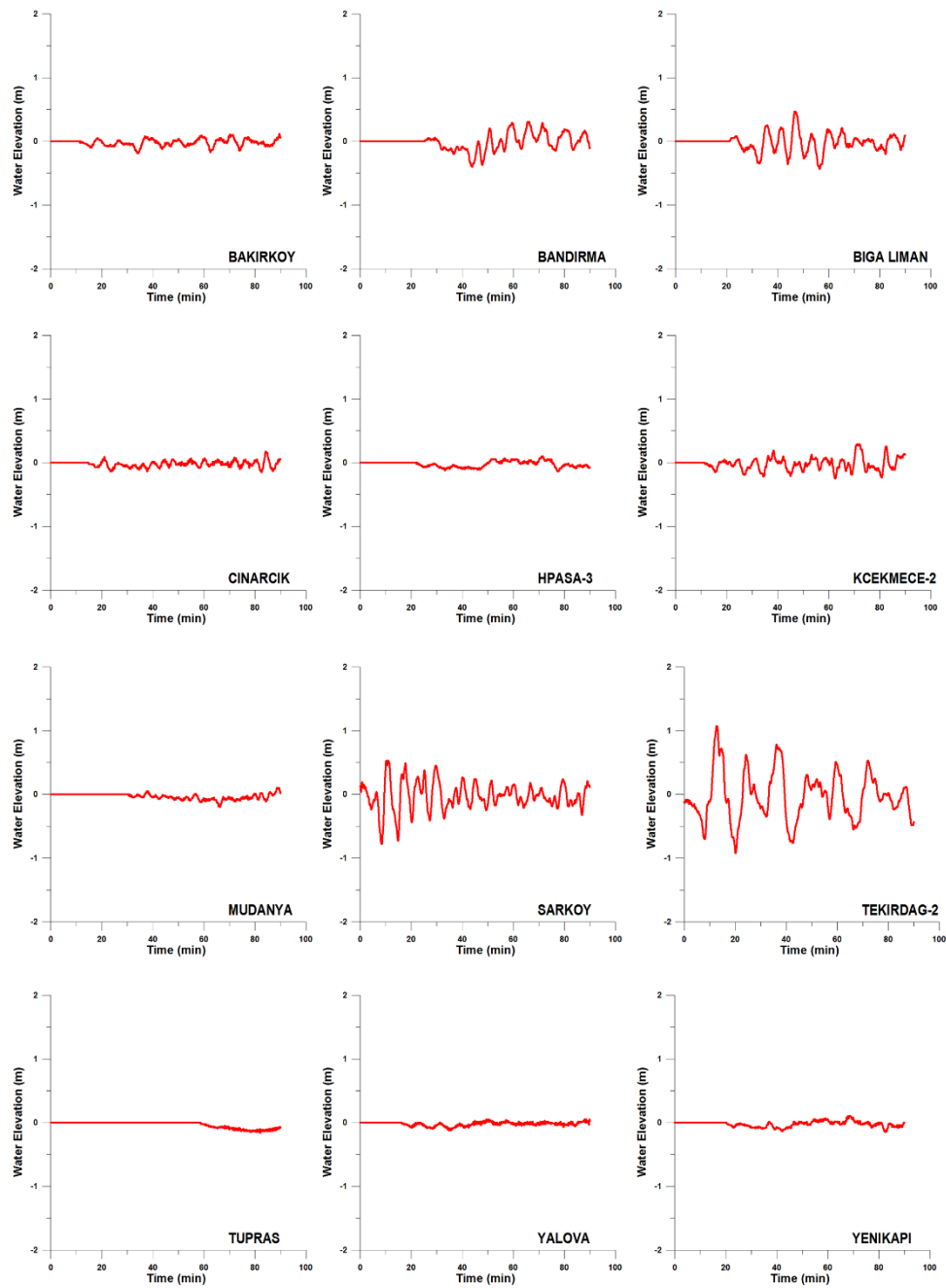


Figure B.12 Time Histories of Water Surface Fluctuations at the Selected Gauge Locations for GA

Table B.5 Results of GA Simulation at the Selected Gauge Points

- **YAN SOURCE**

Table B.6 Results of YAN Simulation at the Selected Gauge Points

Name of gauge pt.	Depth of gauge pt.(m)	X	Y	Arrival time of initial wave (min)	Arrival time of max.wave (min)	Maximum (+) wave amp.(m)	Maximum (-) wave amp.(m)
Bakirkoy	9.0	28.826200	40.952800	0	21	0.5	-0.7
Bandirma	6.6	27.968300	40.360600	44	85	0.9	-0.7
BigaLiman	3.9	27.135900	40.451600	47	85	0.1	-0.2
Cinarcik	4.8	29.136000	40.651500	0	10	2.4	-3.6
Hpasa3	9.1	29.014800	40.995700	0	32	1.0	-0.7
Kcekmece2	5.9	28.723800	40.969300	1	17	0.6	-0.8
Mudanya	8.4	28.908900	40.367500	0	88	0.4	-0.6
Sarkoy	5.3	27.336100	40.744900	27	62	0.1	-0.2
Tekirdag2	9.5	27.519700	40.971100	27	71	0.2	-0.3
Tupras	8.3	29.935000	40.737200	22	78	0.8	-0.8
Yalova	8.1	29.276900	40.663400	0	7	0.5	-1.4
Yenikapi	9.7	28.966500	41.001800	0	41	0.9	-0.7

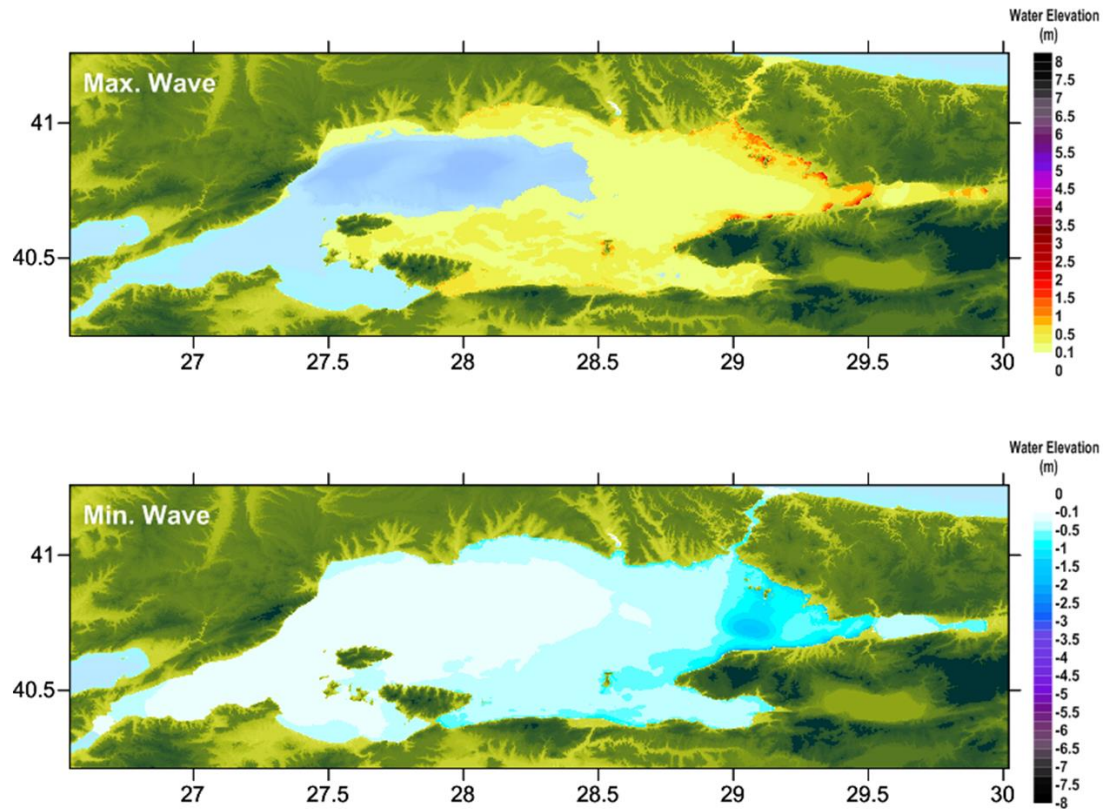


Figure B.13 Distribution of Maximum (+) Wave Amplitude (top) and Minimum (-) Wave Amplitudes

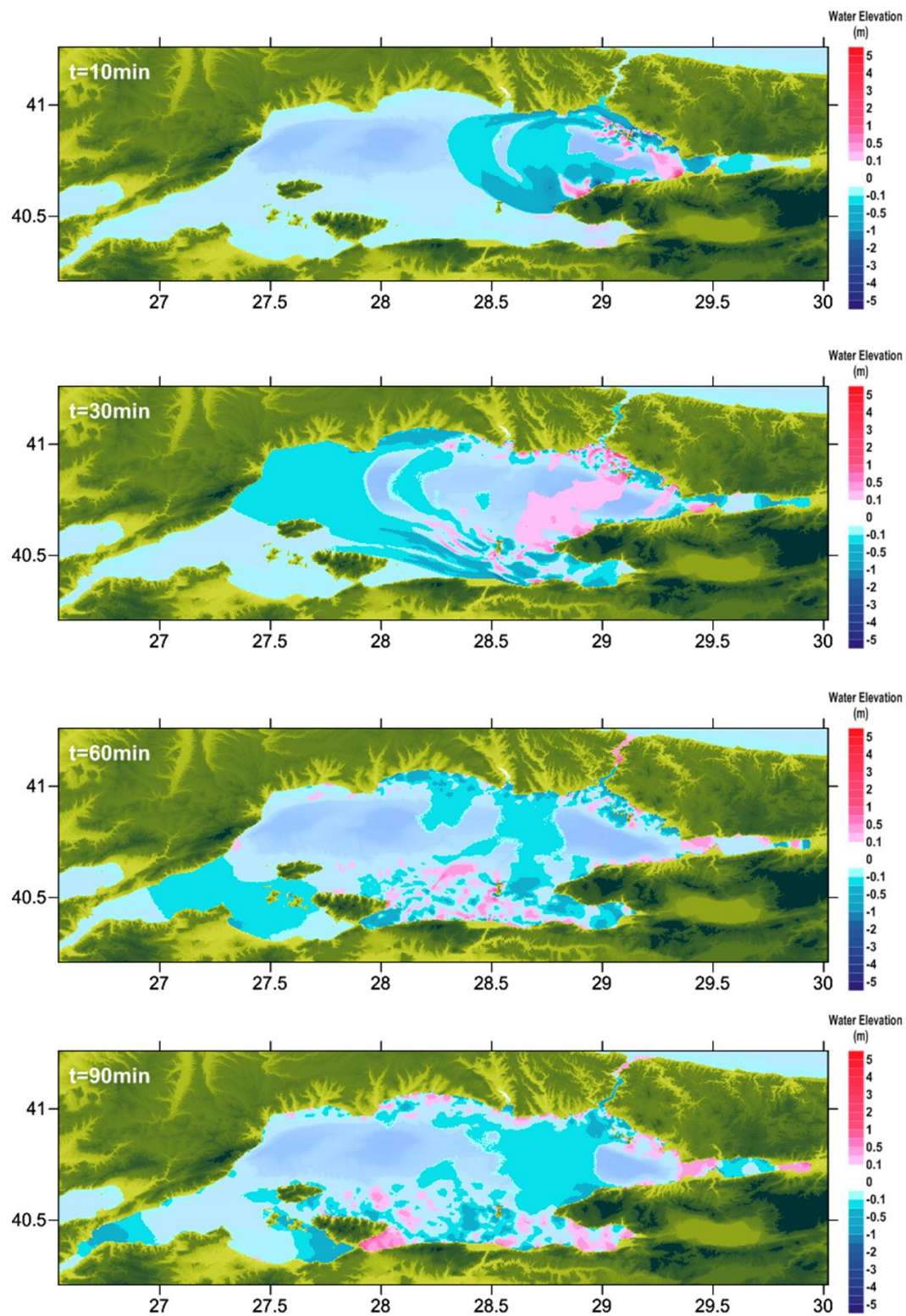


Figure B.14 Sea states at $t=10$, 30, 60, and 90 min respectively according to the tsunami source YAN

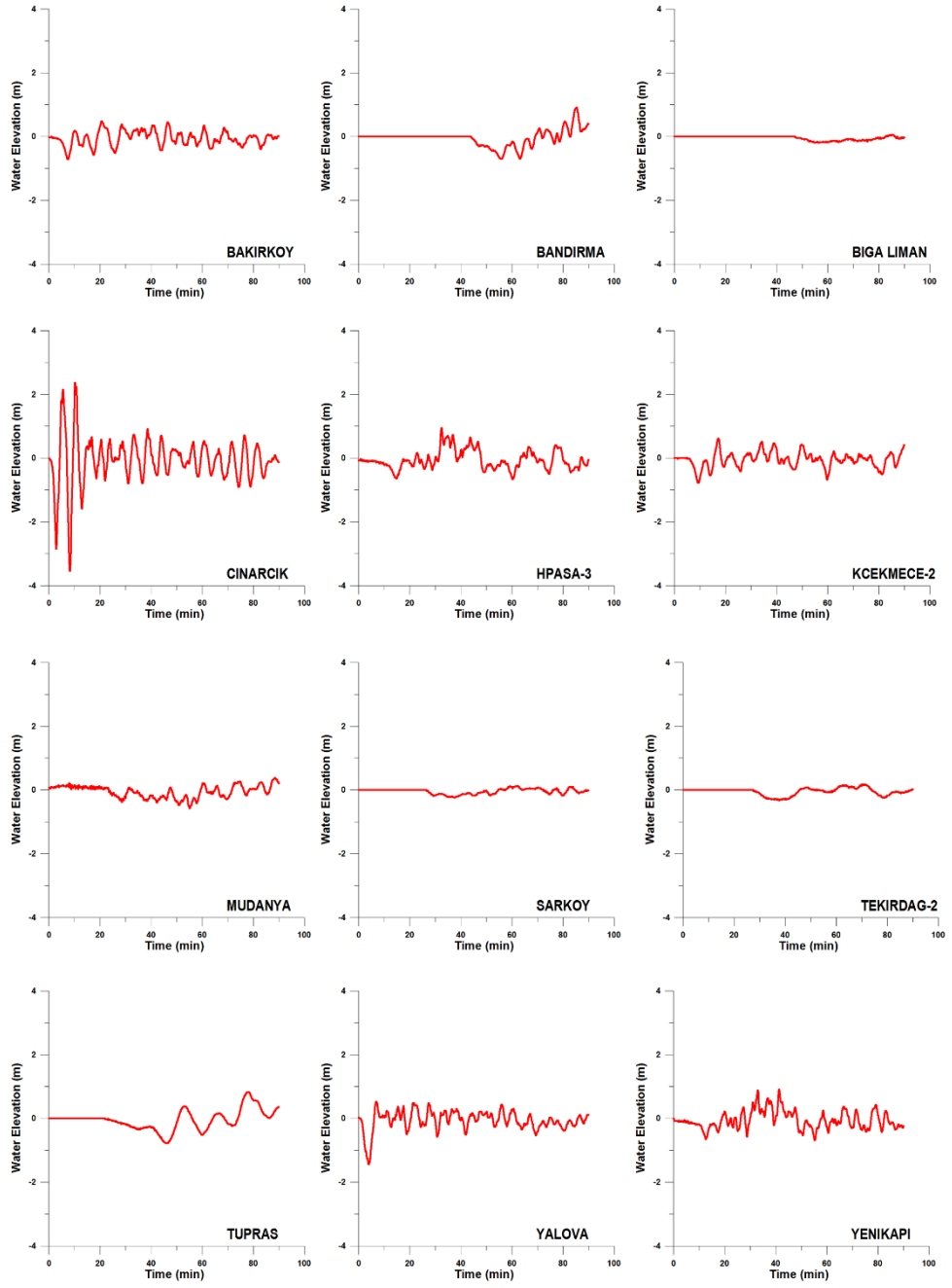


Figure B.15 Time Histories of Water Surface Fluctuations at the Selected Gauge Locations for YAN

- CMN SOURCE

Table B.7 Results of CMN Simulation at the Selected Gauge Points

Name of gauge pt.	Depth of gauge pt.(m)	X	Y	Arrival time of initial wave (min)	Arrival time of max.wave (min)	Maximum (+) wave amp.(m)	Maximum (-) wave amp.(m)
Bakirkoy	9.0	28.826200	40.952800	10	70	0.4	-0.7
Bandirma	6.6	27.968300	40.360600	0	75	1.5	-1.4
BigaLiman	3.9	27.135900	40.451600	17	42	0.7	-0.7
Cinarcik	4.8	29.136000	40.651500	13	78	0.2	-0.4
Hpasa3	9.1	29.014800	40.995700	20	59	0.6	-0.6
Kcekmece2	5.9	28.723800	40.969300	10	87	0.7	-0.8
Mudanya	8.4	28.908900	40.367500	27	84	0.4	-0.8
Sarkoy	5.3	27.336100	40.744900	3	22	0.6	-1.2
Tekirdag2	9.5	27.519700	40.971100	0	46	1.5	-1.8
Tupras	8.3	29.935000	40.737200	56	0	0.0	-0.8
Yalova	8.1	29.276900	40.663400	14	53	0.2	-0.5
Yenikapi	9.7	28.966500	41.001800	18	60	0.4	-0.5

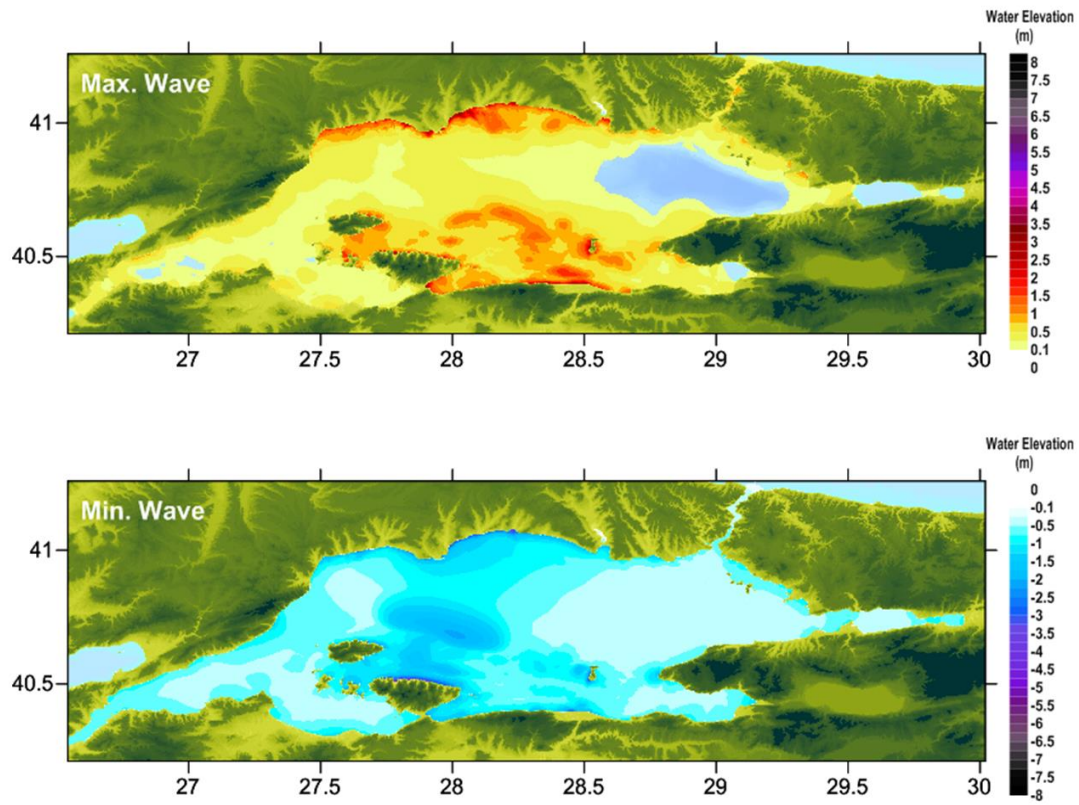


Figure B.16 Distribution of Maximum (+) Wave Amplitude (top) and Minimum (-) Wave Amplitudes

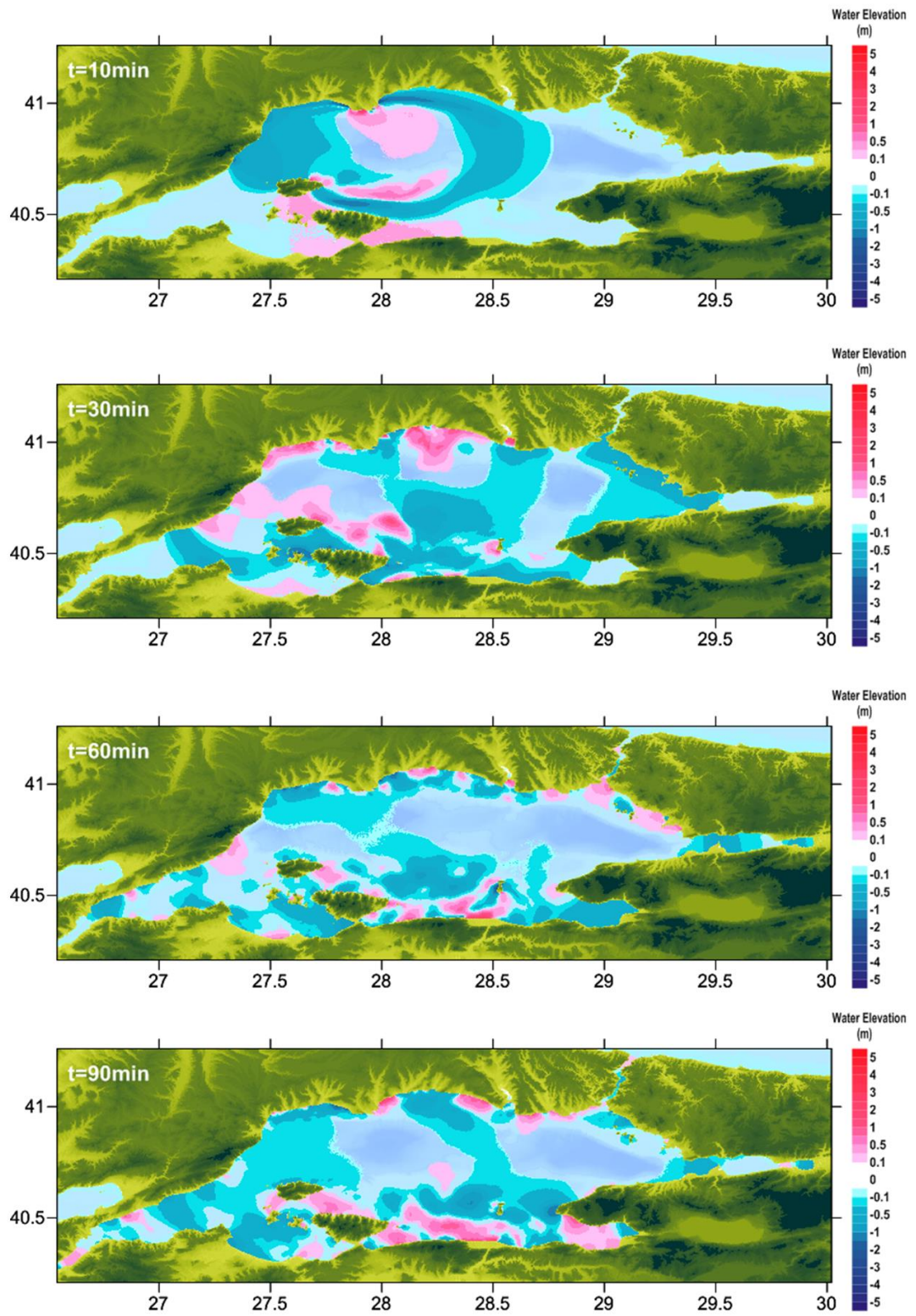


Figure B.17 Sea states at $t=10, 30, 60$, and 90 min respectively according to the tsunami source CMN

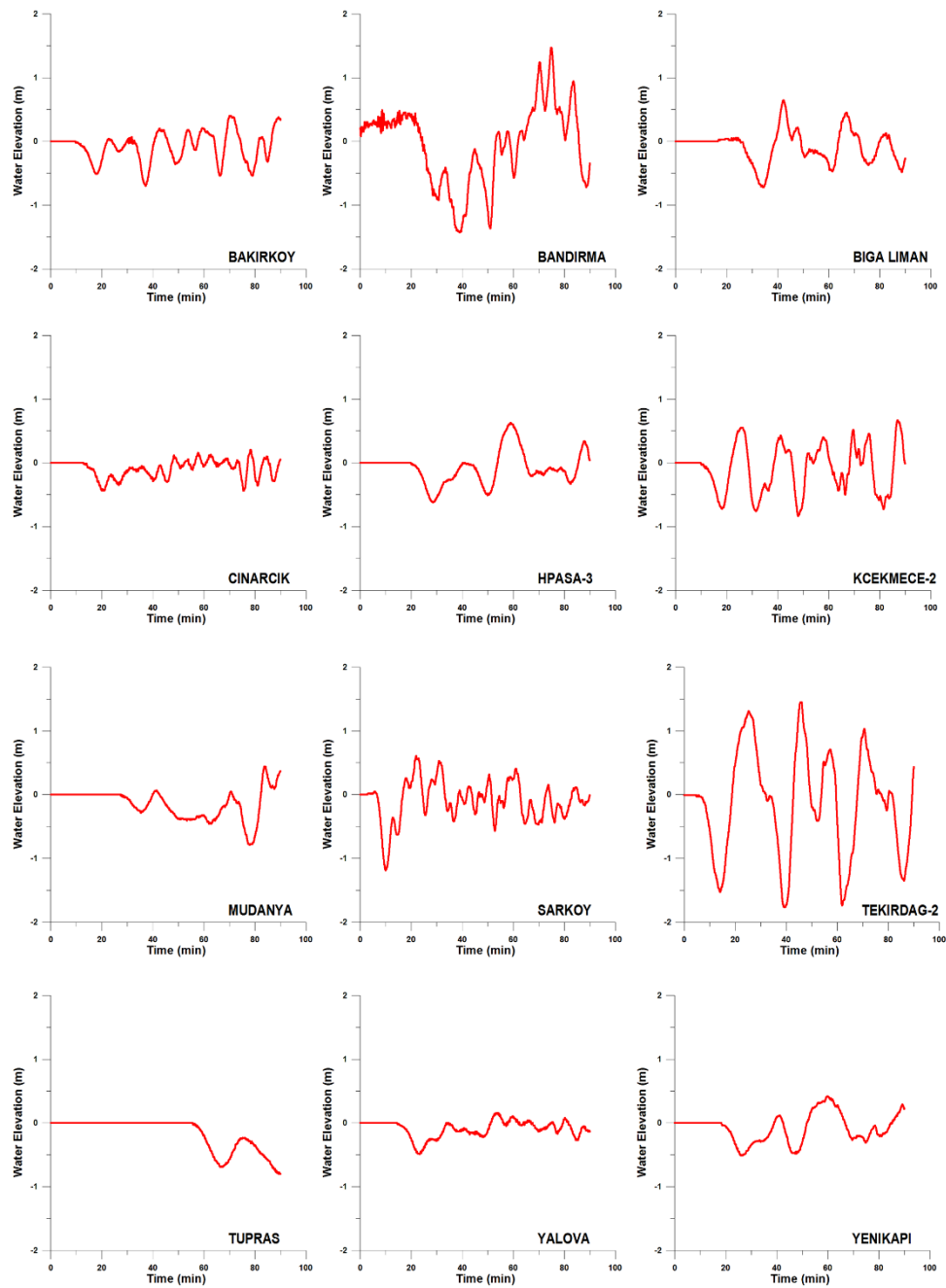


Figure B.18 Time Histories of Water Surface Fluctuations at the Selected Gauge Locations for CMN